Université du Québec
Institut national de la recherche scientifique
Énergie, Matériaux et Télécommunications
(INRS-EMT)

Performance Analysis and Design Optimization of Cooperative Relay Networks

A dissertation submitted in partial fulfillment of the requirements for the degree of Doctor of Philosophy

By
Amir Hossein Forghani

Evaluation Jury

External Examiner	Prof. Reza M. Soleymani, Concordia Univerity
External Examiner	Prof. Benoit Champagne, McGill University
Internal Examiner	Prof. Douglas O'Shaughnessy, INRS-EMT
Research Director	Prof. Sonia Aïssa, INRS-EMT

"If we knew what it was we were doing, it would not be called research, would it?"

Albert Einstein

Abstract

In wireless communications, implementing multiple antennas to provide spatial diversity may not always be feasible in practice. Therefore, cooperative techniques which employ relays to assist communication have emerged as practical solutions to produce spatial diversity without the requirement of having multiple antennas at the transmitters and/or the receivers. In this thesis, cooperative relaying networks are investigated, where relays are employed to improve the communication reliability and coverage area. Two well-known transmission strategies are assumed for the relays in terms of processing their received signal: amplify-and-forward and decode-and-forward. The focus is on the performance evaluation and enhancement of multi-hop multi-branch relaying networks taking into account the practical issue of co-channel interference. With multi-hop transmission along a single branch between the source and the destination, it is possible to achieve higher coverage and decrease the effects of channel impairments. On the other hand, by leveraging different and independent branches instead of one branch, the diversity gain can be increased further. In this case, maximal ratio combining and selection combining are applied at the end receiver. Furthermore, different cooperative schemes are investigated in different scenarios. In particular, interferers affecting the relaying nodes in the network can be of equal power or have different powers. For improved network performance, variable-gain coefficient is used at the relaying nodes. Furthermore, optimal power allocation among the transmit nodes is developed. Also, a selection method, where only the relays which decode the signal correctly during the broadcast phase participate in the relaying phase, is investigated. For the latter case, dual-hop multi-branch relaying is studied. Later on, signal space diversity technique is studied as a mean to improve the performance in a particular relaying network with one relay. Based on the relaying strategy adopted, the network performance is evaluated in terms of several metrics such as the error probability, the outage probability and the Ergodic capacity. Statistics of the end-to-end signal-to-interference-plus-noise

ratio, including cumulative density function, probability density function and moment generating function are used to in to conduct exact, approximate or lower-bound analysis. For instance, by employing approximate analysis to evaluate the system performance without resort to time-consuming simulation experiments, and determining the diversity order of the considered relaying networks. In particular, our result pertaining to the diversity order predicts that an error floor will appear when the ratio of the total transmit power to noise power is high, since the system performance is strictly interference-limited. The analyses conducted in this work allow the understanding of the impact of important system parameters, such as the interference and the number of branches and hops, on the performance of cooperative relaying networks, without resorting to time-consuming simulation experiments, and constitute the main task for providing guidelines as to the configuration to choose in practice.

Acknowledgments

It is a pleasure to thank the many people who made this thesis possible.

First and foremost, I would like to express my deepest gratitude to my advisor, Professor Sonia Aïssa. With her enthusiasm, her inspiration, and her great efforts to explain things clearly and simply, she made the research process more interesting to me. Throughout my PhD program, she provided encouragement, sound advice, good training, good company, and lots of fantastic ideas, but she also always gave me great freedom to expand my research activity.

I am indebted to my colleague, Dr. Salama Ikki, for providing effective consultations. Indeed, I could learn a lot from him. My thanks go also to my other colleague, Dr. Minghua Xia, for insightful technical interactions. My collaboration with them within the *Sensei Wireless Lab* was indeed very fruitful.

I am also thankful to the administration staff at INRS, especially Madam Sabourin, for assisting me in many different ways.

I wish to thank my entire extended family for all their love and encouragement.

Finally, I thank all the members of my thesis committee.

Contents

List of Figures

Chapter 1

Introduction

1.1 Motivation

Cooperative techniques are very important in the current research in wireless communications [1, 2]. Cooperative communication creates spatial diversity by employing relays to assist communication without the need for having multiple antennas [3, 4] at the transmitter and/or the receiver. In fact, the source node and the relay(s) provide a virtual antenna array to alternatively create spatial diversity when multiple antennas are not available. With cooperative communication, it is possible to combat channel impairments and, accordingly, enhance the system performance and coverage area [5]. Generally, the relays as elements that help the communication in a cooperative network, can either decode-and-forward (DF) [6–8] or amplify-and-forward (AF) [9,10] their received signals. Based on the relaying strategy adopted, different cooperative protocols can be implemented to achieve target performance criteria, defined in terms of error probability, outage probability, Ergodic capacity, etc ... [5].

Define a hop as the jumping between two consecutive nodes participating in the communication between the source and the destination, and a branch as a link (with one or more hops) between the source node and the destination node. Generally, two types of cooperation are considered, depending on the number of hops and branches between the source and its end destination. In the first type, cooperation takes places in the form of multi hops along a single branch between the source and the destination [5], while in the second type transmissions occur on multiple branches with each branch consisting of dual hops [11–13]. Clearly, by leveraging different and independent branches instead of one branch, the diversity gain can be increased further. In this case, different combining techniques such as maximal ratio combining (MRC) and selection combining (SC) can be applied at the end receiver (the destination node).

The performance of cooperative networks, in their general form of multi-hop multi-branch (MHMB) relaying networks, highly depends on the operation environment. In a wireless environment, in addition to the radio propagation impairments, co-channel interference (CCI) can affect the performance of the network significantly. CCI is a form of crosstalk that originates from the frequency reuse, i.e. when two or more radio transmitters are active within the same frequency band. In MHMB relaying networks, several nodes outside the target network can be sources of CCI. These undesired signals can degrade the signal quality at the target destination and need to be considered when evaluating the performance of MHMB relaying networks and designing communication strategies that ensure high efficiency in practice. In fact, as it will be shown later in the thesis, the impact of CCI can be significant and requires appropriate countermeasures to improve the performance of these networks. Such countermeasures can range from optimization of the way the resources are split between different participating nodes in the network, to implementation of sophisticated techniques such as signal space diversity.

In recent studies on MHMB networks, the major focus is on the transmission itself over the network in interference-free environments. Nevertheless, studying the impact of CCI on MHMB cooperative networks is not only necessary, it produces tools for the design and operation of practical cooperative wireless systems. The impact of CCI on the efficiency of cooperative systems were analytically investigated in [14–17]. In these papers, the authors assumed that the interference impacts the destination node and the relays for the well-known dual-hop network model. For instance, it is stated in [16] that interference limits the diversity gain of channel state information (CSI)-assisted AF relaying systems and can decrease the performance significantly. In [15], the effect of interference on the outage probability of an AF relaying network performing in a Rayleigh fading environment is analyzed.

Different techniques can be implemented to increase the transmission performance in relaying networks in the presence of interference. These techniques are diverse, and can be combined together in order to improve the performance further. Resource optimization (optimal power allocation), signal space diversity, relay selection and variable-gain relaying are among these techniques. These techniques will be detailed later when specifying the objectives and contributions of this thesis.

1.2 Literature Review

In this section, a review of work related to the subject of thesis is presented. The literature review highlights pertinent papers in three main domains: multi-hop diversity, multi-hop multi-branch cooperative relaying and cooperative relaying in the presence of interference.

1.2.1 Multi-hop Diversity

Besides the spatial diversity provided by multiple relays in cooperative systems [18], multi-hop transmission using multiple relays also provides an efficient way to combat shadowing and path loss, and improves the power efficiency [19].

In [19], the exact symbol error probability of M-ary phase shift keying (M-PSK) for multi-hop communication systems with regenerative relays is determined, where the source node transmits data to the destination node via a set of intermediate relays, which perform hard decisions on the received symbols before forwarding them to their respective subsequent node. Both, time-invariant additive white Gaussian noise (AWGN) channels and frequency-flat fading channels are considered. Furthermore, generic expressions which might be easily evaluated numerically or in closed-form are derived for various cases. However, a network constrained to use only point-to-point links has an average throughput that diminishes to zero as the number of relays approaches infinity [20]. To alleviate this limitation, a multi-hop diversity system was proposed in [21], in which each relay can combine the signals from all preceding transmitting relays before retransmission to the following relays [20–22]. Although the multi-hop diversity system guarantees throughput improvement, each relay requires coherent reception from all preceding relays along with a signal combiner. These requirements are impractical for networks composed of numerous, small, low-cost relays such as wireless sensor networks.

In [20], a practical approach for networks comprising multiple relays operating over orthogonal time slots is proposed based on a generalization of hybrid-automatic repeat request (ARQ). In contrast with conventional hybrid-ARQ, retransmitted packets do not need to come from the original source but could instead be sent by relays that overhear the transmission. An information-theoretic framework is exposed, which establishes the performance limits in a block fading environment. The results indicate a significant improvement in the energy-latency tradeoff when compared with conventional multi-hop protocols implemented as a cascade of point-to-point links.

The authors in [21] considered and four channel models: the decoded relaying multi-hop channel; the amplified relaying multi-hop channel; the decoded relaying multi-hop diversity channel; and the amplified relaying multi-hop diversity channel. Two classifications are discussed: decoded versus amplified relaying, and multi-hop versus multi-hop diversity channels. The channel models are compared through analysis and simulations, with the single hop (direct transmission) reference channel, on the basis of signal-to-noise ratio (SNR), probability of outage, probability of error, and optimal power allocation. Each of the four channel models is shown to outperform the single hop reference channel under the condition that the set of intermediate relaying terminals is selected intelligently. Multi-hop diversity channels are shown to outperform multi-hop channels. Moreover, it is shown that amplified relaying outperforms decoded relaying despite noise propagation. This is attributed to the fact that amplified relaying does not suffer from error propagation which limits the performance of decoded relaying channels to that of their weakest link.

In [22], the performance of multi-hop diversity transmission in Rayleigh fading is studied. Simple closed-form approximations for the outage and bit error probabilities of multi-hop diversity systems employing fixed AF relaying are derived. An exact closed-form expression for the outage probability of a multi-hop diversity transmission scheme employing fixed DF relaying is obtained. In addition, a selective relaying protocol which adapts transmissions at the source and relays based on the instantaneous received SNR at each relay, is developed and analyzed in terms of outage probability and bit error rate (BER). The analysis in [22] shows that multi-hop diversity transmission with fixed DF relaying offer no diversity order gain, while those employing the fixed AF relaying achieve a diversity order equal to the number of hops. It is also shown that multi-hop diversity transmission systems employing fixed AF relaying attain the best outage probability and BER performance, despite the noise amplification at the relays.

The performance of cooperative diversity schemes over log-normal fading channels, is presented in [23]. The authors focus on single-relay cooperative networks with AF relaying and consider three TDMA-based cooperation protocols which correspond to distributed implementations of multi-input multi-output (MIMO), single-input multiple-output (SIMO), and multiple-input single-output (MISO) schemes. For each protocol, the authors derived upper bounds on the pairwise error probability over log-normal channels and quantify the diversity advantages. Based on the minimization of a union bound on the BER performance, they further formulated optimal power allocation schemes which demonstrate significant performance gains over their counterparts with equal power allocation.

1.2.2 Multi-hop Multi-branch Cooperative Relaying

As a general relay-topology based on cooperative diversity, a MHMB cooperative relaying system can employ low-complexity relays, and only the destination combines the signals from the last-hop relays in multiple branches. In addition, the combination of cooperative diversity and multi-hop transmission can mitigate not only multi-path fading but also shadowing and path loss [23–26]. Note that a MHMB cooperative relaying system is not a multi-hop diversity transmission system, but rather a parallel multi-hop transmission system. The end-to-end performance of MHMB cooperative relaying systems was studied in [24–26], but most studies focused on systems using AF relays.

In [24], a performance analysis of MHMB communication over Log-Normal fading channels is presented. The framework allows to estimate the performance of AF relaying methods for both CSI-assisted relays and fixed-gain relays. In particular, by relying on the Gauss quadrature rule (GQR) representation of the moment generation function (MGF) for a Log-Normal distribution, accurate formulas for important performance indexes whose accuracy can be estimated a priori and just depend on GQR numerical integration errors, are developed. Also, in order to simplify the computational burden of the former framework for some system set-ups, various approximations are proposed, which are based on the improved Schwartz-Yeh method. The authors show that the proposed approximations provide a good trade-off between accuracy and complexity for both SC and MRC methods.

In [25], MHMB systems with non-regenerative fixed-gain AF relays are considered. Simple closed-form expressions for the outage and bit error probabilities of these systems are derived. It is shown that while a multi-hop transmission system does not offer diversity gain, it can perform better than a single-hop system if its individual-link average SNRs satisfy a certain condition. In addition, the analysis clearly shows the diversity gains achieved by dual-hop multi-branch systems and MHMB systems. A design criterion is also presented for guaranteeing better outage and BER performance for a MHMB relaying system compared to a dual-hop multi-branch system with the same number of branches.

The Ergodic capacity of rate adaptive, power non-adaptive, MHMB DF relaying networks is analyzed in [26]. Different cases of super-imposed, selection, and orthogonal relaying are investigated. Parallel channel coding and repetition coding are considered for each case. Closed-form expressions for the maximum instantaneous achievable rates are obtained for each case. The distribution functions of the maximum instantaneous achievable rates for a source-relay-symmetric (S-R-sym) case and relay-destination-symmetric (R-D-sym) case are evaluated. The Ergodic capacity of rate adaptive, power non-adaptive, dual-hop multi-branch networks in the S-R-sym and R-D-sym cases are derived for Rayleigh fading. It is observed that parallel channel coding gain can attain as much as 1 bit improvement for the examples considered. Increasing the number of branches deteriorates the performance of the orthogonal relaying scheme, but improves the performance of the other schemes albeit with diminishing returns. The performance of all schemes degrades rapidly as the number of hops per branch increases, such that no scheme is more energy-efficient than direct transmission for more than three hops per branch.

1.2.3 Cooperative Relaying in the Presence of Interference

Most prior work on cooperative relaying considers thermal noise-limited conditions without interference. However, CCI often limits the performance of wireless systems, and since relaying systems are usually used to increase the coverage under dense frequency reuse, they are typically exposed to CCI. The authors in [27–32] provided insights on the effect of CCI in dual-hop AF relaying systems. However, only few studies have examined CCI in dual-hop DF relaying systems [33–35], and these systems cannot be generalized to MHMB relaying systems in a straightforward way.

The performance of a dual-hop CSI-assisted AF system, with CCI at the relay is analyzed in [27]. The system's outage probability and the average BER in the presence of multiple Rayleigh fading interfering signals are investigated. An exact expression for the outage probability and an accurate bound for the average BER are derived.

The outage probability and the average BER of a dual-hop fixed-gain relaying system in the presence of CCI and thermal noise at the relay and at the destination are investigated in [28]. The analysis assumes Rayleigh fading for the source-relay and relay-destination channels and Rician fading for the interfering channels. New closed-form/series expressions for the outage probability and the average BER are presented, which allow for a rapid performance evaluation of fixed-gain relaying in interference-impaired environments. The achievable diversity order is also studied, and it is also shown that the Rician K-factor of the interfering channel has a negative effect on the outage probability and BER performance.

In [29], the performance of a dual-hop non-regenerative relay fading channel in an interference-limited environment is investigated. The relay and destination nodes are corrupted by CCI. New closed-form expressions for the probability density function (PDF) and cumulative distribution function (CDF) of the output signal-to-interference ratio (SIR) are derived. Furthermore, analytical expressions for the outage probability of both the CSI-assisted relay channel and the fixed-gain relay channel are derived.

The outage performance of dual-hop relay networks with CCI, which is a major problem in cellular systems, is investigated in [30]. A realistic channel fading model for micro-cellular radio network is adopted, i.e., the desired signal is assumed to have Rician fading due to the presence of line-of-sight (LOS) propagation, and the interfering signals from neighbouring cells are assumed to experience Rayleigh fading because of the absence of LOS propagation. An upper-bound on the outage probability and the asymptotic expression for AF protocol are derived. The authors also propose an optimal power allocation scheme for the high SIR regime.

The authors in [31] investigate the effect of CCI on the performance of dual-hop AF relaying. Based on the derivation of the effective signal-to-interference-plus-noise ratio (SINR) at the destination node of the system, taking into account CCI, they obtain expressions for the error and outage probabilities. Moreover, they study the performance of the system in the high SINR regime.

In [32], a cooperative diversity system consisting of a source, a destination, and multiple single-hop AF relays is considered, and a mathematical framework for the asymptotic analysis (at high SNR) of this system in generic noise and interference is provided. Assuming independent Rayleigh fading for all links in the network and orthogonal relay-destination channels, the authors obtain simple and elegant closed-form expressions for the asymptotic symbol and bit error rates valid for arbitrary linear modulation formats, arbitrary numbers of relays, and arbitrary types of noise and interference with finite moments including CCI, ultra-wideband interference, generalized Gaussian noise, and Gaussian noise. Furthermore, they exploit the analytical error rate expressions to develop power allocation, relay selection, and relay placement schemes that are asymptotically optimal in environments with generic noise and interference. In general, their power allocation problem results in a geometric program which can be solved efficiently in a numerical way. For the special case of only one relay, they provide a closed-form result for the optimal power allocation. The proposed power allocation, relay selection, and relay placement schemes lead to large performance gains in non-Gaussian noise compared to the conventional counterparts optimized for Gaussian noise.

In [33], the outage performance of DF cooperative systems in interference-limited Nakagami-m fading environment is investigated. More specifically, assuming the presence of multiple co-channel interferers subject to Nakagami-m fading at the DF relay, and a noisy destination, simple accurate closed-form approximations for the end-to-end outage probability are derived. To this end, moment-based estimators are used to attain the appropriate Nakagami-m fading parameters.

Dual-hop AF and DF relaying systems with multiple interferers and Rayleigh fading is analyzed in [34]. The authors derive closed-form expressions for the outage probability where the interferers have arbitrary transmit power. Numerical results verify the validity of the theoretical analysis and comparisons are provided.

On the other hand, [35] analyzes the outage probability of multi-branch dual-hop DF cooperative relaying over non-identical Nakagami/Nakagami fading channels. The work derives an exact closed-form expression for the outage probability with MRC considering both the effect of CCI and AWGN. The results show that a DF cooperative relaying system is more vulnerable to noise than to interference for low and moderate SINR, whereas it is more susceptible to interference for high SINR and high diversity order. The authors also show that the robustness of the destination against CCI is more important than that of the relay.

Even though cooperative relaying networks are known to mitigate the impact of shadowing, most studies examined only multi-path fading. For practical purpose, both small-scale and large-scale fading should be taken into account. However, the performance of cooperative relaying networks under composite shadowing and fading has so far been limited. Renzo et al. presented a workable framework for the performance analysis of MHMB cooperative relaying over shadowed Nakagami fading channels [24], but they considered the AF scheme without CCI. Moreover, most existing literature evaluates the bit error probability through upper bounds [21], [22], by using the Gaussian Q-function [19], [24], or an approximation of the latter. In particular, a closed-form expression for the average symbol error probability (ASEP) for DF MHMB cooperative relaying system has not been obtained so far.

1.3 Research Objectives

This dissertation, focuses on the performance evaluation and enhancement of MHMB relaying networks taking into account the practical issue of CCI. Specifically, the performance of MHMB relaying networks with multiple co-channel interferers affecting all nodes that take part in the end-to-end transmission from the source node to its final destination is investigated. In particular, equal-power interferers or non-equal power interferers are assumed to impact each relay node in the network. The optimal gain, i.e., variable-gain coefficient, is used at each relay as a technique to improve the performance. The performance of the network is assessed in terms of important performance criteria, namely, the bit error probability and the outage probability. Furthermore, optimal power allocation is considered as another technique to improve the overall performance of the network. Later on, signal space diversity (SSD) technique is studied as a technique to improve the performance in a particular relaying network with one relay. Accordingly, the performance of relaying networks benefiting from SSD in terms of error probability, outage probability, Ergodic capacity (for slow fading channels) and outage capacity (for fast fading channels) is investigated. Furthermore, in order to improve the system performance, minimization of the error probability of the considered network subject to constraint on the total energy budget is studied. Optimization of the performance whereby the total energy is minimized under constraint on the error probability, is also conducted. Finally, by using relay selection technique in dual-hop multi-branch relaying network, the system performance is further enhanced. The idea of using a relay decoding set implies that the relays which fail to decode their received signal in the first phase of signal transmission, do not participate in the second phase of signal transmission.

The main techniques that are used to enhance the performance of the relaying networks considered in this thesis can be categorized as follows:

1.3.1 Resource Optimization

Resource optimization among the source node and all the relays can be used to improve the performance and remedy the impacts of CCI. In this work, two optimization processes with different criteria are presented. In both optimization processes, optimal power allocation is carried out among the source node and the relay (s) participating in the signal transmission. In order to improve performance, minimization of the error/outage probability of the system subject to constraint on the total energy budget is performed. In the other form, in order to preserve the total energy, the total energy expenditure of the system is minimized subject to constraint on the error/outage probability.

1.3.2 Signal Space Diversity

SSD also known as modulation diversity, is known as a promising technique to enhance the performance in a relaying network with one relay [36]. The technique can yield gains in terms of time diversity, frequency diversity and spatial diversity. Using SSD, the symbol vectors are rotated by a square spreading matrix in such a way that any two symbol vectors can be distinguished by the maximum number of distinct components [36]. In a cooperative network with one relay, since these components are transmitted through independent paths from the source to the destination (one component is sent through source-destination path while the other component is sent through relay-destination path), the received signal at the destination is more reliable and accordingly, the performance of the network is improved. Indeed, assuming that a deep fade affects only one of the components of the signal vector, the rotated constellation provides more protection against the unfavourable impacts of the noise comparing to the non-rotated constellation, as no two points collapse together.

1.3.3 Relay Selection

Assuming multiple relays, there might be a possibility that one or more relays fail to decode the received signal correctly, assuming that the relays use decode-and forward technique to generate and forward the processed signal to the subsequent relays or the destination. Therefore, in MHMB relaying with multiple DF relays, only the relays which are able to decode their received signal correctly should participate in the signal transmission. Let C define the set of relays which are able to decode their received signal correctly. In the second phase, i.e., the relaying phase, only the relays in C are allowed to be active, and hence forward their processed signals to the subsequent relays or the destination. Using this selection scheme, the performance can be improved, since the relays which fail to decode their received signal do not participate in the signal transmission. This approach is used in IEEE802.16j and LTE release 10 and its practical implementation requires the use of error detection methods such as cyclic redundancy.

1.3.4 Relaying with Variable-Gains

There are many choices for the gain at the relay when AF transmission is considered, e.g., variable-gain or fixed-gain. Variable-gain coefficient is the optimal gain at the relay. Other types of gains may also be used at the relays, but would not yield optimum performance, as they are not optimal gains. In fact, the variable-gain at the relays is used to guarantee the power constraint. Using the variable-gain coefficient at the relay implies that full CSI is available at the relay.

As will be detailed next, these techniques will be used to enhance the performance of the relaying networks studied in this thesis. The focus being also on the analysis of the performance of these networks, we mention the methodology that will be used.

The methodology is mainly based on studying the statistics of the end-to-end SINR in the relaying networks considered. Accordingly, CDF, PDF and MGF of the end-to-end SINR are derived and used for the performance analysis. Closed-form asymptotic and lower-bound analysis are presented for error and outage probabilities of the considered MHMB relaying networks. For the SSD based relaying networks, where the constellation rotation and interleaving are employed, the performance is investigated in terms of error probability, outage probability, Ergodic capacity, and outage capacity.

1.4 Contributions of the Dissertation

1.4.1 Summary of Contributions and Thesis Organization

A summary of the thesis contributions is presented in this section.

In Chapter 2, a closed-form approximate expression for the average bit error probability of MHMB relaying is derived. The cooperative relaying scheme includes M separate branches between the source node and the destination node, and each branch comprises a certain number of AF relays. Independent and non-identical Rayleigh fading links between successive nodes in each branch are considered. Numerical results are provided and compared with Monte Carlo simulations.

Chapter 3 studies the performance of opportunistic AF MHMB relaying in the presence of CCI. Exact and upper-bound expressions for the end-to-end SINR are obtained, assuming transmissions over independent non-identical Rayleigh fading channels. Afterwards, the CDF and PDF of the upper-bound end-to-end SINR are investigated. Then, a lower-bound closed-form expression for the outage probability is obtained. Furthermore, approximation function for the PDF of the end-to-end SINR is derived. Subsequently, simple expressions for the approximate error and outage probabilities are provided. These expressions deliver more understanding on the effect of the system parameters on performance. Moreover, optimization of the power allocation among the transmit nodes is addressed to enhance the overall system performance. As an optimal solution for the resource allocation problem at hand, adaptive power allocation that minimizes the error probability under constraint on the aggregate power over the branch with the maximum SINR is developed. It is shown that by applying the energies obtained through the optimization process, the performance of the network enhances significantly. The accuracy of the analysis is validated by comparing the numerical results with Monte Carlo simulations and insightful discussions are provided.

In Chapter 4, the performance of non-symmetric MHMB relaying using AF protocol and operating in practical environments with unequal-power interferers, is examined. Assuming the channels, for both the desired and the interfering signals, to experience Rayleigh fading, first, exact and upper-bound expressions for the end-to-end SINR are derived. Then, the MGF of the upper-bound SINR is obtained. According to the latter, the error and outage probabilities are assessed in closed form. Further, simple and general asymptotic expressions for the error and outage probabilities, which explicitly show the coding and the diversity gains, are derived and discussed. The analysis is validated by comparing the corresponding numerical results with Monte Carlo simulations, sustained by insightful discussions.

Chapter 5 investigates the performance and optimization of a relaying system benefiting from SSD. The SSD technique involves constellation rotation and interleaving over the components of the signal points. For the decoding output of the received signal at the relay, two cases are possible, successful or unsuccessful. Performance metrics, i.e., error probability, asymptotic error probability, outage probability and Ergodic capacity are obtained for independent non-identical and identical channels. Furthermore, a two-phase optimization procedure is presented. In the first phase, the optimum rotation angle is obtained. In the second phase, the optimum source and relay energies are obtained subject to constraint on the total energy budget in order to minimize the error probability. Applying the two-phase optimization, the performance of the system increases considerably. Moreover, to preserve the total energy, another optimization procedure is presented. Aiming at minimizing the total energy expenditure, the optimum source and relay energies are obtained subject to the error probability constraint. The validity of the proposed framework is authenticated by numerical results and Monte Carlo simulations.

In Chapter 6, the performance of reactive DF multi-branch relaying networks operating in the presence of CCI and Nakagami fading is analytically investigated. Intermediate relays available to assist the communication between the source node and its far-end destination are chosen from a decoding set, consisting of the relays that successfully decode the source message in a reactive way, such that the relay whose corresponding branch results in the highest SINR at the destination is chosen. For this scheme, the exact end-to-end SINR expression is first obtained by considering the general case of Nakagami-m fading. Then, the exact unconditional PDF of the end-to-end SINR is explicitly derived. With the resulting PDF, exact closed-form expressions for the outage and error probabilities are obtained. Moreover, in order to gain insights into the system performance, asymptotic analysis of the error probability is performed. Finally, simulation results are presented to corroborate the analysis and comparative numerical results are discussed.

Following the above-mentioned chapters, a conclusion of the thesis with a summary of future research possibilities in the context of this work are provided in Chapter 7.

1.4.2 Publications

[1] A. H. Forghani, S. S. Ikki, and S. Aïssa, "Novel approach for approximating the performance of multi-hop multi-branch relaying over Rayleigh fading channels," in *Proc. Wireless Days Conf. (WD'11)*, Niagara Falls, Ontario, Canada, Oct. 2011.

[2] A. H. Forghani, S. S. Ikki, and S. Aïssa, "Performance evaluation of multi-hop multi-branch relaying networks with multiple co-channel interferers," in *Proc. IEEE International Conf. Commun. (ICC'12)*, Ottawa, Ontario, Canada, June 2012.

[3] A. H. Forghani, S. S. Ikki, and S. Aïssa, "On the performance and power optimization of multi-hop multi-branch relaying networks with co-channel interferers," *IEEE Trans. Veh. Technol.*, vol. 62, no. 7, pp. 3437–3443, Sep. 2013.

[4] A. H. Forghani, S. S. Ikki, and S. Aïssa, "Performance of non-symmetric relaying networks in the presence of interferers with unequal powers," *IEEE Wireless Commun.*

Lett., vol. 2, no. 1, pp. 106–109, Feb. 2013.

In addition, the following papers are currently under review.

[5] A. H. Forghani and S. Aïssa, “Relaying with signal space diversity: performance analysis and optimization,” Submitted to *IEEE Trans. Veh. Tech.*, Sep. 2014.

[6] A. H. Forghani, M. Xia, and S. Aïssa, “Analysis of reactive multi-branch relaying under interference and Nakagami-m fading,” Submitted to *IEEE Trans. Veh. Tech.*, July 2014.

Chapter 2

Multi-Hop Multi-Branch Relaying [1]

2.1 Introduction

In this Chapter, a closed-form approximate expression for the average bit error probability (ABEP) of MHMB cooperative networks is derived. The cooperative relaying scheme includes M separate branches between the source node and the destination node, and each branch comprises a certain number of relays. Furthermore, independent and non-identical Rayleigh fading links are considered between successive nodes in each branch.

The transmission protocol used is AF. In AF relaying, the relay simply amplifies the received signal and forwards the amplified version to the next node. AF has the advantage of less complexity and easier implementation. In order to conduct the performance analysis, we use the MGF approach instead of PDF method. The MGF-based approach for performance analysis allows us to apply a simple single-integral relation between the MGF of a random variable and the MGF of its inverse [38]. The simple single-integral relation is obtained by making use of some features of the Laplace transform. Just with the usage of the MGF-based method one can estimate symbol error probability (SEP), ABEP and etc.

The remaining of this Chapter is organized as follows. In section II, we introduce the

[1] Part of the material in this chapter is extracted from:
[37] A. H. Forghani, S. S. Ikki, and S. Aïssa, "Novel approach for approximating the performance of multi-hop multi-branch relaying over Rayleigh fading channels," in *Proc. Wireless Days Conference (WD'11)*, Niagara Falls, Ontario, Canada, Oct. 2011.

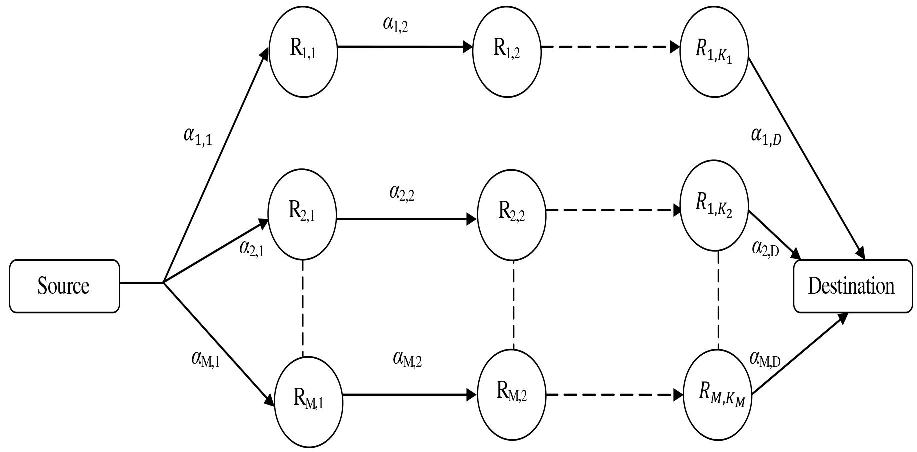

Figure 2.1: Multi-hop multi-branch relaying network.

system and the channel models. In section III, an upper limit expression for the MGF of the inverse SNR is presented. Finding the ABEP by using the MGF pertaining to the overall multi-hop multi-branch cooperative network is presented in section IV. Section V presents some numerical and simulation results to show the accuracy of the proposed performance analysis. Finally in the last section, a conclusion summarizing the contributions of this work is provided.

2.2 System and Channel Models

Consider a multi-hop multi-branch cooperative network with M branches in total and with each branch consisting of a certain number of hops as illustrated in Fig. 2.1. We assume that the number of antennas at the source, the destination and each relay is equal to one. We consider that branch m has K_m hops. The parameter $L = \sum_{m=1}^{M} K_m$ represents the total number of hops between the source node (S) and the destination node (D) in the network. The combining technique at the receiver is MRC. At the $i-th$ relay in branch m $(R_{m,i})$, the signal received at relay $R_{m,i}$ ($m = 1, \ldots, M$ and $i = 2, \ldots, N$) can be expressed as

$$y_{m,i} = \sqrt{E_s}\alpha_{m,i}x_{m,i-1} + n_{m,i}, \tag{2.1}$$

where $\alpha_{m,i}$ represents the channel coefficient related to the $i-th$ hop, $x_{m,i-1}$ is the unit-energy real-valued binary frequency shift keying (BFSK) or complex-valued multiple quadrature amplitude modulation (M-QAM) signal transmitted from the previous node, $n_{m,i}$ is the AWGN at node m,i. The noise component in the above formula is assumed to be independent from the signals and with variance $N_{m,i}$. Also, $x_{m,0}$ represents the unit-energy signal transmitted from the source node.[2] E_s denotes the energy of the transmit signal from the source node and all the other relays. Moreover, we assume that in each time slot only one node transmits in each branch. Further, the entire transmission time is assigned equally among the transmit nodes along the multi-hop links. By assuming CSI-assisted relaying and applying MRC at the destination, the end-to-end (e2e) SNR at the destination (γ_{e2e}) is obtained as [11]:

$$\gamma_{e2e} = \sum_{m=1}^{M} \widetilde{\gamma_m} = \sum_{m=1}^{M} \left[\sum_{i=1}^{K_m} \frac{1}{\widetilde{\gamma_{m,i}}} \right]^{-1}, \tag{2.2}$$

where $\widetilde{\gamma_{m,i}}$ represents the SNR at the relay $R_{m,i}$, which is equal to $\widetilde{\gamma_{m,i}} = \overline{|\alpha_{m,i}|^2} \frac{E_S}{N_{m,i}}$ and $\widetilde{\gamma_m}$ represent the SNR at the destination due to the m^{th} branch. Equation (2.2) is obtained when an ideal relay is able to inverse the channel of the previous hop. It is stated in [11] that γ_{e2e} represents a tight upper bound for the end-to-end SNR.

2.3 Approximate Expression for the MGF

The combining method at the destination is MRC, which means that the SNRs of all branches are added together to obtain the final SNR. In this case, by considering the independence of the fading among branches, the MGF of γ_{e2e} would be the product of the MGFs, $M_{\widetilde{\gamma_m}}(.)$, of the branches' SNRs, i.e., $M_{\gamma_{e2e}}(s) = \prod_{m=1}^{M} M_{\widetilde{\gamma_m}}(s)$ [39, 40]. Also, based on (2.2), the SNR of each branch is obtained by the inverse of the sum of the inverse SNR per hop. Hence, based on the independence of the fading among hops of any branch, the MGF for the inverse of SNR on a branch, $M_{1/\widetilde{\gamma_m}}(.)$ with m denoting the branch number

[2] Note that $x_{1,0} = x_{2,0} = \cdots = x_{M,0}$ since $x_{m,0}$ originates from the source node.

$(m = 1, 2, \ldots, M)$, can be calculated by the product of the MGFs, $M_{1/\widetilde{\gamma_{m,i}}}(.)$ [40], i.e.,

$$M_{1/\widetilde{\gamma_m}}(s) = \prod_{i=1}^{K_m} M_{1/\widetilde{\gamma_{m,i}}}(s). \tag{2.3}$$

We already know from [39] that the PDF of the SNR for Rayleigh fading channel has an exponential distribution. It can be expressed as $f(t) = a_{m,i}e^{-a_{m,i}t}$, with $a_{m,i}$ being the inverse of average SNR for the i^{th} hop in the m^{th} branch, i.e., $a_{m,i} = 1\Big/\left(\overline{|\alpha_{m,i}|^2 \frac{E_S}{N_{m,i}}}\right) = 1\Big/\overline{\widetilde{\gamma_{m,i}}}$. For this hop, the MGF of the SNR is given by

$$M_{\widetilde{\gamma_{m,i}}}(s) = \int_0^\infty e^{-sx} a_{m,i} e^{-a_{m,i}x} dx = \frac{a_{m,i}}{s + a_{m,i}}. \tag{2.4}$$

The MGF of the inverse SNR for this hop in the m^{th} branch is obtained by the following integral relation [41]:

$$M_{1/\widetilde{\gamma_{m,i}}}(s) = \int_0^\infty e^{-sx} x^{-2} f(x^{-1}) dx. \tag{2.5}$$

Considering Rayleigh fading, we have

$$M_{1/\widetilde{\gamma_{m,i}}}(s) = \int_0^\infty a_{m.i} e^{-\left(sx + \frac{a_{m,i}}{x}\right)} x^{-2} dx. \tag{2.6}$$

In order to obtain the MGF of the SNR for the m^{th} branch $M_{\widetilde{\gamma_m}}(s)$, we use the MGF inversion relation provided in [39] and after some mathematical manipulations, the final result will be

$$M_{\widetilde{\gamma_m}}(s) = 1 - 2\sqrt{s} \int_0^\infty J_1(2\beta\sqrt{s}) M_{1\big/\widetilde{\gamma_m}} \left(\beta^2\right) d\beta, \tag{2.7}$$

where $J_1(\cdot)$ represents the first-order Bessel function of the first kind and $M_{1/\widetilde{\gamma_m}}(s) = \prod_{i=1}^{K_m} M_{1/\widetilde{\gamma_{m,i}}}(s)$ [40]. By substituting (2.3) and (2.5) into (2.7), this MGF can be expressed as:

$$M_{\widetilde{\gamma_m}}(s) = 1 - 2\sqrt{s} \int_0^\infty J_1(2\beta\sqrt{s}) \prod_{i=1}^{K_m} \int_0^\infty e^{-\beta^2 x} x^{-2} f(x^{-1}) dx d\beta. \tag{2.8}$$

To the best of our knowledge there is no closed-form solution for the integral relation in (2.8). Considering an upper limit for the MGF of the SNR at the m^{th} branch, $M'_{\widetilde{\gamma_m}}(.)$, closed-form mathematical expressions can be obtained as upper bounds for the error rates. Several steps are needed to reach this upper limit for the error rates. At the first, we suppose an upper bound for $M'_{\widetilde{\gamma_m}}(s)$ as $M'_{1/\widetilde{\gamma_m}}(\beta^2)$. For this task we return to (2.6) again and rewrite it for $s = \beta^2$:

$$M_{1/\widetilde{\gamma_{m,i}}}(\beta^2) = \int_0^{\frac{\sqrt{1+a_{m,i}\beta^2}-1}{\beta^2}} a_{m.i} e^{-\left(\beta^2 x + \frac{a_{m,i}}{x}\right)} x^{-2} dx + \int_{\frac{\sqrt{1+a_{m,i}\beta^2}-1}{\beta^2}}^{\infty} a_{m.i} e^{-\left(\beta^2 x + \frac{a_{m,i}}{x}\right)} x^{-2} dx. \tag{2.9}$$

We claim that $x = \frac{\sqrt{1+a_{m,i}\beta^2}-1}{\beta^2}$ is the value at which $f(x) = a_{m,i} e^{-(\beta^2 x + a_{m,i}/x)} x^{-2}$ takes its maximum, which can be obtained by setting the derivative of $f(x)$ with respect to x equal to zero. For the first integral in the addition part of (2.9), we can express the inequality

$$\int_0^{\frac{\sqrt{1+a_{m,i}\beta^2}-1}{\beta^2}} a_{m.i} e^{-(\beta^2 x + a_{m,i}/x)} x^{-2} dx \leq \frac{a_{m,i}\beta^2}{\sqrt{1+a_{m,i}\beta^2}-1} e^{-\left(\sqrt{1+a_{m,i}\beta^2}-1+\frac{a_{m,i}\beta^2}{\sqrt{1+a_{m,i}\beta^2}-1}\right)}, \tag{2.10}$$

which is the multiplication of variable x whole interval by the point where $f(x)$ takes its maximum, i.e., $f(\frac{\sqrt{1+a_{m,i}\beta^2}-1}{\beta^2})$. For the second integral in the addition part of (2.9), first we make the change of variable x to $1/t$. Accordingly, we have

$$\int_{\frac{\sqrt{1+a_{m,i}\beta^2}-1}{\beta^2}}^{\infty} a_{m.i} e^{-(\beta^2 x + a_{m,i}/x)} x^{-2} dx \overset{x=1/t}{=} \int_0^{\frac{\beta^2}{\sqrt{1+a_{m,i}\beta^2}-1}} a_{m,i} e^{-(\beta^2/t + a_{m,i}t)} dt. \tag{2.11}$$

Considering (2.11), then we can express another inequality such that

$$\int_0^{\frac{\beta^2}{\sqrt{1+a_{m,i}\beta^2}-1}} a_{m.i} e^{-(\beta^2/t + a_{m,i}t)} dt \leq \frac{a_{m,i}\beta^2}{\sqrt{1+a_{m,i}\beta^2}-1} e^{-\left(2\beta\sqrt{a_{m,i}}\right)} \tag{2.12}$$

Based on the obtained results, an upper limit for $M_{1/\widetilde{\gamma_{m,i}}}(\beta^2)$ in (2.9) is obtained as follows

$$M_{1/\widetilde{\gamma_{m,i}}}(\beta^2) \leq \frac{a_{m,i}\beta^2}{\sqrt{1+a_{m,i}\beta^2}-1} e^{-\left(\sqrt{1+a_{m,i}\beta^2}-1+\frac{a_{m,i}\beta^2}{\sqrt{1+a_{m,i}\beta^2}-1}+2\beta\sqrt{a_{m,i}}\right)}. \tag{2.13}$$

As shown in (2.13) $M'_{1/\widetilde{\gamma_m}}(\beta^2) = \frac{a_{m,i}\beta^2}{\sqrt{1+a_{m,i}\beta^2}-1} e^{-\left(\sqrt{1+a_{m,i}\beta^2}-1+\frac{a_{m,i}\beta^2}{\sqrt{1+a_{m,i}\beta^2}-1}+2\beta\sqrt{a_{m,i}}\right)}$. Using (2.7), $M_{\widetilde{\gamma_m}}(s)$ for the m^{th} branch of the multi-hop multi-branch cooperative network under study can be approximated by $M'_{\widetilde{\gamma_m}}(s)$ as follows:

$$M'_{\widetilde{\gamma_m}}(s) = 1-2\sqrt{s}\int_0^\infty J_1(2\beta\sqrt{s})2^{K_m}\left(\frac{\sqrt{1+a_{m,i}\beta^2}}{\beta^2}\right)^{K_m} e^{-\left(\sqrt{1+a_{m,i}\beta^2}-1+\frac{a_{m,i}\beta^2}{\sqrt{1+a_{m,i}\beta^2}-1}+2\beta\sqrt{a_{m,i}}\right)} d\beta. \tag{2.14}$$

With the help of [42, Eq. 6.621.1] and doing the appropriate substitution, $M'_{\widetilde{\gamma_m}}(s)$ can be expressed in closed-form as

$$\begin{aligned} M'_{\widetilde{\gamma_m}}(s) &= 1 - 2\sqrt{s} \times 2^{K_m} \\ &\times \frac{(\sqrt{s}/2A_m)\Gamma(2+K_m)}{(2A_m)^{K_m\Gamma(2)+1}} F_1\left(\frac{2+K_m}{2}, \frac{3+K_m}{2}; 2; -\frac{s}{A_m^2}\right), \end{aligned} \tag{2.15}$$

where $A_m = \sum_{i=1}^{K_m}\left(\sqrt{1+a_{m,i}\beta^2}-1+\frac{a_{m,i}\beta^2}{\sqrt{1+a_{m,i}\beta^2}-1}+2\beta\sqrt{a_{m,i}}\right)$, $\Gamma(.)$ and $F_1(.)$ represent the Gamma and the first hypergeometric multivariate functions, respectively. By considering the independence of the fading gains in every branch, the MGF of γ_{e2e} can be considered as the product of the MGFs, $M_{\widetilde{\gamma_m}}(.)$, of each branch's SNRs [40]. For simplicity $M_{\gamma_{e2e}}(s)$ could be approximated by the product of $M'_{\widetilde{\gamma_m}}(s)$ shown in (2.15) from all the branches, as given by:

$$M_{\gamma_{e2e}}(s) \cong \prod_{m=1}^{M} 1 - 2\sqrt{s} \times 2^{K_m} \times \frac{(\sqrt{s}/2A_m)\Gamma(2+K_m)}{(2A_m)^{K_m\Gamma(2)+1}} F_1\left(\frac{2+K_m}{2}, \frac{3+K_m}{2}; 2; -\frac{s}{A_m^2}\right). \tag{2.16}$$

2.4 Average Error Probability

Based on the above derived MGF, it is possible to analyze the overall performance of the cooperative network. We can find the ABEP for different modulation schemes such as M-ary quadrature amplitude modulation (M-QAM) [39, Eq. 5.73]. The approximate ABEP expression for BFSK modulation is obtained by [43, Eq. 14] as:

$$ABEP_{BFSK} \cong \frac{1}{12} M_{\gamma_{e2e}}\left(\frac{1}{2}\right) + \frac{1}{4} M_{\gamma_{e2e}}\left(\frac{4}{6}\right), \tag{2.17}$$

where $M_{\gamma_{e2e}}(s)$ is given by (16).

2.5 Numerical Examples

In this section, to illustrate the accuracy of the analysis, some numerical results for the ABEP are shown. The impact of changing some parameters such as the number of hops and branches in the cooperative network are investigated, assuming transmission over Rayleigh fading channels. Results are plotted as a function of E_T/N_0 where $E_T = E_S\left(1 + \sum_{m=1}^{M}(K_m - 1)\right)$ denotes the overall energy. The applied modulation scheme is BFSK. Fig. 2.2 depicts the results for ABEP versus SNR for one branch while the number of hops varies from four to five. Simulations and the results of our proposed method are shown. It is illustrated that by adding a new hop, a new term will be added to the average error probability.

In Fig. 2.3, we compare analytical results with the simulation results in a two-branch un-balanced network. The values of SNR for the second branch are considered twice the values of the SNR for the first branch. By adding branches, the error probability will decrease because of gaining diversity.

2.6 Summary

In this Chapter, we considered a MHMB relaying network which takes advantage of the AF transmission protocol. We assumed that the method for combining signals at the receiver is MRC and considered Rayleigh fading channels for the different hops in all branches. The fading channels were assumed to be independent of each other but not necessarily identical. The Chapter has developed closed-form approximations for the MGF to evaluate the performance of the system. The approximation approach can be applied to analyze

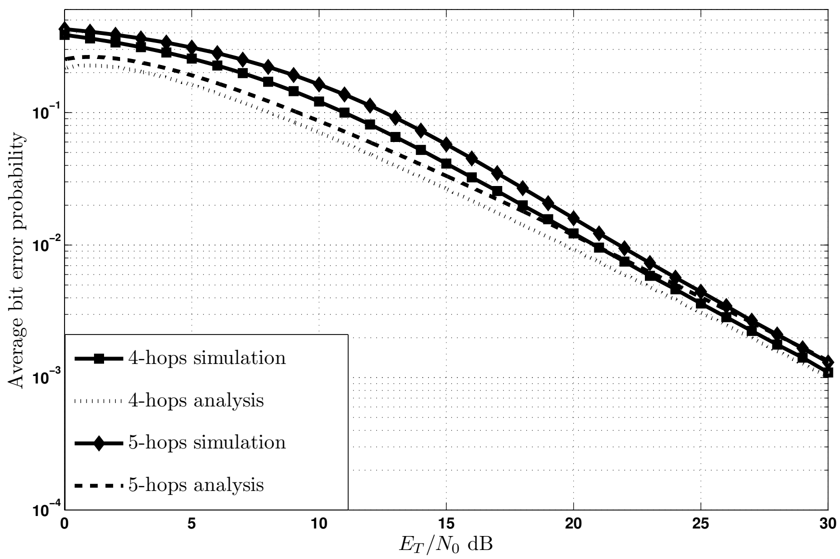

Figure 2.2: Performance of four and five-hop cooperative network assuming one branch and Rayleigh fading channel in each hop.

the performance for a variety of cooperative systems. In order to validate the analysis, numerical and simulation results were provided. In the next Chapter, we investigate the performance of opportunistic MHMB relaying networks operating in the presence of co-channel interferences.

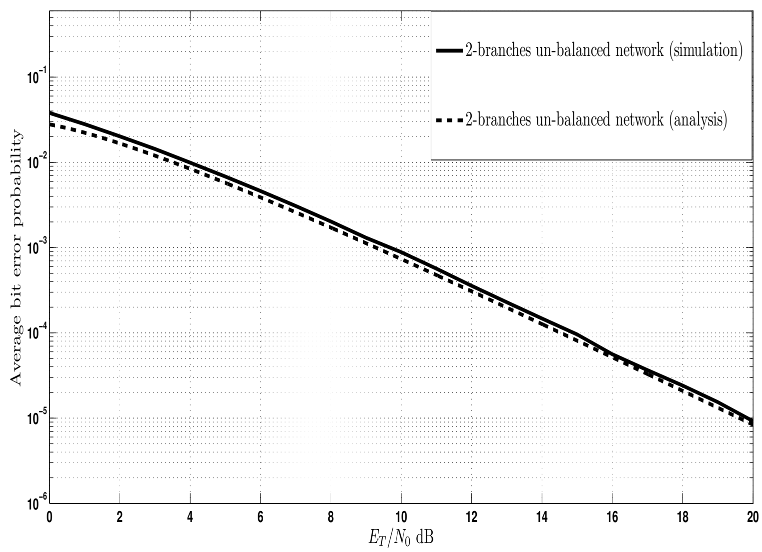

Figure 2.3: Performance of two-branch un-balanced network assuming dual-hop and Rayleigh fading in each hop.

Chapter 3

Multi-Hop Multi-Branch Relaying in the Presence of Equal-Power Interferers [1]

3.1 Introduction

In this Chapter, the performance of opportunistic AF MHMB relaying networks operating in the presence of CCI is studied, whereby the source and the destination are assumed not in direct line-of-sight. Because multiple relays are involved in the transmission of the signal from its source to its end destination in the cooperative network, interference is considered at all the relays and the investigation is conducted in terms of major performance metrics, namely the outage and error probabilities.

The technique of combining the signals at the receiver is selection combining, hence the branch with the highest SINR value is selected at the destination node. Exact and upper-bound expressions for the end-to-end SINR are obtained, assuming transmissions over independent non-identical Rayleigh fading channels for either the desirable or the interference

[1] Part of the material in this chapter is extracted from:
[44] A. H. Forghani, S. S. Ikki, and S. Aïssa, "Performance evaluation of multi-hop multi-branch relaying networks with multiple co-channel interferers," in *Proc. IEEE International Conf. Commun. (ICC'12)*, Ottawa, Ontario, Canada, 2012.
[45] A. H. Forghani, S. S. Ikki, and S. Aïssa, "On the performance and power optimization of multi-hop multi-branch relaying networks with co-channel interferers," *IEEE Trans. Veh. Tech.*, vol. 62, no. 7, pp. 3437–3443, Sep. 2013.

signals. Afterwards, the CDF and the PDF of the upper-bound end-to-end SINR are investigated. According to CDF and PDF of the upper-bound end-to-end SINR, a lower-bound closed-form expression for the outage probability is obtained. Furthermore, approximation function for the PDF of the end-to-end SINR is derived. Subsequently, simple expressions for the approximate error and outage probabilities are provided. These expressions deliver more understanding on the effect of the system parameters. Also, to remedy the adverse effect of the channel fluctuations and therefore enhance the performance of the system, we introduce a power optimization procedure. As an optimal solution for the resource allocation problem at hand, adaptive power allocation is used to minimize the error probability under constraint on the aggregate power over the branch with the maximum SINR. By implementing adaptive power allocation among the source and all the relays, the transmission reliability will be increased. The accuracy of the analysis is validated by comparing the numerical results with Monte Carlo simulations, and insightful discussions are provided.

In detail, section II introduces the network model along with definitions needed for the study, followed by the derivation of an exact expression for the end-to-end SINR. Then in section III, the statistics of the end-to-end SINR are investigated and the performance analysis is conducted. The optimization process is then addressed in section IV. Section V presents numerical and simulation results along with discussions to attest the accuracy of the proposed framework. Finally, the last section summarizes the Chapter's findings.

3.2 Network Model

Consider the MHMB relaying network illustrated in Fig. 3.1, wherein the source communicates with the destination via M different branches. Each branch m, $m = 1, \ldots, M$, consists of N half-duplex relays. Within each branch, the transmission from the source node to the final destination is carried out by the corresponding relays $(R_{m,1}, \cdots, R_{m,n}, \cdots, R_{m,N})$ taking part in the signal transmission. Note that when $n = 1$ for any m, node $R_{m,(n-1)}$ represents the source node. At the destination, the detection and the combination of the M signals are performed in a way that a highly reliable copy of the transmitted packet is generated [46]. In this Chapter, the combining method is assumed selection based, wherein

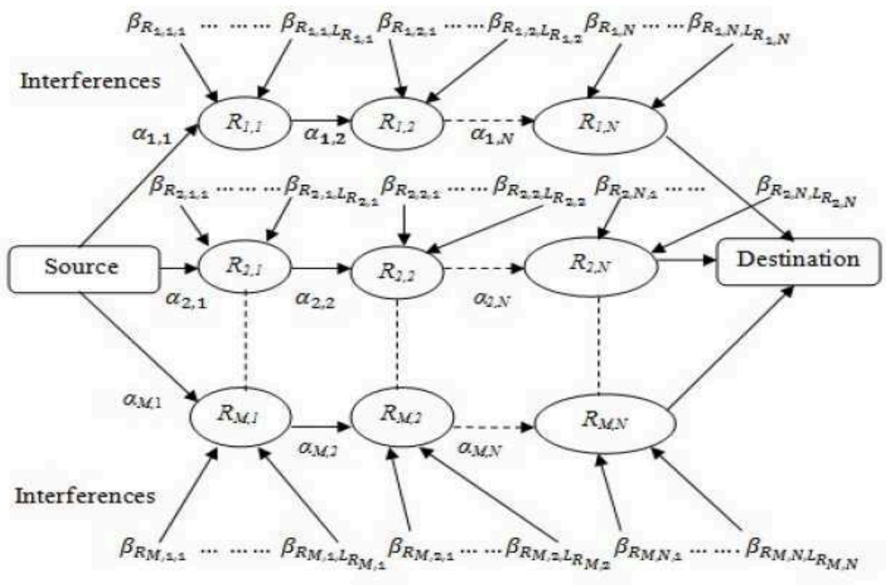

Figure 3.1: Multi-hop multi-branch relaying network with co-channel interference.

the destination selects the branch with the highest SINR among the M branches. The CSI is considered to be only available at the receiving nodes. Also, we assume that in each time slot only one node transmits in each branch. Further, the entire transmission time is assigned equally among the transmit nodes along the multi-hop links.

Considering the n^{th} time slot, the signal received at the $(m,n)^{th}$ relay in the m^{th} branch, $R_{m,n}$, is a combination of a faded noisy signal received from the preceding transmit node, $R_{m,(n-1)}$, and faded CCI signals originating from $L_{R_{m,n}}$ external interfering sources. Then, during the following time slot, the said relay transmits the processed signal to the subsequent node along the same branch, i.e., $R_{m,(n+1)}$. Hence, the signal received by node $R_{m,n}$ over the relay indices $m = 1, \ldots, M$ and $n = 2, \ldots, N$ can be expressed as

$$y_{m,n} = \sqrt{E_{m,(n-1)}}\alpha_{m,n}x_{m,(n-1)} + \sqrt{E_{I_{m,n}}}\sum_{j=1}^{L_{R_{m,n}}} \beta_{R_{m,n,j}} d_{R_{m,n,j}} + w_{m,n}, \tag{3.1}$$

where the fading coefficient of the channel between nodes $R_{m,(n-1)}$ and $R_{m,n}$ is denoted $\alpha_{m,n}$, as shown in Fig. 3.1. With respect to the m^{th} branch, $x_{m,(n-1)}$ represents the unit-energy transmit signal from the previous relay. For the first hop $(n = 1)$ in any branch where $x_{m,0}$ indicates the transmit signal from the source node,[2] $E_{m,(n-1)}$ indicates the energy of the signal transmitted from the $(n-1)^{th}$ node in the m^{th} branch. Further, in the first equation of (3.1), the signal from the j^{th} interferer affecting the $(m,n)^{th}$ relay is represented by $d_{R_{m,n,j}}$ and assumed of unit energy, $L_{R_{m,n}}$ indicates the number of signals which interfere with this relay, with the energy of the interference signal symbolized by $E_{I_{m,n}}$, and the Rayleigh fading coefficient of the j^{th} CCI channel impacting the n^{th} relay in the m^{th} branch is indicated by $\beta_{R_{m,n,j}}$. The final term in the first equation of (3.1), i.e., $w_{m,n}$, denotes the AWGN with variance N_0 and mean zero.

The variable-gain coefficient is defined as $c_{m,n} = \left(\sqrt{E_{m,(n-1)} \left|\alpha_{m,n}\right|^2 + E_{I_{m,n}} \sum_{j=1}^{L_{R_{m,n}}} \left|\beta_{R_{m,n,j}}\right|^2 + N_0}\right)^{-1}$, with $c_{m,0} = 1$ for $m = 1, \ldots, M$, assuming that the CSI of the interferers is available at the relays. [3] Thus, the amplification process at the $(m,n)^{th}$ relay node includes the generation of the signal $x_{m,n} = c_{m,n} y_{m,n}$ and transmitting it to the next relay node.

For the m^{th} branch, the $N+1$ output signals, $y_{m,N},\ y_{m,(N-1)}, \ldots, y_{m,0} = x_{m,0}$, can be expressed by the $N+1$ equations obtained according to (3.1), where for a specific n, $y_{m,n}$ is a function of $x_{m,(n-1)}$. Using these equations, the expression for $y_{m,N}$ can be obtained as a function of $x_{m,0}$ (the source signal) and other network parameters through a recursive process. The obtained expression for $y_{m,N}$ can be split into three different parts: the signal part, the noise part and the interference part, similar to [47, Eqs. 4-6]. The term that comprises $x_{m,0}$ represents the signal part, the $w_{m,n}$ term denotes the noise part, and the term that includes $E_{I_{m,n}}$ indicates the interference part. Using these terms of $y_{m,N}$, we define the end-to-end SINR of the m^{th} branch, γ_{end}^m, as the ratio of the signal part power to the summation of the noise power and the interference power. Thus, similar to [47, Eqs. 7-8], γ_{end}^m can be obtained as:[4]

$$\gamma_{\text{end}}^m = \left[\prod_{n=1}^{N} \left(1 + \frac{1 + \sum_{j=1}^{L_{R_{m,n}}} \gamma_{I_{m,n,j}}}{\gamma_{m,n}}\right) - 1\right]^{-1}, \tag{3.2}$$

[2] Note that $x_{1,0} = x_{2,0} = \cdots = x_{M,0}$ since $x_{m,0}$ originates from the source node.

[3] Other types of gains may also be used at the relays, but would not achieve the optimum performance as they are not optimal gains.

[4] The expression for $y_{m,N}$ with its corresponding signal, noise and interference terms is not detailed here, but can straightforwardly be expanded based on the derivations in [47].

where $\gamma_{m,n} = |\alpha_{m,n}|^2 E_{m,(n-1)}/N_0$ indicates the useful SNR at the n^{th} relay of the m^{th} branch, and $\gamma_{I_{m,n,j}} = \left(E_{I_{m,n}}/N_0\right)\left|\beta_{R_{m,n,j}}\right|^2$ is the interference-to-noise ratio (INR) at the same node ($R_{m,n}$) with reference to the j^{th} interferer ($j = 1, \cdots, L_{R_{m,n}}$). The SINR expressed in (3.2) is an extension of the one obtained in [48] for the special case of dual-hop network. Besides, (3.2) reduces to the SNR presented in [11] when the transmission environment is assumed free of CCI. Furthermore, in a practical relaying network, due to the presence of CCI, considerable deterioration of the SINR can occur by increased noise variance.

3.3 Statistics of the End-To-End SINR and Performance Analysis

3.3.1 Cumulative Distribution Function and Lower-Bound Outage Probability

In this section, taking as a starting point the approach in [47] and [49–51], we resort to a tight upper-bound on the end-to-end SINR to reach simple expressions for performance metrics of interest in the considered multi-hop multi-branch system. A tight upper-bound for Eq. (3.2), denoted γ_{up}^m, is expressed as $\gamma_{\text{end}}^m \leq \gamma_{\text{up}}^m = \min\left(\gamma_{m,1}^{\text{eff}}, \gamma_{m,2}^{\text{eff}}, \cdots, \gamma_{m,n}^{\text{eff}}, \cdots, \gamma_{m,N}^{\text{eff}}\right)$, where the effective SINR at the n^{th} relay in the m^{th} branch is given by $\gamma_{m,n}^{\text{eff}} = \gamma_{m,n}/(1+\sum_{j=1}^{L_{R_{m,n}}} \gamma_{I_{m,n,j}})$. Based on [47, Eq. 15], the CDF of $\gamma_{m,n}^{\text{eff}}$, denoted $F_{\gamma_{m,n}^{\text{eff}}}(\gamma)$, is obtained as

$$F_{\gamma_{m,n}^{\text{eff}}}(\gamma) = 1 - \left(\frac{\bar{\gamma}_{m,n}/\bar{\gamma}_{I_{m,n}}}{\gamma + \bar{\gamma}_{m,n}/\bar{\gamma}_{I_{m,n}}}\right)^{L_{R_{m,n}}} \exp\left(\frac{-\gamma}{\bar{\gamma}_{m,n}}\right). \tag{3.3}$$

Further, we can express the CDF of γ_{up}^m as [52]:

$$F_{\gamma_{\text{up}}^m}(\gamma) = 1 - \prod_{n=1}^{N}\left(1 - F_{\gamma_{m,n}^{\text{eff}}}(\gamma)\right) = 1 - \prod_{n=1}^{N}\left(\frac{\bar{\gamma}_{m,n}/\bar{\gamma}_{I_{m,n}}}{\gamma + \bar{\gamma}_{m,n}/\bar{\gamma}_{I_{m,n}}}\right)^{L_{R_{m,n}}} \exp\left(\frac{-\gamma}{\bar{\gamma}_{m,n}}\right). \tag{3.4}$$

$$F_{\gamma_f}(\gamma) = \prod_{m=1}^{M}\left(1 - \exp\left(-\sum_{n=1}^{N}\frac{\gamma}{\bar{\gamma}_{m,n}}\right)\prod_{n=1}^{N}\left(\frac{\bar{\gamma}_{m,n}/\bar{\gamma}_{I_{m,n}}}{\gamma + \bar{\gamma}_{m,n}/\bar{\gamma}_{I_{m,n}}}\right)^{L_{R_{m,n}}}\right). \tag{3.5}$$

$$P_{\text{out}} = \prod_{m=1}^{M}\left(1 - \exp\left(-\left(2^{N\times r}-1\right)\sum_{n=1}^{N}\frac{1}{\bar{\gamma}_{m,n}}\right)\times\prod_{n=1}^{N}\left(\frac{\bar{\gamma}_{m,n}/\bar{\gamma}_{I_{m,n}}}{(2^{N\times r}-1) + \bar{\gamma}_{m,n}/\bar{\gamma}_{I_{m,n}}}\right)^{L_{R_{m,n}}}\right). \tag{3.6}$$

As the destination node chooses the branch with the highest signal quality among the M received signals, the SINR at the destination, i.e., γ_f, can be expressed as $\gamma_f = \max\left(\gamma_{\text{up}}^1, \gamma_{\text{up}}^2, \cdots, \gamma_{\text{up}}^m, \cdots, \gamma_{\text{up}}^M\right)$, where γ_{up}^m is the SINR with respect to the m^{th} branch. Accordingly, the CDF of the end-to-end SINR can be obtained by multiplying the CDFs of the SINR for all the branches, that is given in (3.5) on the top of this page. Taking the definition of outage, P_{out}, as the probability that the mutual information, I_{AF}, is less than a certain rate, r, i.e., $P_{\text{out}} = Pr(I_{\text{AF}} < r)$, and expressing the mutual information by $I_{\text{AF}} = \frac{1}{N}\log_2(1+\gamma_f)$, where N denotes the number of hops, then the outage probability is given by $P_{\text{out}} = F_{\gamma_f}\left(2^{N\times r}-1\right)$. Consequently, by substituting $(2^{N\times r}-1)$ into (3.5), the outage probability can be obtained, as shown in (3.6) on the top of the current page.

3.3.2 Approximate Performance Analysis

Though the expression (3.5) obtained for $F_{\gamma_f}(\gamma)$ serves for numerical evaluation of the network performance, it may not be computationally acute, and does not provide insight into the impact of the main system parameters. Here, our aim is to simplify the expressions of $F_{\gamma_f}(\gamma)$ and P_{out}. Besides, by applying the approximate technique, a simple expression for the error probability becomes possible.

An approximation to $F_{\gamma_m^{\text{up}}}(\gamma)$ given in (3.4), can be found based on the behavior of $F_{\gamma_m^{\text{up}}}(\gamma)$ around the origin $(\gamma = 0)$ [53,54]. Using the Taylor series expansion of $F_{\gamma_m^{\text{up}}}(\gamma)$ at the origin for $\gamma \geq 0$, $F_{\gamma_m^{\text{up}}}(\gamma)$ can be reexpressed as $F_{\gamma_m^{\text{up}}}(\gamma) = F_{\gamma_m^{\text{up}}}(\gamma)\,|_{\gamma=0} + F'_{\gamma_m^{\text{up}}}(\gamma)\,|_{\gamma=0} \times$

$\gamma + \mathrm{O}\left(\gamma^2, \gamma^3, \ldots\right)$, where $F'_{\gamma_m^{\mathrm{up}}}\left(\gamma\right)|_{\gamma=0}$ denotes the derivative of $F_{\gamma_m^{\mathrm{up}}}\left(\gamma\right)$ with respect to γ calculated at $\gamma = 0$ and $\mathrm{O}\left(\gamma^2, \gamma^3, \ldots\right)$ represents the higher order terms. Using (3.4) gives $F_{\gamma_m^{\mathrm{up}}}\left(\gamma\right)|_{\gamma=0} = 0$. Also, by employing the same equation, i.e. (3.4), $F'_{\gamma_m^{\mathrm{up}}}\left(\gamma\right)\Big|_{\gamma=0}$ is obtained as $F'_{\gamma_m^{\mathrm{up}}}\left(\gamma\right)|_{\gamma=0} = \sum_{n=1}^{N}\left(\frac{1}{\bar{\gamma}_{m,n}}\left(1 + L_{R_{m,n}}\bar{\gamma}_{I_{m,n}}\right)\right)$. Following the above explanations and by ignoring the term $\mathrm{O}\left(\gamma^2, \gamma^3, \ldots\right)$ according to [53, 54], $F_{\gamma_m^{\mathrm{up}}}\left(\gamma\right)$ is approximated as $F_{\gamma_m^{\mathrm{up}}}\left(\gamma\right) \sim \sum_{n=1}^{N}\left(\frac{\gamma}{\bar{\gamma}_{m,n}}\left(1 + L_{R_{m,n}}\bar{\gamma}_{I_{m,n}}\right)\right)$. Consequently, knowing that the receiver employs selection combining on the signals received from the M branches, the approximate CDF of the end-to-end SINR can be obtained as the product of the terms $\sum_{n=1}^{N}\left(\frac{\gamma}{\bar{\gamma}_{m,n}}\left(1 + L_{R_{m,n}}\bar{\gamma}_{I_{m,n}}\right)\right)$ for $m = 1, \ldots, M$, that is

$$F_{\gamma_f}\left(\gamma\right) \sim \prod_{m=1}^{M}\left(\sum_{n=1}^{N}\left(\frac{\gamma}{\overline{\gamma}_{m,n}}\left(1 + L_{R_{m,n}}\overline{\gamma}_{I_{m,n}}\right)\right)\right). \tag{3.7}$$

Thus, by taking derivative with respect to γ, of the right-hand-side (RHS) of (3.7), the approximate PDF of γ_{f} is obtained as

$$f_{\gamma_f}\left(\gamma\right) \sim M\prod_{m=1}^{M}\left(\sum_{n=1}^{N}\left(\frac{1}{\overline{\gamma}_{m,n}}\left(1 + L_{R_{m,n}}\overline{\gamma}_{I_{m,n}}\right)\right)\right)\gamma^{M-1}. \tag{3.8}$$

If we substitute γ with $2^{N\times r} - 1$ in the RHS of (3.7), the approximate outage probability can immediately be obtained. Therefore, for the approximate outage probability, we may write:

$$P_{\mathrm{out}} \sim \left(2^{N\times r} - 1\right)^{M}\prod_{m=1}^{M}\left(\sum_{n=1}^{N}\left(\frac{1}{\bar{\gamma}_{m,n}}\left(1 + L_{R_{m,n}}\bar{\gamma}_{I_{m,n}}\right)\right)\right). \tag{3.9}$$

Now, we resort to the approach presented in [53] to evaluate the error probability performance. First, we recall that the error probability, $P\left(e\right)$, is given by

$$P\left(e\right) = \int_0^{\infty} a\,\mathrm{erfc}\left(\sqrt{b\gamma}\right) f_{\gamma_f}\left(\gamma\right) d\gamma, \tag{3.10}$$

where a and b represent constants which depend on the type of modulation applied (e.g., binary phase shift keying (BPSK): a = 0.5 and b = 1, quadrature phase shift keying (QPSK): a = 0.5 and b = 0.5) and $\mathrm{erfc}\left(x\right)$ is the well-known complementary error function. Subsequently, using (3.8) and (3.10), we obtain the approximate error probability as

$$P(e) \approx \frac{a\Gamma\left(M+\frac{1}{2}\right)}{b^{M}\sqrt{\pi}} \prod_{m=1}^{M} \left(\sum_{n=1}^{N} \left(\frac{1}{\overline{\gamma}_{m,n}} \left(1 + L_{R_{m,n}} \overline{\gamma}_{I_{m,n}}\right)\right)\right), \tag{3.11}$$

where $\Gamma(.)$ denotes the Gamma function. Here, an interesting point can be drawn from the above expression. Indeed, to enhance the error performance all the useful SNRs ($\bar{\gamma}_{m,n}$) should be improved otherwise, the improvement is minimal since the worst link dominates the other links. Besides, it can clearly be seen that as the numbers of CCI signals ($L_{R_{m,n}}$) increase, the error probability increases.

3.4 Performance Optimization

An optimal power allocation between the source and the relays is an important factor to remedy the impact of the CCIs and the channel fluctuations. In the previous sections, it was assumed that the fading coefficients were available to the destination and the relays, while the source does not have any knowledge about the CSI. These settings are useful in applications where feedback of the channel's estimation is not available. Nevertheless, in scenarios such as fixed wireless networks, feedback is possible and therefore we can employ CSI at the source node to enhance performance. Also, in the previous sections, we treated the energy of the nodes as some deterministic parameters.

In this section, we investigate an approach to improve the performance of the system by considering the energy of the nodes as non-deterministic parameters. Moreover, it is assumed that the knowledge of the mean channel gains is available at the source node, which can be achieved by a low-rate feedback for network topologies with slow variations. We assume that the received power is attenuated by the inverse of the distance between two consecutive terminals to the power of the path-loss exponent, $\eta \in [2, 4]$. In each branch, a distance D_m between the source and the destination via N transmitting hops is considered. Furthermore, the n^{th} hop distance between two successive terminals at the m^{th} branch, $R_{m,(n-1)}$ and $R_{m,n}$, is indicated by $d_{m,n}$, where $d_{m,1}+d_{m,2}+\cdots+d_{m,N} = D_m$. The channels are assumed vertically identical but not necessarily identical in horizontal dimension. This

$$\text{minimize} \qquad P(e) = \frac{a\Gamma\left(M+\frac{1}{2}\right)}{b^M\sqrt{\pi}} \times \left(\sum_{n=1}^{N}\left(\frac{N_0}{E_{K,(n-1)}}d_{K,n}^{\eta}\left(1+L_{R_{K,n}}\bar{\gamma}_{I_{K,n}}\right)\right)\right)^M$$

$$\text{subject to :} \qquad E_S + \sum_{n=2}^{N} E_{K,(n-1)} = C, \quad E_S > 0 \quad \text{and} \quad E_{K,(n-1)} > 0,\ n = 2, \cdots, N, \tag{3.12}$$

assumption in a practical network can be actuated by the grouping of relays in clusters while the clusters are not positioned at equal distances, i.e. mathematically, $\bar{\gamma}_{m,n} = \bar{\gamma}_{K,n}$, $\bar{\gamma}_{I_{m,n}} = \bar{\gamma}_{I_{K,n}}$, $d_{m,n} = d_{K,n}$ and $L_{R_{m,n}} = L_{R_{K,n}}$, for $m = 1, 2, \cdots, M$ and $n = 1, 2, \cdots, N$, where K represents the index of the branch with maximum SINR. Therefore, the average error probability obtained in (3.11), reduces to $P(e) = \frac{a\Gamma\left(M+\frac{1}{2}\right)}{b^M\sqrt{\pi}}\left(\sum_{n=1}^{N}\left(\frac{1}{\bar{\gamma}_{K,n}}\left(1+L_{R_{K,n}}\bar{\gamma}_{I_{K,n}}\right)\right)\right)^M$. One of the important parameters involved in the optimization process is the average square of fading coefficient for the channel between nodes $R_{m,(n-1)}$ and $R_{m,n}$, given by $\mathbf{E}\left(\alpha_{m,n}^2\right) = 1/d_{m,n}^{\eta}$, for $m = 1, 2, \cdots, M$ and $n = 1, 2, \cdots, N$. Hence, the average value of the $(m,n)^{th}$ SNR can be expressed as $\bar{\gamma}_{m,n} = \frac{E_{m,(n-1)}}{N_0}d_{m,n}^{-\eta}$.

Now, we derive the optimal power allocation at the source node and the relays in order to minimize the system error probability. The allocation of the energy among the nodes is carried out subject to an aggregate energy limitation. The latter can be interpreted as a sum-power constraint, which is defined over the branch with maximum SINR. Accordingly, using (3.11) and employing the steps mentioned above, the optimization problem aiming at minimizing the error probability can be formulated as shown in (3.12) on the top of the current page, where K is the index of the branch with maximum SINR, C is the unknown constant which will be determined later and $E_S = E_{K,0}$ is the energy of the source node. Thus, the Lagrange cost function can be expressed as

$$\Upsilon = \frac{a\Gamma\left(M+\frac{1}{2}\right)}{b^M\sqrt{\pi}}\left(\sum_{n=1}^{N}\left(\frac{N_0}{E_{K,(n-1)}}d_{K,n}^{\eta}\left(1+L_{R_{K,n}}\bar{\gamma}_{I_{K,n}}\right)\right)\right)^M$$

$$+\ \phi\left(E_S + \sum_{n=2}^{N} E_{K,(n-1)} - C\right), \tag{3.13}$$

where ϕ represents the Lagrange parameter. Then, determining the derivatives of Υ with

$$\frac{\partial \Upsilon}{\partial E_S} = -M \frac{a\Gamma\left(M+\frac{1}{2}\right)}{b^M\sqrt{\pi}} \frac{N_0}{E_S^2} d_{K,1}^{\eta}\left(1+L_{R_{K,1}}\bar{\gamma}_{I_{K,1}}\right)$$
$$\left(\sum_{n=1}^{N}\left(\frac{N_0}{E_{K,(n-1)}} d_{K,n}^{\eta}\left(1+L_{R_{K,n}}\bar{\gamma}_{I_{K,n}}\right)\right)\right)^{M-1} + \phi = 0. \tag{3.14}$$

$$\frac{\partial \Upsilon}{\partial E_{K,(n-1)}} = -M \frac{a\Gamma\left(M+\frac{1}{2}\right)}{b^M\sqrt{\pi}} \frac{N_0}{E_{K,(n-1)}^2}\left(1+L_{R_{K,n}}\bar{\gamma}_{I_{K,n}}\right) \times d_{K,n}^{\eta}$$
$$\left(\sum_{n=1}^{N}\left(\frac{N_0}{E_{K,(n-1)}} d_{K,n}^{\eta}\left(1+L_{R_{K,n}}\bar{\gamma}_{I_{K,n}}\right)\right)\right)^{M-1} + \phi = 0. \tag{3.15}$$

---

respect to E_S and $E_{K,(n-1)}$ ($n = 2, \cdots, N$), and setting them to zero, we obtain (3.14) and (3.15). Also, taking the derivative of Υ with respect to ϕ, and setting it to zero, (3.16) is obtained as

$$\frac{\partial \Upsilon}{\partial \phi} = E_S + \sum_{n=2}^{N} E_{K,(n-1)} - C = 0. \tag{3.16}$$

Then, we apply some simplifications to obtain the energies of the nodes, E_S and $E_{K,(n-1)}$ for $n = 2, \cdots, N$. Specifically, we define G as

$$G = M \frac{a\Gamma\left(M+\frac{1}{2}\right)}{b^M\sqrt{\pi}} N_0 \times \left(\sum_{n=1}^{N}\left(\frac{N_0}{E_{K,(n-1)}} d_{K,n}^{\eta}\left(1+L_{R_{K,n}}\bar{\gamma}_{I_{K,n}}\right)\right)\right)^{M-1}. \tag{3.17}$$

Consequently, the energies of the nodes in terms of ϕ can be obtained as $E_S = \sqrt{\frac{G d_{K,1}^{\eta}\left(1+L_{R_{K,1}}\bar{\gamma}_{I_{K,1}}\right)}{\phi}}$ and $E_{K,(n-1)} = \sqrt{\frac{G d_{K,n}^{\eta}\left(1+L_{R_{K,n}}\bar{\gamma}_{I_{K,n}}\right)}{\phi}}$ for $n = 2, \cdots, N$. Using (3.16), by adding the energies of the nodes, ϕ can be obtained in terms of C: $\phi = \frac{G\left(\sum_{n=1}^{N}\sqrt{d_{K,n}^{\eta}\left(1+L_{R_{K,n}}\bar{\gamma}_{I_{K,n}}\right)}\right)^2}{C^2}$.

Taking into account the value obtained for ϕ, E_S and $E_{K,(n-1)}$ ($n = 2, \cdots, N$) can be rewritten as

$$E_S = C \frac{\sqrt{d_{K,1}^{\eta}\left(1 + L_{R_{K,1}} \bar{\gamma}_{I_{K,1}}\right)}}{\sum\limits_{n=1}^{N} \sqrt{d_{K,n}^{\eta}\left(1 + L_{R_{K,n}} \bar{\gamma}_{I_{K,n}}\right)}}. \tag{3.18}$$

$$E_{K,(n-1)} = C \frac{\sqrt{d_{K,n}^{\eta}\left(1 + L_{R_{K,n}} \bar{\gamma}_{I_{K,n}}\right)}}{\sum\limits_{n=1}^{N} \sqrt{d_{K,n}^{\eta}\left(1 + L_{R_{K,n}} \bar{\gamma}_{I_{K,n}}\right)}} \quad n = 2, \cdots, N. \tag{3.19}$$

The energies obtained above are expressed in terms of C, which is an unknown constant. Hence, to express the energies in a closed-form format in terms of the main system parameters, we need to determine the value of C. For such, we resort to the total energy constraint which is given by $E_S + \sum_{m=1}^{M} \sum_{n=2}^{N} E_{m,(n-1)} = E_T$, where E_T denotes the total energy budget. Therefore, assuming that $E_{m,(n-1)} = E_{K,(n-1)}$ for $m = 1, 2, \cdots, M$, the total energy constraint can be expressed as

$$E_S + M \times \sum_{n=2}^{N} E_{K,(n-1)} = E_T. \tag{3.20}$$

Replacing the energies in (3.20) with the ones presented in (3.18) and (3.19), constant C is obtained and, accordingly, we can express the energies of the nodes in terms of the total energy as

$$E_S = \frac{E_T \sqrt{d_{K,1}^{\eta}\left(1 + L_{R_{K,1}} \bar{\gamma}_{I_{K,1}}\right)}}{\sqrt{d_{K,1}^{\eta}\left(1 + L_{R_{K,1}} \bar{\gamma}_{I_{K,1}}\right)} + M \sum\limits_{n=2}^{N} \sqrt{d_{K,n}^{\eta}\left(1 + L_{R_{K,n}} \bar{\gamma}_{I_{K,n}}\right)}}. \tag{3.21}$$

$$E_{K,(n-1)} = \frac{E_T \sqrt{d_{K,n}^{\eta}\left(1 + L_{R_{K,n}} \bar{\gamma}_{I_{K,n}}\right)}}{\sqrt{d_{K,1}^{\eta}\left(1 + L_{R_{K,1}} \bar{\gamma}_{I_{K,1}}\right)} + M \sum\limits_{n=2}^{N} \sqrt{d_{K,n}^{\eta}\left(1 + L_{R_{K,n}} \bar{\gamma}_{I_{K,n}}\right)}}$$

$$n = 2, \cdots, N. \tag{3.22}$$

3.5 Numerical Examples and Discussions

In this section, we present numerical results for (*i*) the error performance when assuming that the modulation scheme is BPSK, (*ii*) the outage performance and (*iii*) the power optimization scheme. The results are provided for unbalanced (non-identical) hops. For Figs. 3.2 and 3.5, in addition to the results pertaining to the unbalanced case, results for balanced (identical) scenario are also provided. We analyze the effect of altering the principal parameters, namely, the number of branches, hops and CCI signals. We also investigate the impact of changing the average INR values, i.e., $\overline{\gamma}_{I_{m,n}}$, on performance. Here, we assume that the distance between the source and the destination nodes in each branch is normalized to one and that the path-loss exponent is $\eta = 3$. The results are illustrated as a function of E_T/N_0 where $E_T = E_S + \sum_{m=1}^{M} \sum_{n=1}^{N-1} E_{m,n}$ and E_S represents the energy of the signal transmitted from the source node.

For all the example networks, we assume that three interferers affect each relay ($L_{R_{m,n}} = 3$, but for simplicity we refer to this number by L_R). The plots pertaining to the performance in the interference-free case are also shown.

Moreover, for Figs. 3.2 to 3.4, E_T is distributed equally among all the nodes, including the source node.[5] For these figures, the analytical results are compared with Monte Carlo simulations. It is attested that our analytical results are in fair agreement with the simulation results. The analytical results for Figs. 3.2 and 3.3 are produced according to the expression for the error probability presented in (3.11). For these figures, it is assumed that each CCI signal has an average INR value, $\overline{\gamma}_{I_{m,n}}$, equal to $0.003E_T/N_0$.

Fig. 3.2 depicts the error probability for cooperative networks with $N = 3$ or 5 hops and a single branch in each. For the scenario with balanced hops, i.e., $d_{1,n} = \frac{1}{N}$ for $n = 1, \ldots, N$, it is clearly verified that the network with $N = 5$ outperforms the ones with $N = 3$, because of the shorter distances between the nodes. Also, as seen for a fixed N, networks with unbalanced hops, i.e., $d_{1,1} = 0.6,\ d_{1,2} = 0.3$ and $d_{1,3} = 0.1$ for $N = 3$ and $d_{1,1} = 0.5,\ d_{1,2} = 0.2$ and $d_{1,3} = d_{1,4} = d_{1,5} = 0.1$ for $N = 5$, outperform

[5]The assumption of equally distributing E_T among all nodes does not necessarily provide the condition of balanced hops, since equal distance between two successive nodes is another factor for the hops to be balanced. Here, we create unbalanced hops by considering unequal distances between successive nodes.

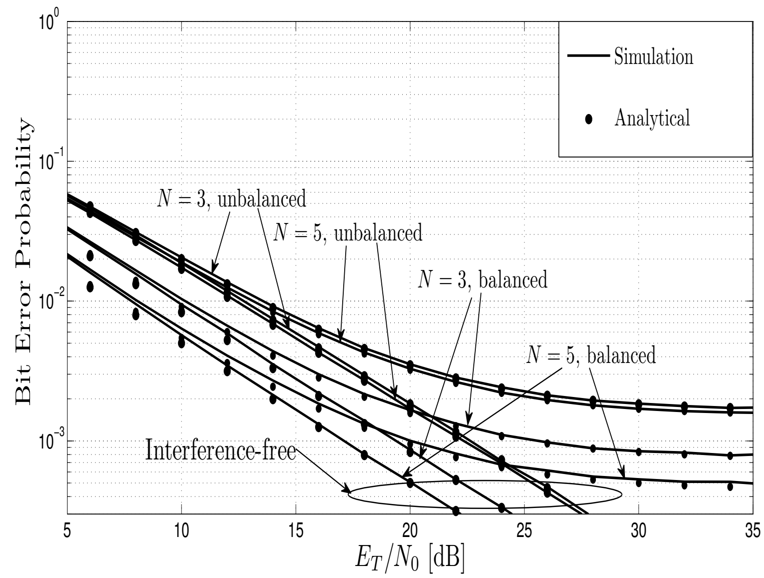

Figure 3.2: Performance of single-branch multi-hop networks (balanced vs. unbalanced) with $N = 3,\ 5$ relays, each impacted by $L_R = 3$ interferers with individual average INR $\bar{\gamma}_{I_{m,n}} = 0.003\frac{E_T}{N_0}$, in comparison with the interference-free case.

the considered counterpart networks with balanced hops. Further, we observe that at high E_T/N_0, the phenomenon of error floor begins to appear due to the presence of CCI which impacts the performance independently of the values of E_T/N_0. On the other hand, as E_T/N_0 increases in the low to medium ranges, an improvement in the error probability performance is observed because of the fact that the dominant factor in these ranges is the AWGN.

In Fig. 3.3, we hold the parameters of unbalanced dual-hop systems, i.e., $d_{m,1} = 0.8$ and $d_{m,2} = 0.2$ for $m = 1,\ \ldots, M$, with triple-branch $(M = 3)$, dual-branch $(M = 2)$ and single-branch $(M = 1)$. It is authenticated by Fig. 3.3 that the dual-hop triple-branch network achieves a better performance compared to the dual-hop dual-branch network and dual-hop single-branch network due to the diversity.

Fig. 3.4 demonstrates the effect of altering the average INR values, $\overline{\gamma}_{I_{m,n}}$, on the outage performance in unbalanced dual-hop networks, i.e., $d_{m,1} = 0.8$ and $d_{m,2} = 0.2$ for $m = 1,\ \ldots, M$, with $M = 1$ as in single-branch and $M = 2$ as in dual-branch. The analytical results pertaining to the lower-bound outage probability are provided based on

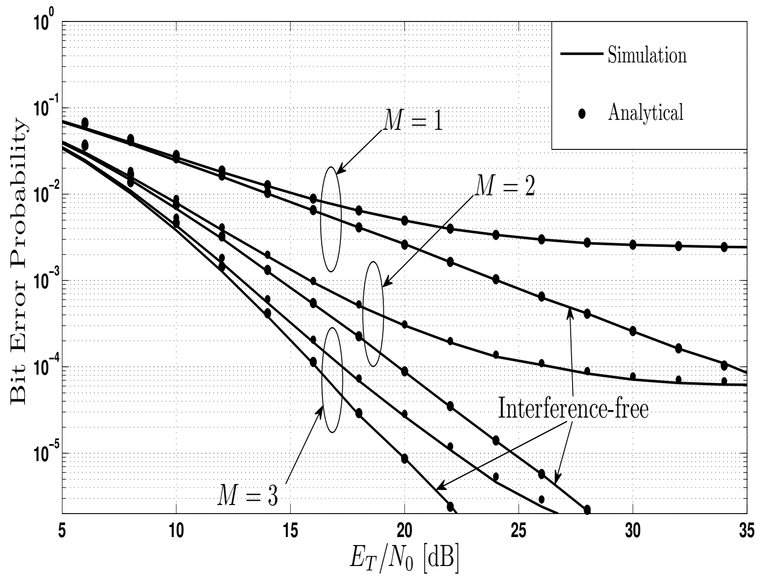

Figure 3.3: Performance of unbalanced dual-hop networks with $M = 1,\ 2,$ or 3 branches in the presence of CCI ($L_R = 3$, average INR of each interferer $\bar{\gamma}_{I_{m,n}} = 0.003\frac{E_T}{N_0}$), in comparison with the interference-free case.

(3.6). Besides, the analytical results corresponding to the approximate outage performance, are also provided, according to (3.9). The outage probability is shown for the specific rate of $r = 1.25$, while the average INR of each interfering signal takes different values, i.e., $\bar{\gamma}_{I_{m,n}} = INR_1 = 0.001$, $\bar{\gamma}_{I_{m,n}} = INR_2 = 0.003$ and $\bar{\gamma}_{I_{m,n}} = INR_3 = 0.006\ E_T/N_0$. As seen, the dual-hop dual-branch network with $\overline{\gamma}_{I_{m,n}} = INR_1 = 0.001E_T/N_0$ achieves the maximum performance among the others due to achieving more diversity.

Finally, Fig. 3.5 compares the performance of the adaptive power allocation algorithm with that of the equal power scheme. The results are provided for an unbalanced dual-hop dual-branch network, i.e., $d_{m,1} = 0.8$ and $d_{m,2} = 0.2$ for $m =\ 1, 2$. We assume two different scenarios in the presence of CCI. In the first, each interferer affecting the $(1,1)^{th}$ and the $(2,1)^{th}$ hops, has average INR, $\bar{\gamma}_{I_{1,1}}$ and $\bar{\gamma}_{I_{2,1}}$, equal to $INR_1 = 0.015E_T/N_0$. For this scenario, the average INR of every CCI signal that impacts the $(1,2)^{th}$ and the $(2,2)^{th}$ hops, $\bar{\gamma}_{I_{1,2}}$ and $\bar{\gamma}_{2,2}$, is equal to $INR_2 = 0.005E_T/N_0$. In the second scenario, $\bar{\gamma}_{I_{1,1}}$ and $\bar{\gamma}_{I_{2,1}}$ are equal to $INR_3 = 0.006E_T/N_0$ while $\bar{\gamma}_{I_{1,2}}$ and $\bar{\gamma}_{2,2}$ are equal to $INR_4 = 0.002E_T/N_0$. As observed, the adaptive power allocation algorithm outperforms the equal power allocation

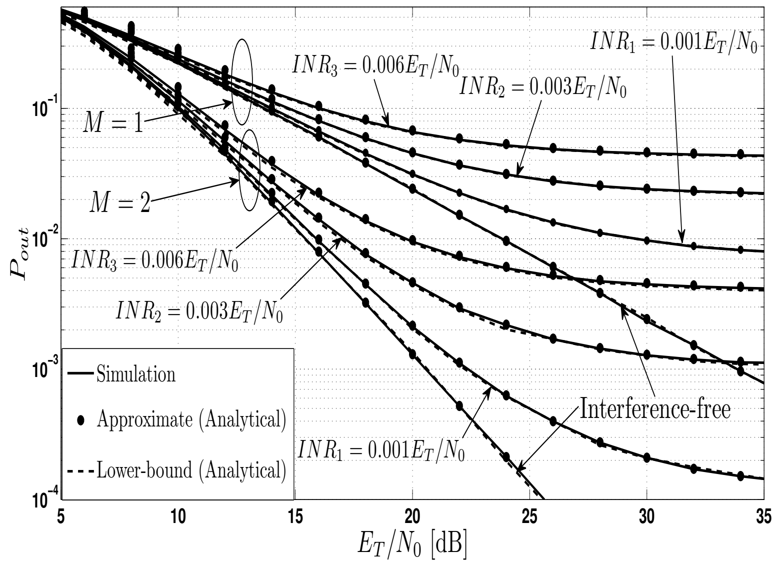

Figure 3.4: Outage probability of unbalanced dual-hop networks with $M = 1$ or 2 branches in the presence of CCI ($r = 1.25$, $L_R = 3$), for different values of the average INR of each interferer ($\bar{\gamma}_{I_{m,n}} = 0.001\frac{E_T}{N_0}$, $0.003\frac{E_T}{N_0}$ or $0.006\frac{E_T}{N_0}$), in comparison with the interference-free case.

scheme. Moreover, the optimal power solution has a very little impact on the system error performance in the low E_T/N_0 range. This is because of the fact that in the low E_T/N_0 range, AWGN is the most dominant factor on performance. Furthermore, at high E_T/N_0, the error floor in schemes with adaptive power allocation decreases significantly compared to the case with equal power allocation. It is also attested that as the average INR value decreases, i.e., $\bar{\gamma}_{I_{1,1}}$ and $\bar{\gamma}_{I_{2,1}}$ decrease from $INR_1 = 0.015E_T/N_0$ to $INR_3 = 0.006E_T/N_0$ and $\bar{\gamma}_{I_{1,2}}$ and $\bar{\gamma}_{2,2}$ decrease from $INR_2 = 0.005E_T/N_0$ to $INR_4 = 0.002E_T/N_0$, the performance of both the adaptive power allocation and the equal-power scheme is improved as compared to the performance in the interference-free case.

3.6 Summary

The effect of CCI on the performance of MHMB wireless systems with AF relaying technique was studied in this Chapter. We assumed that the desired signal and all the interfering signals are subject to independent Rayleigh fading. All the interfering signals were

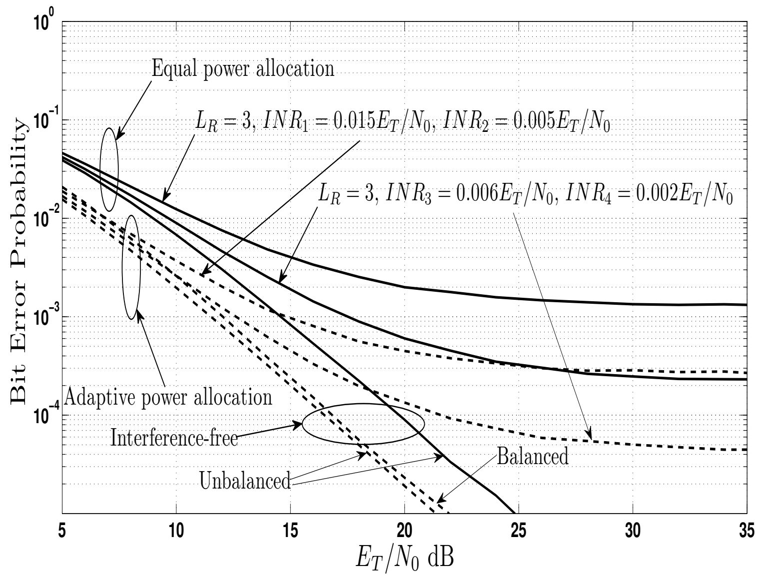

Figure 3.5: Performance of the adaptive algorithm in comparison with equal power allocation for an unbalanced dual-hop dual-branch network, considering two different scenarios in the presence of CCI with $L_R = 3$, and the interference-free case.

presumed to take arbitrary INR values. We obtained exact and upper-bound expressions for the end-to-end SINR. Following that, a lower-bound on the outage probability was derived in closed-form. Besides, we derived approximate expressions for the error and outage probabilities. The analysis is valid for arbitrary numbers of branches, hops and interferers, and for different average INR values. Finally, aiming at optimizing the system performance in terms of minimizing the error probability, we investigated adaptive power allocation at the source node and all the relays. Correspondingly, we derived closed-form expressions for the energies of the nodes. Our results verified that by applying the energies obtained through the optimization process, the performance of the system can improve significantly. Such optimization is indeed very important for the deployment of relaying networks in practical environments with CCI. In the following Chapter, we examine the performance of MHMB relaying networks using AF protocol and operating in practical environments with unequal-power interferers.

Chapter 4

Non-Symmetric Multi-Hop Multi-Branch Relaying in the Presence of Interferers with Unequal Powers [1]

4.1 Introduction

In this Chapter, the performance of non-symmetric MHMB relaying networks using AF protocol and operating in practical environments with unequal-power interferers, is examined. In particular, because multiple relays take part in the data transmission, CCI is considered at all the relaying nodes. Assuming the channels, for both the desired and the interfering signals, to experience Rayleigh fading and implementing MRC at the end receiver, first, exact and upper-bound expressions for the end-to-end SINR are derived. Then, the MGF of the upper-bound end-to-end SINR is obtained. According to the latter, the error and outage probabilities are assessed in closed form. Further, simple and general asymptotic expressions for the error and outage probabilities, which explicitly show the coding and the diversity gains, are derived and discussed. Finally, the analysis is validated

[1] Part of the material in this chapter is extracted from:
[55] A. H. Forghani, S. S. Ikki, and S. Aïssa, "Performance of non-symmetric relaying networks in the presence of interferers with unequal powers," *IEEE Wireless Commmun. Lett.*, vol. 2, no. 1, pp. 106–109, Feb. 2013.

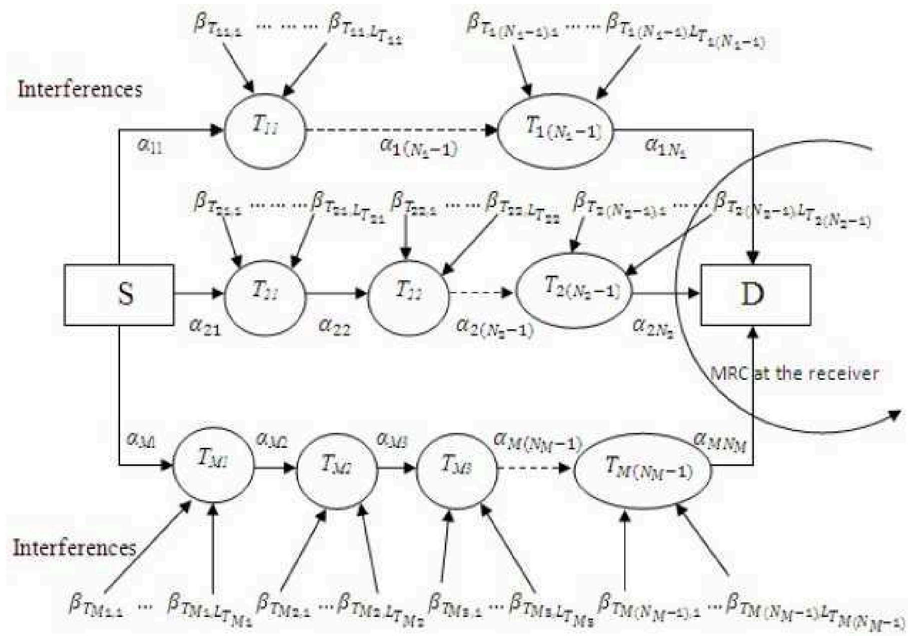

Figure 4.1: Non-symmetric multi-hop multi-branch relaying network with unequal-power interferers and MRC at the end receiver.

by comparing the corresponding numerical results with Monte Carlo simulations, sustained by insightful discussions.

4.2 Network Model

As illustrated in Fig. 4.1, in the non-symmetric MHMB relaying network, the connection between the source and the destination is performed through M different branches, with each consisting of N_m hops. At the m^{th} branch, the respective relays ($T_{mn},\ n = 1, \cdots, N_m - 1$) contribute in the process of data transmission from the source node to its ultimate destination (when $n = 1$ for any m, node $T_{m(n-1)}$ corresponds to the source node). The channel assigned to the source is split into orthogonal sub-channels across time. The medium access control takes advantage of a time-division scheme to provide half-duplex transmission for the relays. Furthermore, it is assumed that in each time slot only one node in each branch transmits. The signal received at the $(mn)^{th}$ relay, T_{mn}, consists of a faded noisy signal received from the formerly transmitting node, $T_{m(n-1)}$, and some faded CCI signals from $L_{T_{mn}}$ external interfering sources. After processing by the $(mn)^{th}$ relay, the received signal is transmitted in the following time slot to the subsequent node along the same branch, i.e., $T_{m(n+1)}$. Thus, in the m^{th} branch ($m = 1, \cdots, M$), the signal received by the n^{th} relay, T_{mn}, can be expressed as

$$y_{mn} = \sqrt{E_{m(n-1)}}\alpha_{mn}x_{m(n-1)} + \sum_{j=1}^{L_{T_{mn}}}\sqrt{E_{I_{mn,j}}}\beta_{T_{mn,j}}d_{T_{mn,j}} + w_{mn}, \tag{4.1}$$

where α_{mn} denotes the Rayleigh fading coefficient of the channel between nodes $T_{m(n-1)}$ and T_{mn}, $x_{m(n-1)}$ represents the unit-energy signal transmitted from the previous relay on the same branch (for the first hop $(n = 1)$ in any branch, x_{m0} originates from the source node), and $E_{m(n-1)}$ denotes the energy of the signal transmitted from the $m(n-1)^{th}$ node in the same branch. In the second term of the right-hand-side (RHS) of the first equation in (4.1), $d_{T_{mn,j}}$ denotes the signal from the j^{th} interferer affecting the $(mn)^{th}$ relay, assumed of unit energy. Further, $L_{T_{mn}}$ denotes the number of signals which interfere with the $(mn)^{th}$ relay, $E_{I_{mn,j}}$ represents the energy of the j^{th} interferer at the $(mn)^{th}$ relay, and $\beta_{T_{mn,j}}$ denotes the Rayleigh fading coefficient of the j^{th} interference channel impacting the n^{th} relay in the m^{th} branch. The last term in the RHS of the first equation in (4.1), i.e., w_{mn}, represents the AWGN with zero mean and variance N_0. We assume that the CSI of the interferers is available at the relays, and consider variable-gain amplification. The entire transmission time is allocated equally among transmitting nodes across the multi-hop paths. The variable amplification coefficient at the n^{th} relay in the m^{th} branch is denoted g_{mn}, expressed as $g_{mn} = \left(E_{m(n-1)}\left|\alpha_{mn}\right|^2 + \sum_{j=1}^{L_{T_{mn}}} E_{I_{mn,j}}\left|\beta_{T_{mn,j}}\right|^2 + N_0\right)^{-1/2}$, with consideration that $g_{m0} = 1$ for $m = 1, 2, \cdots, M$. Hence, the amplification process at the $(mn)^{th}$ relay node consists in generating the signal $x_{mn} = g_{mn}y_{mn}$ and transmitting it to the next relay node. To advance with the analysis, we present a theorem for the PDF of the sum of independent random variables with exponential distribution that will be applied to determine the statistics of the final SINR.

Next, we reproduce the following result from [52] which will be used later in our analysis.

$Theorem\,1$: For independent exponential random variables R_k, $k = 1, \cdots, K$, with

PDF $f_{R_k}(r) = \exp\left(-r/\bar{R}_k\right)/\bar{R}_k$ and mean value $\bar{R}_k$, the PDF of $Y = \sum_{k=1}^{N} R_k$ is given by [52]:

$$f_Y(y) = \sum_{k=1}^{N} \frac{\tau_k}{\bar{R}_k} \exp\left(-\frac{y}{\bar{R}_k}\right), \tag{4.2}$$

where $\tau_k = \prod_{i=1,\, i\neq k}^{N} \frac{\bar{R}_k}{\left(\bar{R}_k - \bar{R}i\right)}$.

We define $\gamma_{I_{mn,j}} = \left(E_{I_{mn,j}}/N_0\right)\left|\beta_{T_{mn,j}}\right|^2$ as the INR at the $(mn)^{th}$ relay with reference to the j^{th} interferer ($j = 1, \cdots, L_{T_{mn}}$). Recall that the PDF of $\gamma_{I_{mn,j}}$ is exponential with average $\bar{\gamma}_{I_{mn,j}} = \mathbf{E}\left[\left|\beta_{T_{mn,j}}\right|^2\right] E_{I_{mn,j}}/N_0$ ($\mathbf{E}[\cdot]$ is the expectation operator). Then, applying Theorem 1, the PDF of $\sum_{j=1}^{L_{T_{mn}}} \gamma_{I_{mn,j}}$ can be expressed as

$$f_{\sum_{j=1}^{L_{T_{mn}}} \gamma_{I_{mn,j}}}(\gamma) = \sum_{j=1}^{L_{T_{mn}}} \frac{\rho_{mn,j}}{\bar{\gamma}_{I_{mn,j}}} \exp\left(-\frac{\gamma}{\bar{\gamma}_{I_{mn,j}}}\right), \tag{4.3}$$

where $\rho_{mn,j} = \prod_{i=1, i\neq j}^{L_{T_{mn}}} \left(\frac{\bar{\gamma}_{I_{mn,j}}}{\bar{\gamma}_{I_{mn,j}} - \bar{\gamma}_{I_{mn,i}}}\right)$. Also, the effective SINR at the n^{th} relay in the m^{th} branch is denoted by

$$\gamma_{mn}^{\text{eff}} = \gamma_{mn} \bigg/ \left(1 + \sum_{j=1}^{L_{T_{mn}}} \gamma_{I_{mn,j}}\right), \tag{4.4}$$

where $\gamma_{mn} = |\alpha_{mn}|^2 E_{m(n-1)}/N_0$ represents the SNR at node T_{mn} which follows the exponential PDF $f_{\gamma_{mn}}(\gamma) = \exp\left(-\gamma/\bar{\gamma}_{mn}\right)/\bar{\gamma}_{mn}$ with average $\bar{\gamma}_{mn} = \mathbf{E}\left[|\alpha_{mn}|^2\right] E_{m(n-1)}/N_0$. Using (4.4) and knowing that the m^{th} branch consists of N_m relays, the end-to-end SINR for said branch, denoted γ_{end}^m, is obtained as

$$\gamma_{\text{end}}^m = \left[\prod_{n=1}^{N_m} \left(1 + \frac{1 + \sum_{j=1}^{L_{T_{mn}}} \gamma_{I_{mn,j}}}{\gamma_{mn}}\right) - 1\right]^{-1}. \tag{4.5}$$

MRC is applied for combining the signals at the destination, which means that the end-to-end SINR is obtained by summation of the SINR values of the M independent branches. Thus, the end-to-end SINR is given by $\gamma_{\text{end}} = \sum_{m=1}^{M} \gamma_{\text{end}}^m$, where γ_{end}^m is obtained in (4.5). Considering (4.4), the PDF of the γ_{mn}^{eff} can be written as

$$f_{\gamma_{mn}^{\text{eff}}}(\gamma) = \int_0^{\infty} (x+1) f_{\gamma_{mn}}\left((x+1)\gamma\right) f_{\sum_{j=1}^{L_{T_{mn}}} \gamma_{I_{mn,j}}}(x)\, dx. \tag{4.6}$$

After solving (4.6), the CDF of γ_{mn}^{eff}, i.e., $F_{\gamma_{mn}^{\text{eff}}}(\gamma) = \int_0^{\infty} f_{\gamma_{mn}^{\text{eff}}}(\gamma) d\gamma$ is obtained as

$$F_{\gamma_{mn}^{\text{eff}}}(\gamma) = 1 - \exp\left(-\frac{\gamma}{\bar{\gamma}_{mn}}\right) \sum_{j=1}^{L_{T_{mn}}} \frac{\bar{\gamma}_{mn}\rho_{mn,j}}{\gamma\bar{\gamma}_{I_{mn,j}} + \bar{\gamma}_{mn}}. \tag{4.7}$$

4.3 End-to-End Performance Analysis

4.3.1 MGF of the Upper-Bound SINR

It is extremely difficult to analyze the exact SINR given in (4.5) even for the interference-free scenario. To facilitate the derivation of the statistics of the output SINR and conduct a performance evaluation of the systems under study, we first make use of a pertinent upper-bound technique introduced in [56]. Accordingly,

$$\gamma_{\text{end}}^{m} \leq \gamma_{\text{up}}^{m} = \min\left(\gamma_{m1}^{\text{eff}}, \gamma_{m2}^{\text{eff}}, \cdots, \gamma_{mn}^{\text{eff}}, \cdots, \gamma_{mN_m}^{\text{eff}}\right). \tag{4.8}$$

Afterwards, the CDF of γ_{up}^{m} can be obtained by $F_{\gamma_{\text{up}}^{m}}(\gamma) = 1 - \prod_{n=1}^{N_m}\left(1 - F_{\gamma_{mn}^{\text{eff}}}(\gamma)\right)$, which can be expressed as

$$F_{\gamma_{\text{up}}^{m}}(\gamma) = 1 - \exp\left(-\gamma\sum_{n=1}^{N_m}\frac{1}{\bar{\gamma}_{mn}}\right) \prod_{n=1}^{N_m}\sum_{j=1}^{L_{T_{mn}}} \frac{\bar{\gamma}_{mn}\rho_{mn,j}}{\gamma\bar{\gamma}_{I_{mn,j}} + \bar{\gamma}_{mn}}. \tag{4.9}$$

Further, by substituting (4.7) into $1 - \prod_{n=1}^{N_m}\left(1 - F_{\gamma_{mn}^{\text{eff}}}(\gamma)\right)$, and applying partial fraction, $F_{\gamma_{\text{up}}^{m}}(\gamma)$ obtained in (4.9), is simplified to:

$$F_{\gamma_{\text{up}}^{m}}(\gamma) = 1 - \exp\left(-\gamma\sum_{n=1}^{N_m}\frac{1}{\bar{\gamma}_{mn}}\right) \sum_{n=1}^{N_m}\sum_{j=1}^{L_{T_{mn}}} \frac{\varphi_{mn,j}}{\gamma + \frac{\bar{\gamma}_{mn}}{\bar{\gamma}_{I_{mn,j}}}}, \tag{4.10}$$

where

$$\varphi_{mn,j} = \prod_{n=1}^{N_m} \left. \frac{\sum_{l=1}^{L_{T_{mn}}} \rho_{mn,l}\frac{\bar{\gamma}_{mn}}{\bar{\gamma}_{I_{mn,l}}} \prod_{k=1,k\neq l}^{L_{T_{mn}}}\left(\gamma + \frac{\bar{\gamma}_{mn}}{\bar{\gamma}_{I_{mn,k}}}\right)}{\prod_{l=1,l\neq j}^{L_{T_{mn}}}\left(\gamma + \frac{\bar{\gamma}_{mn}}{\bar{\gamma}_{I_{mn,l}}}\right)} \right|_{\gamma = -\frac{\bar{\gamma}_{mn}}{\bar{\gamma}_{I_{mn,j}}}} \tag{4.11}$$

Accordingly, by using (4.10), the MGF of $\gamma_{\rm up}^{m}$ can be obtained as

$$\begin{aligned} M_{\gamma_{\rm up}^{m}}(s) &= \mathbf{E}_{\gamma_{\rm up}^{m}}(\exp(-s\gamma)) = \int_0^\infty sF_{\gamma_{\rm up}^{m}}(\gamma)\exp(-s\gamma)\,d\gamma \\ &= 1+\sum_{n=1}^{N_m}\sum_{j=1}^{L_{T_{mn}}} s\varphi_{mn,j}\exp(a_m b_{mn,j})\,\mathrm{E_i}(-a_m b_{mn,j}), \end{aligned} \tag{4.12}$$

where $\mathrm{E_i}(x) = \int_{-\infty}^{x}\frac{\exp(t)}{t}dt$ denotes the Exponential integral and constants $(a_m, b_{mn,j})$ are defined by: $a_m = s+\sum_{n=1}^{N_m}\frac{1}{\bar{\gamma}_{mn}}$, $b_{mn,j} = \frac{\bar{\gamma}_{mn}}{\bar{\gamma}_{I_{mn,j}}}$. Hence, given that transmission is carried out through M branches which are independent of each other, the final MGF can be expressed as $M_{\gamma_f}(s) = \prod_{m=1}^{M} M_{\gamma_{\rm up}^{m}}(s)$, where $M_{\gamma_{\rm up}^{m}}(s)$ is shown in (4.12).

4.3.2 Lower-Bound Performance

The MGF obtained in (4.12) is general and can be used with any type of modulation to determine the error and outage probabilities of the network. For instance, considering coherently detected L-PSK modulation and making use of [57, Eq.(8. 23)], the probability of error can be calculated using

$$P(e) = \frac{1}{\pi}\int_0^{\Theta} M_{\gamma_f}\left(\frac{g_{\rm PSK}}{\sin^2\theta}\right)d\theta, \tag{4.13}$$

where $\Theta = (L-1)\pi/L$ and $g_{\rm PSK} = \sin^2(\pi/L)$. Thus, by substituting the MGF formula (4.12) into the above expression, $P(e)$ can be written as [58, Eq.(10)]:

$$P(e) = \frac{\Theta}{2\pi}M_{\gamma_f}(g_{\rm PSK})+\frac{1}{4}M_{\gamma_f}\left(\frac{4}{3}g_{\rm PSK}\right)+\left(\frac{\Theta}{2\pi}-\frac{1}{4}\right)M_{\gamma_f}\left(\frac{g_{\rm PSK}}{\sin^2\Theta}\right), \tag{4.14}$$

thus yielding a closed form for the error probability.

Now, we determine a lower-bound for the outage probability of the network. The latter is defined as the probability that the end-to-end SINR is less than a threshold value $\gamma_{\rm th}$: $P_{\rm out} = P(\gamma_f<\gamma_{\rm th})$. This definition for outage probability is equivalent to the definition provided in the previous Chapter, given that the mutual information (I) is a function of end-to-end SINR and can be defined as $I = \frac{1}{N}\log_2(1+\gamma_{\rm end})$, where N denotes the number of hops.

Since the MGF is just the Laplace transform of the PDF, then the outage probability can be found by the inverse Laplace transform of the ratio $M_{\gamma_f}(s)/s$, evaluated at γ_{th}. Thus, the outage probability can be expressed as

$$P_{\text{out}} = \frac{1}{2\pi j}\int_{\sigma-j\infty}^{\sigma+j\infty} \frac{M_{\gamma_f}(s)}{s} \exp\left(-s\gamma_{\text{th}}\right) ds, \tag{4.15}$$

where σ is chosen within the convergence region of the integral in the complex S plane. Considering (4.12), the integral in (4.15) can be evaluated by finding the residues of the function inside the integral, using numerical tools.

4.3.3 Asymptotic Performance

Since the lower-bound metrics derived above do not give sufficient insights about the performance of the network, we now resort to an approximation of the MGF of the end-to-end SINR to derive asymptotic expressions for the error and outage metrics. First, taking the derivative from $F_{\gamma_{\text{up}}^m}(\gamma)$, shown in (4.9), with respect to γ, the PDF of γ_{up}^m is obtained as

$$\begin{aligned} f_{\gamma_{\text{up}}^m}(\gamma) = \exp\left(-\gamma \sum_{n=1}^{N_m} \frac{1}{\bar{\gamma}_{mn}}\right)&\left(\sum_{n=1}^{N_m} \frac{1}{\bar{\gamma}_{mn}} \prod_{n=1}^{N_m} \sum_{j=1}^{L_{T_{mn}}} \frac{\bar{\gamma}_{mn}\rho_{mn,j}}{\gamma\bar{\gamma}_{I_{mn,j}} + \bar{\gamma}_{mn}}\right. \\ &\left. + \sum_{n=1}^{N_m} \sum_{j=1}^{L_{T_{mn}}} \frac{\bar{\gamma}_{I_{mn,j}}\bar{\gamma}_{mn}\rho_{mn,j}}{\left(\gamma\bar{\gamma}_{I_{mn,j}} + \bar{\gamma}_{mn}\right)^2} \prod_{l=1,\, l\neq n}^{N_m} \sum_{k=1}^{L_{T_{mn}}} \frac{\bar{\gamma}_{ml}\rho_{ml,k}}{\gamma\bar{\gamma}_{I_{ml,k}} + \bar{\gamma}_{ml}}\right). \end{aligned} \tag{4.16}$$

According to [53], approximating $f_{\gamma_{\text{up}}^m}(\gamma)$ can be done based on the behaviour of $f_{\gamma_{\text{up}}^m}(\gamma)$ around $\gamma = 0$. By engaging the Taylor series expansion of $f_{\gamma_{\text{up}}^m}(\gamma)$ at $\gamma = 0$ (the Maclaurin series) for $\gamma \geq 0$, (4.16) can be reformulated as $f_{\gamma_{\text{up}}^m}(\gamma) = f_{\gamma_{\text{up}}^m}(0)$. Consequently, calculating (4.16) at $\gamma = 0$, $f_{\gamma_{\text{up}}^m}(0)$ can be written as

$$f_{\gamma_{\text{up}}^m}(0) = \sum_{n=1}^{N_m} \frac{1}{\bar{\gamma}_{mn}} + \sum_{n=1}^{N_m} \sum_{j=1}^{L_{T_{mn}}} \frac{\bar{\gamma}_{I_{mn,j}}\rho_{mn,j}}{\bar{\gamma}_{mn}} \prod_{l=1,\, l\neq n}^{N_m} \sum_{k=1}^{L_{T_{mn}}} \rho_{ml,k}. \tag{4.17}$$

Next, according to the definition of $\rho_{mn,j}$ expressed in (4.3), i.e., $\rho_{mn,j} = \prod_{i=1,i\neq j}^{L_{T_{mn}}} \frac{\bar{\gamma}_{I_{mn,j}}}{\bar{\gamma}_{I_{mn,j}} - \bar{\gamma}_{I_{mn,i}}}$, we have

$$\sum_{j=1}^{L_{T_{mn}}} \bar{\gamma}_{I_{mn,j}} \rho_{mn,j} = \sum_{j=1}^{L_{T_{mn}}} \bar{\gamma}_{I_{mn,j}} \text{ and } \sum_{k=1}^{L_{T_{mn}}} \rho_{ml,k} = 1. \tag{4.18}$$

Using (4.18), equation (4.17) can be rewritten as $f_{\gamma_{\mathrm{up}}^{m}}(0) = \sum_{n=1}^{N_m} \frac{1+\sum_{j=1}^{L_{T_{mn}}} \bar{\gamma}_{I_{mn,j}}}{\bar{\gamma}_{mn}}$. Subsequently, we may write $f_{\gamma_{\mathrm{up}}^{m}}(\gamma) \sim \sum_{n=1}^{N_m} \frac{1+\sum_{j=1}^{L_{T_{mn}}} \bar{\gamma}_{I_{mn,j}}}{\bar{\gamma}_{mn}}$. Having obtained the latter expression as the approximate PDF of γ_{up}^{m} and knowing that the receiver at the destination node performs MRC on the M independent branches, the MGF of the end-to-end SINR is the product of the individual MGFs pertaining to each branch:

$$M_{\gamma_{\mathrm{f}}}(s) \to \frac{1}{s^M} \prod_{m=1}^{M} \sum_{n=1}^{N_m} \left(\frac{1}{\bar{\gamma}_{mn}} \left(1 + \sum_{j=1}^{L_{T_{mn}}} \bar{\gamma}_{I_{mn,j}} \right) \right). \tag{4.19}$$

Following that, by substituting (4.19) into (4.13), the error probability can be obtained as

$$P(e) \to \frac{1}{\pi} \prod_{m=1}^{M} \sum_{n=1}^{N_m} \left(\frac{1}{\bar{\gamma}_{mn}} \left(1 + \sum_{j=1}^{L_{T_{mn}}} \bar{\gamma}_{I_{mn,j}} \right) \right) \times \frac{1}{(g_{PSK})^M} \left(-\frac{\cos(\Theta)}{2M} Q + \frac{(2M-1)!!}{2^M M!} \Theta \right), \tag{4.20}$$

where Q is defined as

$$Q = \sin^{2M-1}(\Theta) + \sum_{k=1}^{M-1} \frac{\sin^{2M-2k-1}(\Theta)}{2^k} \frac{\prod_{i=1}^{2k-1}(2M-i)}{\prod_{j=1}^{k}(M-j)}, \tag{4.21}$$

with i taking odd integer values and $(2M-1)!!$ denoting the double factorial, i.e. $(2M-1)!! = 1 \times 3 \times \cdots \times (2M-1)$. Also, putting (4.19) into (4.15), a closed-form expression for the outage probability can be obtained as

$$P_{\mathrm{out}} \to \prod_{m=1}^{M} \sum_{n=1}^{N_m} \left(\frac{1}{\bar{\gamma}_{mn}} \left(1 + \sum_{j=1}^{L_{T_{mn}}} \bar{\gamma}_{I_{mn,j}} \right) \right) \times \frac{(\gamma_{\mathrm{th}})^M}{M!}. \tag{4.22}$$

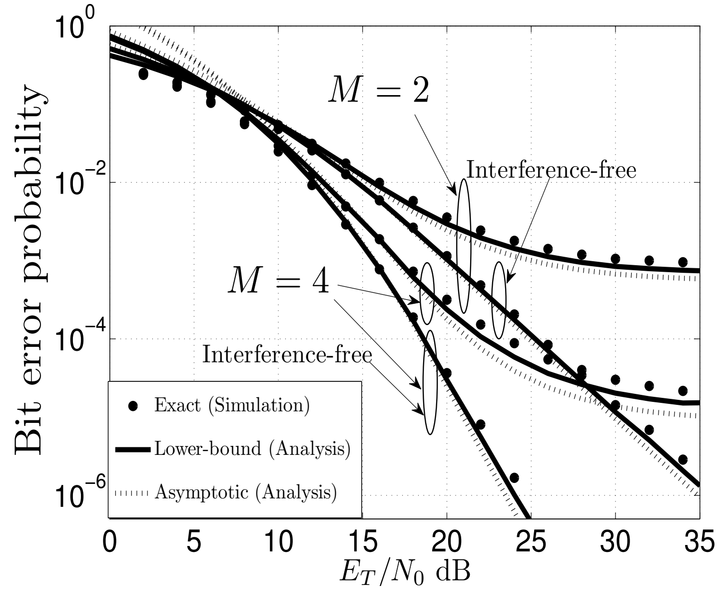

Figure 4.2: Error performance of dual-hop ($N_m = 2,\ m = 1, \cdots, M$) AF networks with $M = 2$ or 4 branches in the presence of $L = 3$ interferers with unequal power, in comparison with the interference-free case.

It is seen from (4.22) that for any $n = 1, \ldots, N_m$ and $m = 1, \ldots, M$, as $L_{T_{mn}}$ or $\bar{\gamma}_{I_{mn,j}}$ increases, the outage performance deteriorates, while it improves as $\bar{\gamma}_{mn}$ increases. Similar observation applies for the error performance.

4.4 Numerical Results

Now, we provide numerical results for (i) the error probability considering that the modulation scheme is BPSK and (ii) the outage probability. We analyze the effect of varying the main parameters: number of branches, number of hops and number of interferers. Results are plotted as a function of E_T/N_0 where $E_T = E_S + \sum_{m=1}^{M} \sum_{n=1}^{N_m - 1} E_{mn}$ denotes the overall energy and E_S represents the energy of the transmit signal from the source.

First, the average error probability is analyzed in Figs. 4.2 and 4.3. In the examples shown, it is assumed that three interferers ($L_{T_{mn}} = 3$, denoted here by L for simplicity) impact each relay with average INR of 0.001, 0.003 and $0.005 E_T/N_0$. The figures depict the lower-bound according to (4.14) and the asymptotic performance based on (4.20) and

(4.21) along with the simulation results. Plots pertaining to the interference-free scenario are also shown.

In Fig. 4.2 we assume two dual-hop ($N_m = 2,\ m = 1, \cdots, M$) networks with $M = 2$ or 4 branches. The network with 4 branches yields better performance because of the enhancement in diversity gain.

In Fig. 4.3, configurations with $M = 2$ branches and $N_1 = N_2 = 3$ or $N_1 = N_2 = 5$ hops are compared. The network with $N_1 = N_2 = 3$ outperforms its counterpart with $N_1 = N_2 = 5$. Figs. 4.2 and 4.3 also show error floors because of the CCI, which impacts the performance independently of E_T/N_0. Further, as E_T/N_0 increases in its low and medium ranges, an improvement in performance occurs because the dominant factor in these ranges is the AWGN.

Fig. 4.4 depicts the lower-bound and asymptotic outage probability based on (4.15) and (4.22), along with simulation results. A dual-hop setting is considered, with $M = 3$ or 4 branches and $L = 3$ or 5 interferers impacting each relay. For the case with $L = 3$, the average INR values are 0.002, 0.003 and $0.004 E_T/N_0$. For the other scenario with $L = 5$, the average INRs are 0.002, 0.005, 0.006, 0.007 and $0.009 E_T/N_0$. Results are plotted as a function of E_T/N_0 normalized to γ_{th}. Obviously, as the number of interfering signals increases, a degradation in performance occurs. Also, the performance improves, as the number of branches increases. Finally, at high $\frac{E_T/N_0}{\gamma_{\text{th}}}$, error floors start to emerge due to the CCI, which affects the outage probability regardless of the E_T/N_0 values.

4.5 Summary

The effect of co-channel interferers with unequal powers on the performance of non-symmetric MHMB relaying systems was investigated. We assumed AF protocol and that the signals are subject to Rayleigh fading. Exact and upper-bound expressions for the SINR were derived. Moreover, closed-form expressions for the lower-bound error and outage probabilities were obtained. Further, asymptotic expressions for the error and outage probabilities were derived. The analysis establishes a suitable tool for the design of practical non-symmetric MHMB relaying networks. In the next Chapter, we investigate the perfor-

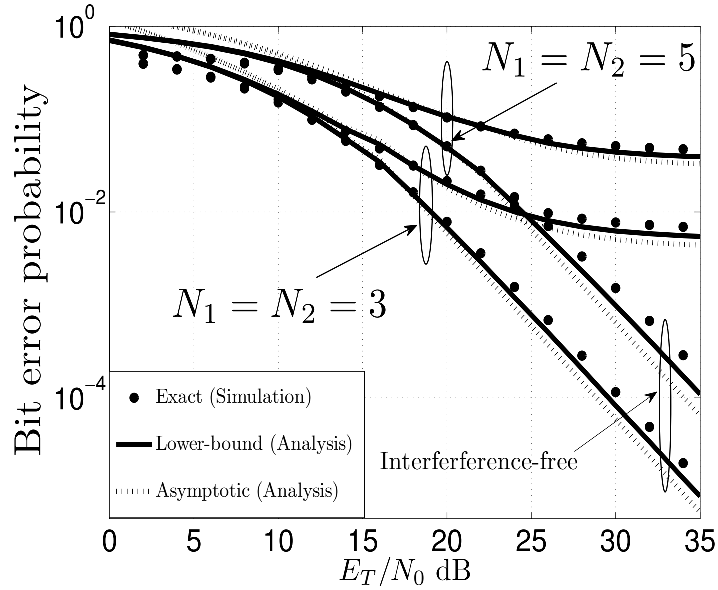

Figure 4.3: Performance of dual-branch ($M = 2$) AF relaying networks with $N_1 = N_2 = 3$ or $N_1 = N_2 = 5$ hops in the presence of $L = 3$ interferers with unequal power, in comparison with the interference-free scenario.

mance of relaying systems benefiting from signal space diversity.

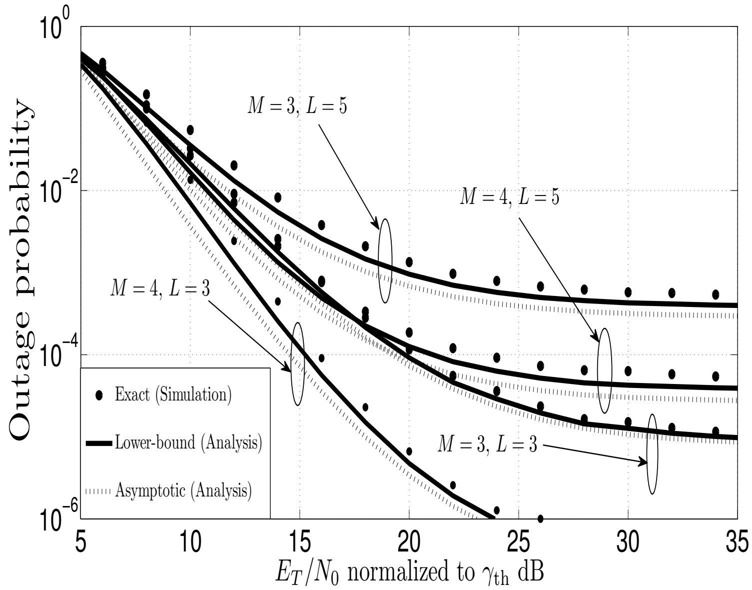

Figure 4.4: Outage performance of dual-hop ($N_m = 2,\ m = 1, \cdots, M$) AF networks with $M = 3$ or 4 branches, for different numbers of co-channel interferers ($L = 3,\ 5$) with unequal power impacting each relay node.

Chapter 5

Signal Space Diversity Based Relaying [1]

5.1 Introduction

In this Chapter, the performance and optimization of a three-terminal relaying system benefiting from signal space diversity are investigated. SSD is applied to enhance the performance and transmission reliability. SSD is an uncoded multidimensional modulation scheme that can increase the diversity order and countermeasure the fading effects in transmissions over wireless channels [36, 60, 61]. The technique of SSD yields gains in terms of spatial diversity when the channels are MIMO [62]. In this technique, first, the information bits are mapped into symbols of a classic constellation, e.g., QPSK and further grouped into vectors [36], [60, 61, 63–67]. Then, the symbol vectors are rotated by a square spreading matrix in such a way that any two symbol vectors can be distinguished by the maximum number of distinct components. Indeed, assuming that a deep fade affects only one of the components of a signal vector, the rotated constellation provides more protection against the unfavourable impacts of the noise, as no two points collapse together. After the symbol vectors are rotated, employing interleaving guarantees that each component of the signal vector is affected by independent fading. Therefore, the diversity order can be increased to the minimum number of distinct components between any two constellation points, which

[1] Part of the material in this chapter is extracted from:
[59] A. H. Forghani and S. Aïssa, "Relaying with signal space diversity: performance analysis and optimization," Submitted to *IEEE Trans. Veh. Tech.*, Sep. 2014.

is the minimum Hamming distance. The resultant diversity gain is obtained at the cost of complexity in maximum-likelihood (ML) decoding. To overcome such complexity, coordinate interleaved space-time codes were introduced in [68, 69], which benefit from the combination of SSD and spatial diversity. These space-time codes are recognized to be single-symbol decodable and, hence, do not add more complexity to ML decoding at the receiver [70].

The importance and popularity of cooperative systems are due to the diversity gain through the use of relays to assist communication without the need of multiple antennas at the transceivers [3, 4]. In its basic form, a cooperative system consists of a source node, a relay node and a destination node, whereby the signal transmitted from the source is received at the destination through independent source-destination and relay-destination paths. By applying the SSD technique, the diversity order of the cooperative system can be enhanced significantly [36]. A typical SSD based relaying system is investigated in [63], where the authors determined the diversity order of the considered system but left investigation in terms of key performance metrics, e.g., error probability, outage probability and Ergodic capacity, open. In particular, in [63], the diversity order is determined by using an approximation for the $Q\left(\right)$ function based on its exponential upper-bound function.

A typical cooperative system is considered which involves a relay node to help the communication between a source and its end destination, and make use of SSD to enhance the system performance. During the broadcast phase of the communication process, the relay remains silent in case of failure in decoding the message originating from the source. Otherwise, when the relay correctly decodes the broadcast signal, it generates the processed signal and forwards it to the destination. Considering Rayleigh fading and the general case of non-identical channels as well as the special case of identical channels, we derive main performance metrics, namely, error probability, asymptotic error probability, outage probability and Ergodic capacity, and determine the system diversity gain as well. In particular, all the expressions for the said performance metrics are obtained according to the $Q\left(\right)$ function rather than its upper-bound exponential function. Furthermore, in order to improve performance, we minimize the error probability of the system subject to constraint on the total energy budget, i.e., with respect to the total energy function. We also consider the optimization of the performance whereby the total energy is minimized under constraint on the error probability. Apart from their novelty, the results obtained constitute a convenient tool for the design and management of SSD based relaying systems and for the performance analysis and optimization of such systems in scenarios where, for instance, multiple relays are available for the communication between the source and its final destination or that relay selection techniques are implemented.

The remaining of the Chapter is organized as follows: In section II, we detail the concept of SSD and the system model. Two different cases are examined: the relay successfully decodes the received signal or it fails to do so. Section III investigates the performance of the SSD based relaying system under study. First, the error probability is obtained and then, we derive the asymptotic error probability for two cases: independent and non-identically distributed (i.n.i.d) and independent and identically distributed (i.i.d.) Rayleigh fading channels. Following that, the outage probability and Ergodic capacity are obtained. In section IV, the optimization procedure is presented. Two scenarios are considered. In the first, we obtain the optimum energy values for use at the source and the relay to minimize the error probability of the system subject to a constraint on the energy budget. The second optimization scenario aims at minimizing the total energy expenditure. In this case, we determine the optimum source and relay energies subject to a given error probability. Numerical and simulation results along with insightful discussions are presented in section V and, finally, we summarize the Chapter's findings in the last section.

5.2 Relaying with Signal Space Diversity

5.2.1 Signal Space Diversity

SSD was previously shown to provide significant diversity gain in single-antenna systems [36], [71]. In this part, we describe the main concept of the SSD technique, which is applied in the relaying system under study in order to enhance the advantages of the collaboration between the source and the relay during the signal transmission. The technique of SSD involves two main operations.

Constellation Rotation

In the first step, a rotated constellation, say χ, is generated by applying a transformation, Φ, to a classical constellation, e.g. M-PSK. An exhaustive list of the angle of rotation corresponding to the transformation Φ in multi-dimensional signal spaces is obtained in [72]. In the two-dimensional signal space, the transformation Φ is a 2-by-2 rotation matrix with elements, $\Phi_{11} = \cos\theta$, $\Phi_{12} = -\sin\theta$, $\Phi_{21} = \sin\theta$ and $\Phi_{22} = \cos\theta$, where θ denotes the angle of rotation. By selecting an appropriate θ, it is possible to uniquely identify each signal point in the constellation χ from its in-phase or quadrature components. Assuming any two constellation points in the original constellation, e.g. c_k and c_m, their corresponding points in the rotated constellation are given by

$$x_k = c_k \exp(j\theta) \text{ and } x_m = c_m \exp(j\theta), \tag{5.1}$$

respectively. Fig. 5.1 illustrates the idea of rotation on 4-PSK modulation. In fact, if we assume that a deep fade hits only one of the components of the transmitted signal point, then we can see that the constellation in Fig. 5.1 (b) provides more protection against the effects of noise, since no two points collapse together as would happen in Fig. 5.1 (a).

Interleaving

During the transmission, the in-phase and quadrature components of each signal point are assumed to be affected separately by independent fading [36]. For such, in the relaying system under consideration, a component interleaver is used at the source node and a corresponding deinterleaver is employed at the destination node. This ensures that different components of each constellation point are transmitted through independent paths to the destination, i.e., on the source-destination link and on the relay-destination link. The two points in the rotated constellation which were defined above as x_k and x_m, can be rewritten as $x_k = \Re(x_k) + j\Im(x_k)$ and $x_m = \Re(x_m) + j\Im(x_m)$, where $\Re(x)$ and $\Im(x)$ represent the in-phase and quadrature components of x, respectively. Interleaving between the components

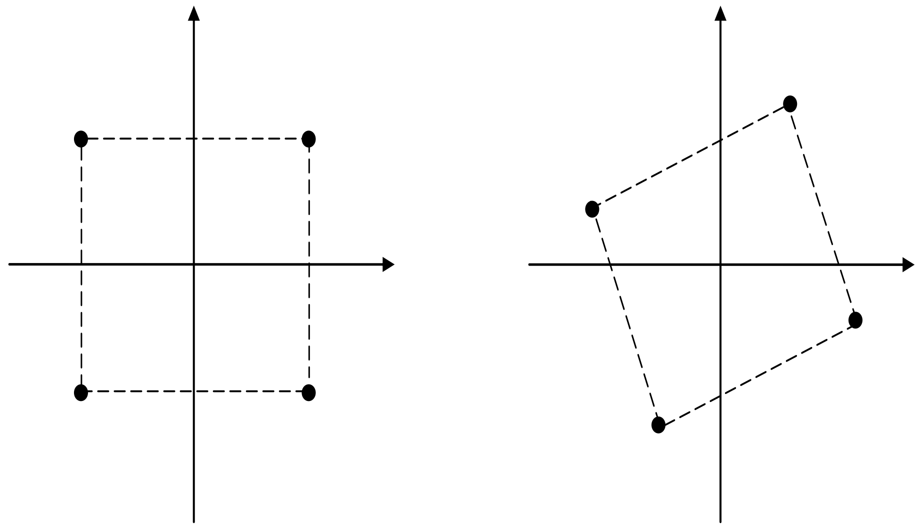

(a) (b)

Figure 5.1: Increasing the diversity by rotation (a) diversity is equal to one and (b) diversity is equal to two [36].

of x_k and x_m, forms new constellation points w_b and w_r, where

$$w_b = \Re(x_k) + j\ \Im(x_m) \text{ and } w_r = \Re(x_m) + j\ \Im(x_k). \tag{5.2}$$

Therefore, each point in the new constellation, denoted W, consists of two components with each one representing a specific constellation point in the rotated constellation χ. At the receiver, the inverse operation, i.e., deinterleaving, along with ML detection are performed to recover the points in the rotated constellation.

The two operations summarized above imply that the diversity order can be determined by the distinct components of each constellation point in the new constellation W. Maximum diversity can be achieved by optimally performing the rotation and separately interleaving the components of the signals. In general, it is possible to employ SSD in a N complex dimension to achieve a diversity order of N [73]. In [36], [71, 73], it was shown that the maximum diversity gain can be achieved if any two signal points in the system constellation have the maximum number of distinct components.

5.2.2 System and Channel Models

In the considered SSD based relaying system, the source node (S) communicates with the destination node (D) over a phase-equalized Rayleigh fading channel with coefficient $h_{S,D}$, where $h_{S,D}$ is real valued and greater than zero. A relay node (R) may also assist the communication between the source and its end destination as will be detailed shortly. The channel coefficient between nodes S and R ($h_{S,R}$) is subject to phase-equalized Rayleigh fading as well, i.e., $h_{S,R}$ is real valued and greater than zero. The channel coefficient between nodes R and D ($h_{R,D}$) is assumed to have a Rayleigh distributed magnitude (amplitude) with a uniform distributed phase within the interval of $\left[0, \frac{\pi}{2}\right)$. The PDFs of $h_{S,D}$ and $h_{S,R}$ are formulated by

$$g_{h_{X,Y}}\left(h_{X,Y}\right) = \frac{2h_{X,Y}}{\mathbf{E}\left(\left|h_{X,Y}\right|^2\right)} \exp\left(-h_{X,Y}^2/\mathbf{E}\left(\left|h_{X,Y}\right|^2\right)\right), \tag{5.3}$$

where $\mathbf{E}\left(\left|h_{X,Y}\right|^2\right)$ denotes the mean channel power with respect to link $X \to Y$ and $\mathbf{E}(.)$ is the expectation operator. Also, the PDF of the $h_{R,D}$ envelope, i.e., $|h_{R,D}|$, is formulated by

$$g_{\left|h_{R,D}\right|}\left(\left|h_{R,D}\right|\right) = \frac{2\left|h_{R,D}\right|}{\mathbf{E}\left(\left|h_{R,D}\right|^2\right)} \exp\left(-\left|h_{R,D}\right|^2/\mathbf{E}\left(\left|h_{R,D}\right|^2\right)\right), \tag{5.4}$$

where $\mathbf{E}\left(\left|h_{R,D}\right|^2\right)$ represents the mean channel power with reference to link $R \to D$. Further, it is considered that $h_{S,R}$, $h_{S,D}$ and $h_{R,D}$ are mutually independent. For all the links, we assume AWGN, with zero mean and equal variance N_0.

The instantaneous SNR of the $S \to R$ link is given by $\gamma_{S,R} = E_S h_{S,R}^2/N_0$, where E_S denotes the energy of the source transmitted signal. Accordingly, the average SNR of the $S \to R$ link is given by $\bar{\gamma}_{S,R} = \frac{E_S}{N_0}\mathbf{E}\left(h_{S,R}^2\right)$. Further, $\gamma_{S,D} = E_S h_{S,D}^2/N_0$ is the instantaneous SNR of the source-destination link, with $\bar{\gamma}_{S,D} = \frac{E_S}{N_0}\mathbf{E}\left(h_{S,D}^2\right)$ as average SNR.

In the broadcast phase, the destination and the relay receive a noisy faded version of the signal w_b (defined earlier as $w_b = \Re(x_k) + j\ \Im(x_m)$) transmitted from the source. In order for the relay to generate its processed signal and forward it to the destination, it needs to perform ML detection on its received signal and verify the correctness of the decoding result. The ML detection rule at the relay, to detect x_k and x_m from w_b, is given by

$$\hat{w}_b = \arg\min_{w \in W} \left[h_{S,R}\sqrt{E_S} w_b + n_{S,R} - h_{S,R}\sqrt{E_S} w \right], \tag{5.5}$$

where W denotes the constellation formed after the interleaving operation on the rotated constellation χ, and $n_{S,R}$ represents the AWGN noise in the $S \rightarrow R$ link. Based on the decoding output of the received signal at the relay, two cases are possible.

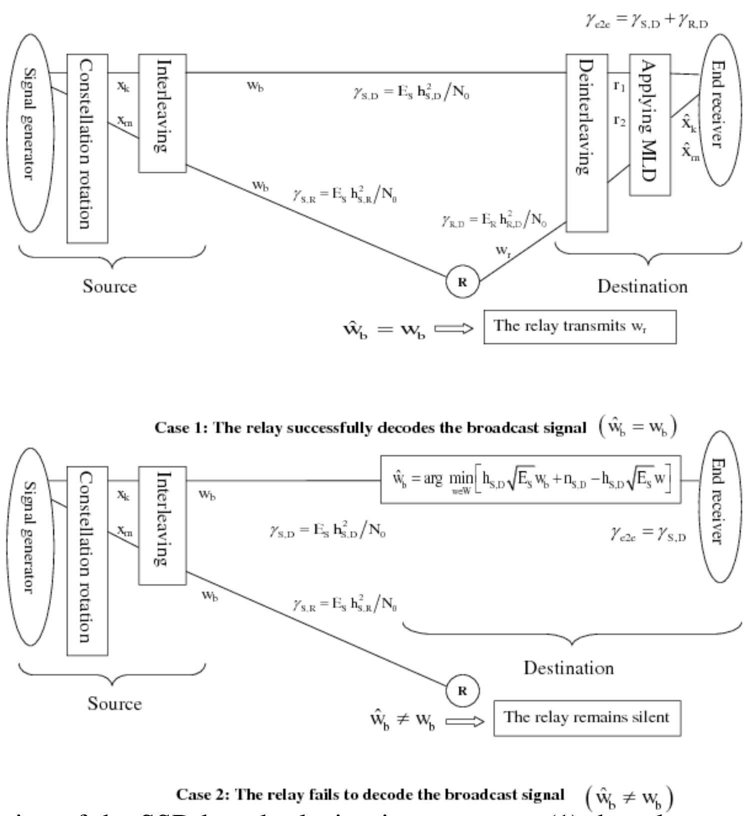

Figure 5.2: Operation of the SSD based relaying in two cases: (1) the relay successfully decodes the broadcast signal ($\hat{w}_b = w_b$) and (2) the relay fails to decode the broadcast signal ($\hat{w}_b \neq w_b$).

Successful Decoding at the Relay

After the broadcast phase, the relay is able to cooperate in the signal transmission provided that it decodes its received signal correctly. As shown in Fig. 5.2, in case of successful decoding ($\hat{w}_b = w_b$), x_k and x_m are correctly detected and the relay transmits the signal w_r (defined earlier as $w_r = \Re(x_m) + j\ \Im(x_k)$) to the destination node D. Similar to the broadcast phase, the relay transmitted signal, i.e. w_r, also carries sufficient information to uniquely identify the two constellation points in the rotated constellation, i.e., x_k and x_m.

In this case, the end-to-end SNR, denoted γ_{e2e}, is given by $\gamma_{\text{e2e}} = \gamma_{S,D} + \gamma_{R,D}$, where $\gamma_{R,D}$ is the instantaneous SNR of the relay-destination link given by $\gamma_{R,D} = E_R h_{R,D}^2 / N_0$, with E_R representing the energy of the transmit signal from the relay and $\bar{\gamma}_{R,D} = \frac{E_R}{N_0}\mathbf{E}\left(h_{R,D}^2\right)$ the average SNR of the $R \rightarrow D$ link.

The PDFs of $\gamma_{S,D}$ and $\gamma_{R,D}$ can be written as $f_{\gamma_{S,D}}(\gamma) = \frac{1}{\bar{\gamma}_{S,D}} \exp\left(-\frac{\gamma}{\bar{\gamma}_{S,D}}\right)$ and $f_{\gamma_{R,D}}(\gamma) = \frac{1}{\bar{\gamma}_{R,D}} \exp\left(-\frac{\gamma}{\bar{\gamma}_{R,D}}\right)$, respectively. Therefore, the PDF of end-to-end SNR in this case, is obtained as

$$f_{\gamma_{S,D}+\gamma_{R,D}}(\gamma) = \begin{cases} \frac{1}{\bar{\gamma}_{S,D}-\bar{\gamma}_{R,D}} \left(\exp\left(-\frac{\gamma}{\bar{\gamma}_{S,D}}\right) - \exp\left(-\frac{\gamma}{\bar{\gamma}_{R,D}}\right)\right), & \text{if } \bar{\gamma}_{S,D} \neq \bar{\gamma}_{R,D} \\ \frac{\gamma}{\bar{\gamma}^2} \exp\left(-\frac{\gamma}{\bar{\gamma}}\right), & \text{if } \bar{\gamma}_{S,D} = \bar{\gamma}_{R,D} = \bar{\gamma}. \end{cases} \tag{5.6}$$

At the end of each transmission block, the destination detects the source message by combining signals received from the source during the broadcast phase and from the relay in the relaying phase. Given the interleaving, different components of each signal point in the rotated constellation are subject to independent channel fading. To detect the source message, the destination reorders the received components. After this deinterleaving operation, the resulting signals can be expressed as

$$\begin{aligned} r_1 &= \Re\left(h_{S,D}\sqrt{E_S}w_b + n_{S,D}\right) + j\Im\left(h_{R,D}\sqrt{E_R}w_r + n_{R,D}\right), \\ r_2 &= \Re\left(h_{R,D}\sqrt{E_R}w_r + n_{R,D}\right) + j\Im\left(h_{S,D}\sqrt{E_S}w_b + n_{S,D}\right), \end{aligned} \tag{5.7}$$

where $n_{S,D}$ and $n_{R,D}$ denote the AWGN noise in the $S \rightarrow D$ and $R \rightarrow D$ links, respectively.

Finally, ML detection is applied on the reordered signals. Thus,

$$\hat{x}_k = \arg\min_{x\in\chi}\left(|\Re(r_1) - \sqrt{E_S}h_{S,D}\Re(x)|^2 + |\Im(r_1) - \sqrt{E_R}h_{R,D}\Im(x)|^2\right),$$
$$\hat{x}_m = \arg\min_{x\in\chi}\left(|\Re(r_2) - \sqrt{E_R}h_{R,D}\Re(x)|^2 + |\Im(r_2) - \sqrt{E_S}h_{S,D}\Im(x)|^2\right). \quad (5.8)$$

Fig. 5.2 provides an illustration for the operation of the system in Case 1, i.e., when the relay successfully decodes the broadcast signal and is active in the relaying phase.

Unsuccessful Decoding at the Relay

As depicted in Fig. 5.2, there is a possibility that the relay fails to decode its received signal ($\hat{w}_b \neq w_b$) and, thus, is not able to produce w_r correctly. In this case, the relay remains silent [2] and the destination detects the source signal based on w_b only, since w_b carries enough information to detect both signal points, x_k and x_m. In other words, to detect the source signal, node D relies on w_b which was received during the broadcast phase:

$$\hat{w}_b = \arg\min_{w\in W}\left[h_{S,D}\sqrt{E_S}w_b + n_{S,D} - h_{S,D}\sqrt{E_S}w\right]. \quad (5.9)$$

In this case, the end-to-end SNR is $\gamma_{\text{e2e}} = \gamma_{S,D}$. Thus, the PDF of γ_{e2e} is given by $f_{\gamma_{S,D}}(\gamma) = \frac{1}{\bar{\gamma}_{S,D}}\exp\left(-\frac{\gamma}{\bar{\gamma}_{S,D}}\right)$.

5.3 Performance Analysis

In this section, we assess the performance of the SSD based relaying system. The analysis is based on the end-to-end SNR that we obtained in the previous section, i.e., $\gamma_{\text{e2e}} = \gamma_{S,D} + \gamma_{R,D}$ for the case when the relay successfully decodes the broadcast signal and $\gamma_{\text{e2e}} = \gamma_{S,D}$ when the relay fails to do so. The performance criteria are the error probability, asymptotic error probability, outage probability and Ergodic capacity, which offer good insights into system performance and also provide suitable tools for the design of SSD based relaying systems.

[2] We assume that the relay knows that it has failed to decode the received signal, and must hence remain silent.

5.3.1 Error Probability

Given the independence between the channel coefficients, $h_{S,D}$, $h_{R,D}$ and $h_{S,R}$, the average error probability of the SSD based relaying system can be written as

$$\bar{P}_e = \bar{P}_R \bar{P}_{\text{Direct}} + (1 - \bar{P}_R)\bar{P}_{\text{Coop}}, \tag{5.10}$$

where $\bar{P}_R$ is the average probability that the relay decodes the source signal incorrectly at the end of the broadcast phase, $\bar{P}_{\text{Direct}}$ is the average error probability at the destination when the relay fails to decode the source message and $\bar{P}_{\text{Coop}}$ denotes the average error probability at the destination when the relay is active in the relaying phase. We define $E(x;\hat{x})$ as the error event denoting that $\hat{x}$ is selected at the decoder instead of x. If all signal points in the original constellation have equal probability of occurrence, then, by applying the union bound, the conditional error probability that the relay decodes the source message incorrectly at the end of the broadcast phase upon deterministic source-relay channel can be upper-bounded as follows:

$$P_R = \frac{1}{|W|} \sum_{x \in \chi} \bigcup_{\hat{x} \neq x} E(x, \hat{x}|h_{S,R}) \leq \frac{1}{|W|} \sum_{x \in \chi} \sum_{\hat{x} \neq x} \texttt{PEP}(x, \hat{x}|h_{S,R}), \tag{5.11}$$

where $\texttt{PEP}(x, \hat{x}|h_{S,R})$ is the conditional pairwise error probability of selecting $\hat{x}$ at the relay when x is transmitted and where $|W|$ represents the number of constellation points in the new constellation. As we assume that the channel coefficients are constant during each transmission block, for M-PSK modulation $\texttt{PEP}(x, \hat{x}|h_{S,R})$ can be expressed as [57, Eq.(13. 12)]:

$$\texttt{PEP}(x, \hat{x}|h_{S,R}) = Q\left(\sqrt{\frac{E_S h_{S,R}^2 |x - \hat{x}|^2}{2N_0}}\right). \tag{5.12}$$

Therefore, Eq. (5.11) can be rewritten as

$$P_R \leq \frac{1}{|W|}\sum_{x\in\chi}\sum_{\hat{x}\neq x} Q\left(\sqrt{\frac{E_S h_{S,R}^2 |x-\hat{x}|^2}{2N_0}}\right) \leq (|W|-1)Q\left(\sqrt{\frac{d_{\min}(W)}{2}\gamma_{S,R}}\right), \tag{5.13}$$

where $d_{\min}(W)$ denotes the minimum distance in the constellation W, defined by $d_{\min}(W) = \min_{w_1,w_2\in W}(|w_1-w_2|^2)$. Finally, the average error probability that the relay decodes the source message incorrectly at the end of the broadcast phase, can be upper-bounded using

$$\bar{P}_R \leq (|W|-1)\int_0^\infty Q\left(\sqrt{\frac{d_{\min}(W)}{2}\gamma_{S,R}}\right) f_{\gamma_{S,R}}(\gamma_{S,R})d\gamma_{S,R}, \tag{5.14}$$

where $f_{\gamma_{S,R}}(\gamma) = \frac{1}{\bar{\gamma}_{S,R}}\exp\left(-\frac{\gamma}{\bar{\gamma}_{S,R}}\right)$ is the PDF of $\gamma_{S,R}$. It is easy to show that the integral in (5.14) can be solved as

$$\bar{P}_R \leq \frac{|W|-1}{2}\left[1-\sqrt{\frac{d_{\min}(W)\bar{\gamma}_{S,R}/4}{1+d_{\min}(W)\bar{\gamma}_{S,R}/4}}\right]. \tag{5.15}$$

Using a similar approach, an upper-bound for the average error probability at the destination when the relay fails to decode the source message, P_{Direct}, can be written as:

$$\bar{P}_{\text{Direct}} \leq \frac{|W|-1}{2}\left[1-\sqrt{\frac{d_{\min}(W)\bar{\gamma}_{S,D}/4}{1+d_{\min}(W)\bar{\gamma}_{S,D}/4}}\right]. \tag{5.16}$$

As for $\bar{P}_{\text{Coop}}$, the average error probability at the destination when the relay is active in the relaying phase, a corresponding upper-bound can be obtained by applying the union bound to the conditional error probability of P_{Coop} assuming that $h_{S,D}$ and $h_{R,D}$ are deterministic. Thus,

$$P_{\text{Coop}} \leq (|\chi|-1)\,\texttt{PEP}(x,\hat{x}|h_{R,D},h_{S,D}), \tag{5.17}$$

where $|\chi|$ represents the number of constellation points in the rotated constellation. Assuming that for any x and y, $d_{\min}(W) \leq (\Re(x) - \Re(y))^2$ and $d_{\min}(W) \leq (\Im(x) - \Im(y))^2$ [74, Eq.(16, 17)], then the conditional pairwise error probability can be written as [57, Eq.(13. 12)]:

$$\mathtt{PEP}(x, \hat{x}|h_{R,D}, h_{S,D}) = Q\left(\sqrt{\frac{E_S}{2N_0}\left(h_{S,D}^2\left(\Re(x) - \Re(y)\right)^2\right) + \frac{E_R}{2N_0}\left(h_{R,D}^2\left(\Im(x) - \Im(y)\right)^2\right)}\right)$$

$$\leq Q\left(\sqrt{\frac{d_{\min}(W)}{2}\left(\gamma_{S,D} + \gamma_{R,D}\right)}\right). \tag{5.18}$$

Then, by resorting to (5.6) and (5.18), the average error probability at the destination when the relay is active in the relaying phase, can be obtained as

$$\bar{P}_{\text{Coop}} = (|\chi| - 1)\times$$

$$\begin{cases} 1 - \frac{\bar{\gamma}_{S,D}}{\bar{\gamma}_{S,D}-\bar{\gamma}_{R,D}}\sqrt{\frac{d_{\min}(W)\bar{\gamma}_{S,D}/4}{1+d_{\min}(W)\bar{\gamma}_{S,D}/4}} + \frac{\bar{\gamma}_{R,D}}{\bar{\gamma}_{S,D}-\bar{\gamma}_{R,D}}\sqrt{\frac{d_{\min}(W)\bar{\gamma}_{R,D}/4}{1+d_{\min}(W)\bar{\gamma}_{R,D}/4}}, & \text{if } \bar{\gamma}_{S,D} \neq \bar{\gamma}_{R,D} \\ \frac{1}{4} - \frac{1}{2}\sqrt{\frac{d_{\min}(W)\bar{\gamma}}{4+d_{\min}(W)\bar{\gamma}}} + \frac{1}{4} \times \frac{d_{\min}(W)\bar{\gamma}}{4+d_{\min}(W)\bar{\gamma}} & \text{if } \bar{\gamma}_{S,D} = \bar{\gamma}_{R,D} = \bar{\gamma}. \end{cases} \tag{5.19}$$

Finally, substituting (5.19), (5.16) and (5.15) into (5.10), a closed-form expression for the average error probability of the SSD based relaying system can be written as

$$\bar{P}_e \approx \frac{|W| - 1}{2}\left[1 - \sqrt{\frac{d_{\min}(W)\bar{\gamma}_{S,R}/4}{1 + d_{\min}(W)\bar{\gamma}_{S,R}/4}}\right] \times \frac{|W| - 1}{2}\left[1 - \sqrt{\frac{d_{\min}(W)\bar{\gamma}_{S,D}/4}{1 + d_{\min}(W)\bar{\gamma}_{S,D}/4}}\right]$$

$$+ \left(1 - \frac{|W| - 1}{2}\left[1 - \sqrt{\frac{d_{\min}(W)\,\bar{\gamma}_{S,R}/4}{1 + d_{\min}(W)\,\bar{\gamma}_{S,R}/4}}\right]\right) \times (|\chi| - 1)\times \tag{5.20}$$

$$\begin{cases} 1 - \frac{\bar{\gamma}_{S,D}}{\bar{\gamma}_{S,D}-\bar{\gamma}_{R,D}}\sqrt{\frac{d_{\min}(W)\bar{\gamma}_{S,D}/4}{1+d_{\min}(W)\bar{\gamma}_{S,D}/4}} + \frac{\bar{\gamma}_{R,D}}{\bar{\gamma}_{S,D}-\bar{\gamma}_{R,D}}\sqrt{\frac{d_{\min}(W)\bar{\gamma}_{R,D}/4}{1+d_{\min}(W)\bar{\gamma}_{R,D}/4}}, & \text{if } \bar{\gamma}_{S,D} \neq \bar{\gamma}_{R,D} \\ \frac{1}{4} - \frac{1}{2}\sqrt{\frac{d_{\min}(W)\bar{\gamma}}{4+d_{\min}(W)\bar{\gamma}}} + \frac{1}{4} \times \frac{d_{\min}(W)\bar{\gamma}}{4+d_{\min}(W)\bar{\gamma}} & \text{if } \bar{\gamma}_{S,D} = \bar{\gamma}_{R,D} = \bar{\gamma}. \end{cases} \tag{5.21}$$

5.3.2 Asymptotic Analysis

The expression obtained above for the average error probability cannot offer insight into the system performance in an explicit way. In this part, we conduct an asymptotic analysis to evaluate the diversity order of the SSD based relaying system under study. An asymptotic expression for the error probability formula presented in (5.10) can be written as

$$\bar{P}_e = \bar{P}_R \bar{P}_{\text{Direct}} + \underbrace{(1 - \bar{P}_R)}_{\to 1} \bar{P}_{\text{Coop}} < \bar{P}_R \bar{P}_{\text{Direct}} + \bar{P}_{\text{Coop}}. \tag{5.22}$$

Using a similar approach as in [75], asymptotic expressions for $\bar{P}_R$, $\bar{P}_{\text{Direct}}$ and $\bar{P}_{\text{Coop}}$ can be found as

$$\bar{P}_R = \frac{|W|-1}{d_{\min}(W)} \frac{1}{\bar{\gamma}_{S,R}} = \frac{|W|-1}{\mathbf{E}\left(h_{S,R}^2\right) d_{\min}(W)} \left(\frac{1}{E_S/N_0}\right), \tag{5.23}$$

$$\bar{P}_{\text{Direct}} = \frac{|W|-1}{d_{\min}(W)} \frac{1}{\bar{\gamma}_{S,D}} = \frac{|W|-1}{\mathbf{E}\left(h_{S,D}^2\right) d_{\min}(W)} \left(\frac{1}{E_S/N_0}\right), \tag{5.24}$$

$$\bar{P}_{\text{coop}} = \frac{3(|\chi|-1)}{(d_{\min}(W))^2} \frac{1}{\bar{\gamma}_{S,D}\bar{\gamma}_{R,D}} = \frac{3(|\chi|-1)}{\mathbf{E}\left(h_{S,D}^2\right)\mathbf{E}\left(h_{R,D}^2\right)(d_{\min}(W))^2} \left(\frac{1}{(E_S/N_0)(E_R/N_0)}\right), \tag{5.25}$$

where $|W|$ and $|\chi|$ are the sizes of the new and the rotated constellations, respectively. Then, representing E_R as $E_R = \kappa E_S$, where $\kappa > 0$, the system's average error probability can be upper-bounded as

$$\bar{P}_e \leq \left[\frac{(|W|-1)^2}{\mathbf{E}\left(h_{S,R}^2\right)\mathbf{E}\left(h_{S,D}^2\right)(d_{\min}(W))^2} + \frac{3(|\chi|-1)}{\kappa \mathbf{E}\left(h_{S,D}^2\right)\mathbf{E}\left(h_{R,D}^2\right)(d_{\min}(W))^2}\right] \left(\frac{1}{E_S/N_0}\right)^2, \tag{5.26}$$

which implies that the diversity order of the system is two, since the power of E_S/N_0 in the right-hand-side of (5.26) is two. Indeed, a part of the diversity is due to the multiplication of $\bar{P}_R$ and $\bar{P}_{\text{Direct}}$ for the case that the relay fails to decode the broadcast signal, i.e., the term $\frac{(|W|-1)^2}{\mathbf{E}\left(h_{S,R}^2\right)\mathbf{E}\left(h_{S,D}^2\right)(d_{\min}(W))^2} \times \left(\frac{1}{E_S/N_0}\right)^2$ in (5.26). The other part of diversity is due to $\bar{P}_{\text{coop}}$ for the case that the relay successfully decodes the broadcast signal, i.e., the term $\frac{3(|\chi|-1)}{\kappa\mathbf{E}\left(h_{S,D}^2\right)\mathbf{E}\left(h_{R,D}^2\right)(d_{\min}(W))^2} \times \left(\frac{1}{E_S/N_0}\right)^2$ in (5.26).

5.3.3 Outage Probability

Considering N as the number of hops of the cooperative link, then the outage probability is defined as the probability that the mutual information, $I = \frac{1}{N}\log_2\left(1+\gamma_{\text{e2e}}\right)$, is less than a certain rate r. Taking into account that the relay can detect the signal correctly or not, the outage probability can be written as

$$\begin{aligned}
P_{\text{out}} &= \bar{P}_R P\left(\frac{1}{2}\log_2\left(1+\gamma_{S,D}\right)<r\right) + \left(1-\bar{P}_R\right)P\left(\frac{1}{2}\log_2\left(1+\gamma_{S,D}+\gamma_{R,D}\right)<r\right) \\
&= \bar{P}_R P\left(\gamma_{S,D}<2^{2r}-1\right) + \left(1-\bar{P}_R\right)P\left(\left(\gamma_{S,D}+\gamma_{R,D}\right)<2^{2r}-1\right) \\
&= \bar{P}_R \int_0^{2^{2r}-1} f_{\gamma_{S,D}}(\gamma)\,d\gamma + \left(1-\bar{P}_R\right)\int_0^{2^{2r}-1} f_{\gamma_{S,D}+\gamma_{R,D}}(\gamma)\,d\gamma, \qquad (5.27)
\end{aligned}$$

where $N=2$, given that the number of hops of the cooperative link is equal to two.

For the case that $\bar{\gamma}_{S,D} \neq \bar{\gamma}_{R,D}$, replacing $\bar{P}_R$, $f_{\gamma_{S,D}}(\gamma)$ and $f_{\gamma_{S,D}+\gamma_{R,D}}(\gamma)$ with their corresponding expressions obtained before, the outage probability is obtained as

$$\begin{aligned}
P_{\text{out}} \approx{} & 1 - K\exp\left(-\frac{2^{2r}-1}{\bar{\gamma}_{S,D}}\right) \\
& + (1-K)\left(\frac{\bar{\gamma}_{R,D}\exp\left(-\frac{2^{2r}-1}{\bar{\gamma}_{R,D}}\right) - \bar{\gamma}_{S,D}\exp\left(-\frac{2^{2r}-1}{\bar{\gamma}_{S,D}}\right)}{\bar{\gamma}_{S,D}-\bar{\gamma}_{R,D}}\right), \qquad (5.28)
\end{aligned}$$

where constant K is given by $K = \frac{|W|-1}{2}\left[1-\sqrt{\frac{d_{\min}(W)\bar{\gamma}_{S,R}/4}{1+d_{\min}(W)\bar{\gamma}_{S,R}/4}}\right]$.

Also, for the scenario that $\bar{\gamma}_{S,D} = \bar{\gamma}_{R,D} = \bar{\gamma}$, the outage probability is expressed as

$$P_{\text{out}} \approx 1 - K \times \exp\left(-\frac{2^{2r}-1}{\bar{\gamma}}\right) + (1-K) \times \left(-\left(1+\frac{2^{2r}-1}{\bar{\gamma}}\right)\exp\left(-\frac{2^{2r}-1}{\bar{\gamma}}\right)\right). \tag{5.29}$$

5.3.4 Ergodic vs. Outage Capacity

Ergodic capacity is the maximum achievable rate whereby errors are recovered through the transmission process. Taking into account that the relay can detect the broadcast signal correctly or not, the Ergodic capacity can be obtained, in [bits/sec/Hz], by

$$C_{\text{Ergodic}} = \frac{1}{N}\mathbf{E}\left[\log_2\left(1+\gamma_{\text{e2e}}\right)\right]$$

$$= \bar{P}_R \times \int_0^{\infty} \frac{1}{2}\log_2\left(1+\gamma\right) f_{\gamma_{S,D}}\left(\gamma\right) d\gamma + \left(1-\bar{P}_R\right)\int_0^{\infty} \frac{1}{2}\log_2\left(1+\gamma\right) f_{\gamma_{S,D}+\gamma_{R,D}}\left(\gamma\right) d\gamma, \tag{5.30}$$

where N was defined earlier as the number of hops of the cooperative link, i.e., N is equal to two. Considering non-identical source-destination and relay-destination links, i.e., $\bar{\gamma}_{S,D} \neq \bar{\gamma}_{R,D}$, and substituting $\bar{P}_R$, $f_{\gamma_{S,D}}\left(\gamma\right)$ and $f_{\gamma_{S,D}+\gamma_{R,D}}\left(\gamma\right)$ with their respective expressions obtained before, the Ergodic capacity can be expressed as

$$C_{\text{Ergodic}} \approx K\left(-\frac{1}{2\times\ln\left(2\right)}\exp\left(\frac{1}{\bar{\gamma}_{S,D}}\right)\text{E}_{\text{i}}\left(-\frac{1}{\bar{\gamma}_{S,D}}\right)\right)$$

$$+\left(1-K\right)\frac{1}{2\times\ln\left(2\right)\left(\bar{\gamma}_{S,D}-\bar{\gamma}_{R,D}\right)}$$

$$\times\left(-\bar{\gamma}_{S,D}\exp\left(\frac{1}{\bar{\gamma}_{S,D}}\right)\text{E}_{\text{i}}\left(-\frac{1}{\bar{\gamma}_{S,D}}\right)+\bar{\gamma}_{R,D}\exp\left(\frac{1}{\bar{\gamma}_{R,D}}\right)\text{E}_{\text{i}}\left(-\frac{1}{\bar{\gamma}_{R,D}}\right)\right), \tag{5.31}$$

where $\mathrm{E_i}(x) = \int_{-\infty}^{x} \frac{\exp(t)}{t} dt$ denotes the Exponential integral.

Using a similar approach, in the scenario with $\bar{\gamma}_{S,D} = \bar{\gamma}_{R,D} = \bar{\gamma}$, the Ergodic capacity reduces to

$$C_{\text{Ergodic}} \approx \frac{1}{2 \times \ln(2)} \left(\left(\frac{1}{\bar{\gamma}} - 1 \right) \exp\left(\frac{1}{\bar{\gamma}} \right) \mathrm{E_i}\left(-\frac{1}{\bar{\gamma}} \right) + 1 \right)$$

$$- \frac{1}{2 \times \ln(2)} K \left(\left(\frac{1}{\bar{\gamma}} \right) \exp\left(\frac{1}{\bar{\gamma}} \right) \mathrm{E_i}\left(-\frac{1}{\bar{\gamma}} \right) + 1 \right). \tag{5.32}$$

For slowly varying channels, outage capacity is used where the instantaneous SNR (γ_{e2e}) is considered to be constant for large number of symbols. For received SNRs below a threshold value, i.e., $\gamma_{\min}$, the received signal cannot be successfully decoded, and hence, the system is in outage. Since the instantaneous CSI is not known at the transmitter, the system transmits considering a fixed data rate, $C_{\text{out}} = \frac{1}{N} \log_2(1 + \gamma_{\min})$, which is successfully decoded with probability $1 - P_{\text{out}}$ and $\gamma_{\min} = 2^{2r} - 1|_{r=r_{\min}}$.

5.4 System Optimization

Based on the analysis presented so far, in this section we present two optimization processes for the SSD based relaying system. First, we investigate an optimization procedure aiming at minimizing the error probability and accordingly, enhancing the system performance. In the second scenario, we introduce an optimization procedure to minimize the energy expenditure while satisfying a constraint on the error probability.

5.4.1 Minimizing the Error Probability

Here, we introduce a two-phase optimization procedure. Indeed, it is feasible to minimize the error probability by maximizing the minimum distance of the new constellation W in one phase, and, by allocating the energy resource optimally between the source and the relay subject to a constraint on the total energy budget, in a second phase. In fact, since the minimum distance of the new constellation and the source energy are two major factors in determining the error probability, the optimization procedure can be accomplished in two steps as follows.

Phase 1

In the SSD technique, the minimum distance of the new constellation W is a function of the rotation angle θ [36]. On the other hand, the said minimum distance has an important impact the system's performance, as shown in the expressions obtained for the different performance metrics in the previous section. For instance, maximizing the minimum distance among the signal points in the new constellation, i.e. $d_{\min}(W)$, can effectively reduce the error probability at the relay and contribute to enhancing the overall performance. Therefore, the value of θ should properly be chosen. For any modulation used, we need to determine the optimum rotation angle. As an example, for QPSK modulation, the new constellation is symmetric with respect to the real and the imaginary axes. As such, two distance criteria can be defined as [74, Eqs. (22, 23)]:

$$d_1 = 2\cos\left(\theta + \frac{\pi}{4}\right) \quad \text{and} \quad d_2 = \sin\left(\theta + \frac{\pi}{4}\right) - \cos\left(\theta + \frac{\pi}{4}\right), \tag{5.33}$$

where the rotation angle θ takes values in the range of 0 to $\frac{\pi}{4}$ radian. For any θ, the minimum distance is $d_{\min}(W) = \min(d_1, d_2)$. Maximizing the minimum distance requires $d_1 = d_2$. Therefore, the optimum rotation angle is determined by $d_1 = d_2$, that is by solving $2\cos\left(\theta + \frac{\pi}{4}\right) = \sin\left(\theta + \frac{\pi}{4}\right) - \cos\left(\theta + \frac{\pi}{4}\right)$, which yields $\theta_{\text{opt}} = 0.4643$ radian ≈ 27 degrees.

Phase 2

In order to obtain minimum error probability in the system, the energy budget, E_T, is optimally split between the source and the relay. For such, resorting to the expressions given in (5.21), (5.22), (5.23) and using the fact that $\bar{P}_e \leq \bar{P}_R \bar{P}_{\text{Direct}} + \bar{P}_{\text{coop}}$, we can formulate the optimization problem as

$$\text{minimize} \qquad \bar{P}_e = a\left(\frac{N_0}{E_S}\right)^2 + b\frac{N_0^2}{E_S \times E_R}$$

$$\text{subject to :}\qquad E_S + E_R \leq E_T,\quad E_S > 0 \quad \text{and} \quad E_R > 0, \tag{5.34}$$

where $a = \frac{(|W|-1)^2}{\mathbf{E}\left(h_{S,R}^2\right)\mathbf{E}\left(h_{S,D}^2\right)(d_{\min}(W))^2}$ and $b = \frac{3(|\chi|-1)}{\mathbf{E}\left(h_{S,D}^2\right)\mathbf{E}\left(h_{R,D}^2\right)(d_{\min}(W))^2}$. The objective function in (5.34) decreases as E_S and E_R increase. Thus, the optimal solution occurs when the summation of E_S and E_R takes its maximum value, i.e., E_T. The Lagrange cost function can be expressed as

$$\Upsilon = a\left(\frac{N_0}{E_S}\right)^2 + b\frac{N_0^2}{E_S \times E_R} + \lambda\left(E_S + E_R - E_T\right), \tag{5.35}$$

where λ denotes the Lagrange parameter. Then, evaluating the derivatives of Υ with respect to E_S, E_R and λ, and setting them to zero, we obtain

$$\frac{\partial \Upsilon}{\partial E_S} = -2aN_0^2 E_S^{-3} - bN_0^2 E_R^{-1} E_S^{-2} + \lambda = 0. \tag{5.36}$$

$$\frac{\partial \Upsilon}{\partial E_R} = -bN_0^2 E_S^{-1} E_R^{-2} + \lambda = 0. \tag{5.37}$$

$$\frac{\partial \Upsilon}{\partial \lambda} = E_S + E_R - E_T = 0. \tag{5.38}$$

Solving the above equations, the optimal energy values for E_S and E_R in the two-phase optimization procedure are obtained as

$$E_S^* = E_T\left(\frac{2\lambda - \tau - \sqrt{\tau^2 + 4\lambda\tau}}{2\left(\lambda - 2\tau\right)}\right), \tag{5.39}$$

$$E_R^* = E_T\left(1 - \frac{2\lambda - \tau - \sqrt{\tau^2 + 4\lambda\tau}}{2\left(\lambda - 2\tau\right)}\right), \tag{5.40}$$

where $\lambda = 2\left(|W|-1\right)^2 \mathbf{E}\left(h_{R,D}^2\right)$ and $\tau = 3\left(|\chi|-1\right)\mathbf{E}\left(h_{S,R}^2\right)$. As observed, the optimum energies obtained are independent of the minimum distance of the new constellation,

$d_{\min}(W)$.

5.4.2 Minimizing the Total Energy

Now we present an optimization procedure that aims at minimizing the energy expenditure at the source and the relay subject to an error probability requirement. This optimization problem is formulated as follows:

$$\text{minimize} \quad E_S + E_R = E_T,$$

$$\text{subject to : } a\left(\frac{N_0}{E_S}\right)^2 + b\frac{N_0^2}{E_S \times E_R} \leq \bar{P}_e^{\max},\ E_S > 0 \text{ and } E_R > 0, \tag{5.41}$$

where $\bar{P}_e^{\max}$ denotes the maximum value tolerated for $\bar{P}_e$. The constraint function $a\left(\frac{N_0}{E_S}\right)^2 + b\frac{N_0^2}{E_S \times E_R}$ increases as E_S and E_R decrease. Hence, the optimal solution for the above optimization problem occurs when $a\left(\frac{N_0}{E_S}\right)^2 + b\frac{N_0^2}{E_S \times E_R}$ takes its maximum value, $\bar{P}_e^{\max}$. The Lagrange cost function can be written as

$$\Upsilon = E_S + E_R + \lambda\left(a\left(\frac{N_0}{E_S}\right)^2 + b\frac{N_0^2}{E_S \times E_R} - \bar{P}_e^{\max}\right), \tag{5.42}$$

where λ is the Lagrange parameter. Specifying the derivatives of Υ with respect to E_S, E_R and λ, and setting them to zero, we obtain

$$\frac{\partial \Upsilon}{\partial E_S} = 1 - 2\lambda a N_0^2 E_S^{-3} - \lambda b N_0^2 E_R^{-1} E_S^{-2} = 0. \tag{5.43}$$

$$\frac{\partial \Upsilon}{\partial E_R} = 1 - \lambda b N_0^2 E_S^{-1} E_R^{-2} = 0. \tag{5.44}$$

$$\frac{\partial \Upsilon}{\partial \lambda} = a\left(\frac{N_0}{E_S}\right)^2 + b\frac{N_0^2}{E_S \times E_R} - \bar{P}_e^{\max} = 0. \tag{5.45}$$

Then solving the equations (5.43), (5.44) and (5.45), the optimal energy values for E_S and E_R in the optimization procedure with constraint on the error probability, are obtained as:

$$E_S^* = N_0 \sqrt{\frac{2a + b + \sqrt{8ab + b^2}}{2\bar{P}_e^{\max}}}. \tag{5.46}$$

$$E_R^* = \frac{2b}{b + \sqrt{8ab + b^2}} N_0 \sqrt{\frac{2a + b + \sqrt{8ab + b^2}}{2\bar{P}_e^{\max}}}\ . \tag{5.47}$$

5.5 Numerical Results and Discussions

In this section, the performance of the SSD relaying system is discussed based on the analysis and optimization presented before. The two possible cases for the decoding output of the received signal at the relay are considered. For the scenario with successful decoding at the relay, the PDF of the end-to-end SNR follows the first condition in (5.6) when the $S \to D$ and $R \to D$ links are not identical ($\bar{\gamma}_{R,D} \neq \bar{\gamma}_{S,D}$). This situation is applied in Figs. 5.4 and 5.6. For the situation that $\bar{\gamma}_{S,R} = \bar{\gamma}_{R,D} = \bar{\gamma}_{S,D}$, the said PDF follows the second condition in (5.6). Such situation is applied in Figs. 5.3 and 5.5.[3] In the discussion, we focus on the impact of important parameters such as the rotation angle and the energies, at the source and the relay, on the system performance. For all figures shown, except Fig. 5.5, the results are plotted as a function of E_T/N_0 where $E_T = E_S + E_R$. For these figures, the precision of the analysis is validated by comparing the analytical results with Monte Carlo simulations. Furthermore, the error probability curves are obtained using QPSK modulation.

Fig. 5.3 illustrates the system error probability for different values of the rotation angle, $\theta = 5, 10, 15, 27, 35$ degrees based on (5.20). As observed, the minimum error probability is achieved at the rotation angle of 27 degrees, which is confirmed by analysis and simulation. Hereafter, the angle $\theta = 27^o$, unless otherwise stated.

[3]Note that the effect of the average SNR values of links $S \to R$, $R \to D$ and $S \to D$ on the system performance is equivalent to the effect of the source and the relay energies when these channels are identical, i.e., $\mathbf{E}\left(\left|h_{S,R}^2\right|\right) = \mathbf{E}\left(\left|h_{R,D}^2\right|\right) = \mathbf{E}\left(\left|h_{S,D}^2\right|\right)$.

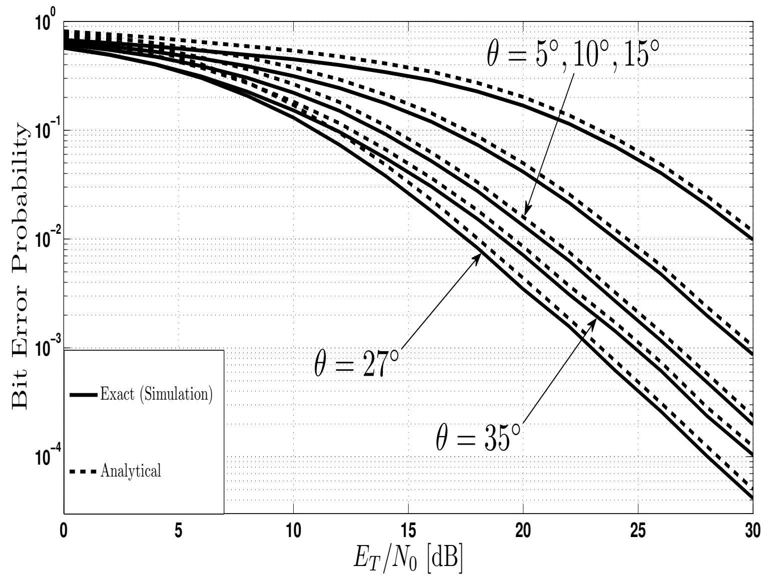

Figure 5.3: Error probability of the SSD relaying system for different values of the rotation angle θ.

To show the impact of the source node energy on the system performance, Fig. 5.4 plots the error probability according to (5.20) for several energy values, $E_S = 0.1, 0.2, 0.3, 0.5$ and $0.88E_T$, where $E_S = 0.5E_T$ represents the source energy for the equal-power allocation scheme and $E_S^* = 0.88E_T$ represents the energy obtained in two-phase optimization procedure according to (5.39). As observed, the error probability is minimized for the source energy $E_S^* = 0.88E_T$. Further, as expected, the curve obtained using the two-phase optimization procedure outperforms the one with equal-power allocation.

Fig. 5.5 is produced in association with the optimization procedure wherein the energy is minimized. The goal is to illustrate the source energy at which the total energy is minimized. In the figure, total energy curves (E_T/N_0 curves considering that the noise power is unity) are shown versus bit error probability for different values of the source node energy E_S. Note that according to the constraint function in (5.41) where $\bar{P}_e^{\max}$ is the maximum value of $\bar{P}_e$, the relay energy can be expressed as $E_R = \frac{bN_0^2 E_S}{\bar{P}_e^{\max} E_S^2 - aN_0^2}$. As $E_R > 0$, then $\bar{P}_e^{\max} E_S^2 - aN_0^2 > 0$ and, thus, $E_S > \sqrt{a/\bar{P}_e^{\max}}$. For the system under study, a is given as $a = 141.72$, then $E_S > \frac{11.90}{\sqrt{\bar{P}_e^{\max}}}$. Plots in Fig. 5.5 are generated for source energy values satisfying the latter condition. Also, using (5.46) and the fact that b is obtained as $b = 5.67$

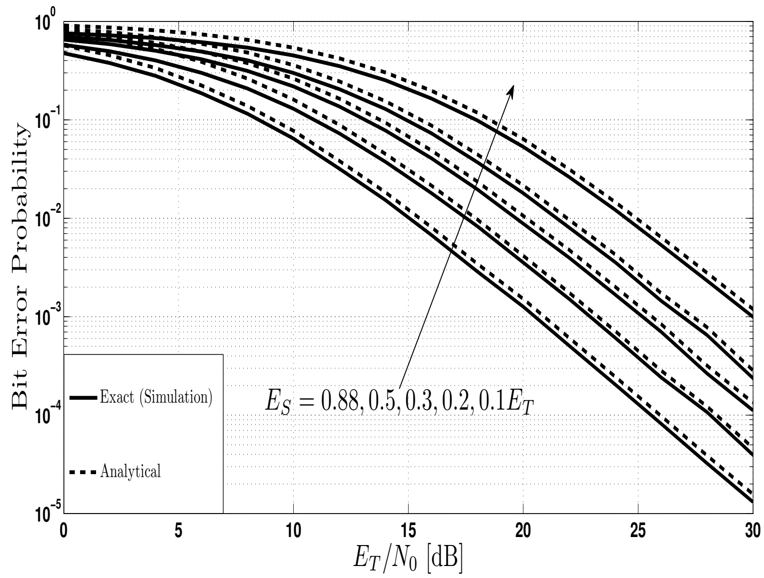

Figure 5.4: Error probability of the SSD based relaying system for different values of the source energy E_S.

for the considered system, the optimized source energy is obtained as $E_S^* = \frac{13.60}{\sqrt{\bar{P}_e^{\max}}}$. The figure illustrates that the total energy is minimized for this E_S^*. In this case, the relay energy is given by $E_R = \frac{1.79}{\sqrt{\bar{P}_e^{\max}}}$ and the minimum total energy is $E_T = \frac{15.39}{\sqrt{\bar{P}_e^{\max}}}$.

Fig. 5.6 shows the effect of the rate and the source energy on the outage performance. The results are obtained according to (5.28). Three different rates, $r = 0.75, 1.5$ and 2.25, and two values of the source energy, $E_S = 0.4E_T$ and $E_S = 0.65E_T$, are considered. As verified by simulation and analysis, the outage probability increases as the rate gets higher. Moreover, it is seen that the plot corresponding to $(E_S = 0.4E_T, r = 1.5)$ almost coincides with that of the case with $(E_S = 0.65E_T, r = 2.25)$. Indeed, the outage degradation due to increasing rate, e.g., from $r = 1.5$ to $r = 2.25$, can be compensated by increasing the source energy, e.g., from $E_S = 0.4E_T$ to $E_S = 0.65E_T$.

Finally, numerical results illustrating the Ergodic capacity of the SSD based relaying system are shown in Fig. 5.7. Here, the impacts of the source energy and of the rotation angle are examined. Two different source energy values are taken: $E_S = 0.5E_T$ which corresponds to the equal-power allocation scheme and $E_S = 0.88E_T$ represents the source

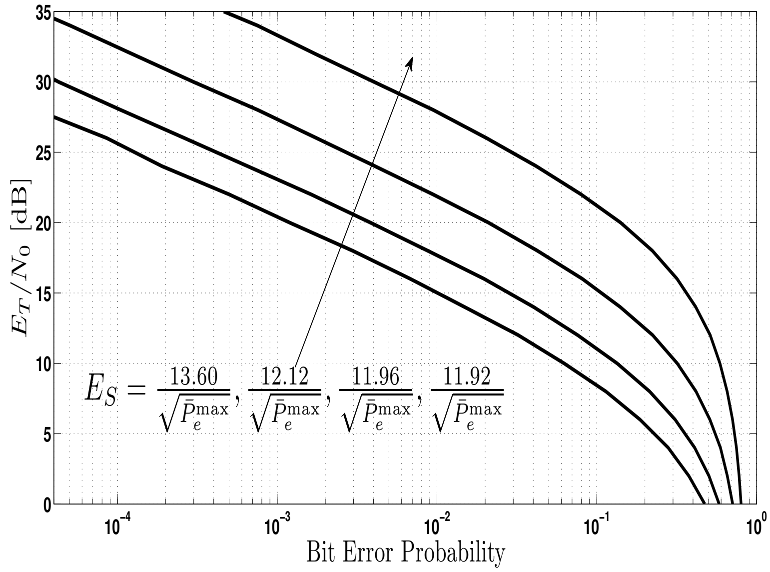

Figure 5.5: Total energy of the proposed SSD based relaying system for various source energy values.

energy for the two-phase optimization procedure. The results pertaining to $E_S = 0.5E_T$ and $E_S = 0.88E_T$ are obtained based on (5.32) and (5.31), respectively. As observed, the Ergodic capacity with the two phase-optimization procedure outperforms the result of the equal-power allocation scenario. We also consider two different rotation angles: 27^o (the optimal angle) and 44^o. As confirmed, the capacity is maximized at the optimal rotation angle and optimized source energy of $E_S = 0.88E_T$.

5.6 Summary

In this Chapter, cooperative communication based on SSD technique was investigated. For the case that the relay successfully decodes the broadcast signal, the receiver at the destination applies ML detection on the reordered signals to detect the source message from the outcome of the broadcasting and relaying phases. When the relay fails to decode the broadcast signal, the detection at the receiver relies on the signal received in the broadcasting phase. Considering Rayleigh fading and the general case of non-identical channels as well

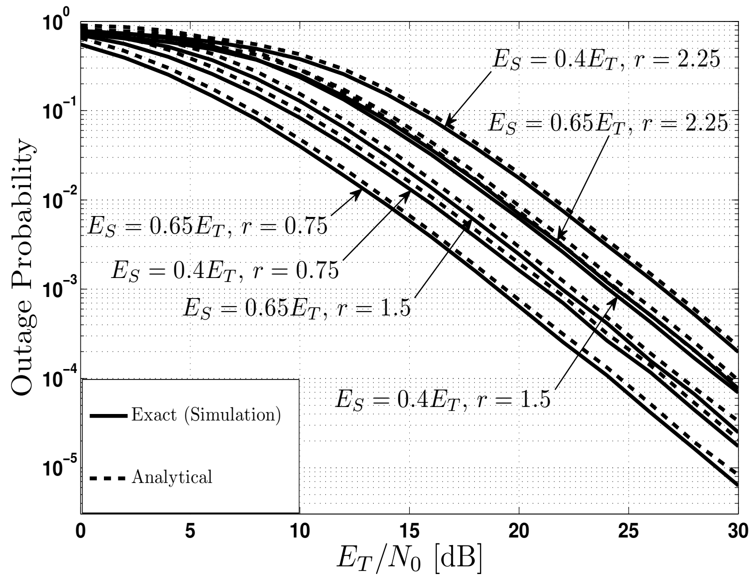

Figure 5.6: Outage probability of the SSD based relaying system for several values of the rate r and with different source energy values.

as the special case of identical channels, we conducted performance analysis in terms of error probability, outage probability and Ergodic capacity. Further, aiming at minimizing the error probability, we presented a two-phase optimization procedure to find the optimal transformation angle and the optimum source and relay energies. Following that, in order to minimize the total energy expenditure, we introduced an optimization procedure wherein the optimum source and relay energies were obtained subject to an error probability requirement. Numerical results were provided and the validity of the analysis was confirmed through simulations.

In the next Chapter, we study the performance of decode-and-forward multi-branch relaying networks operating in the presence of CCI.

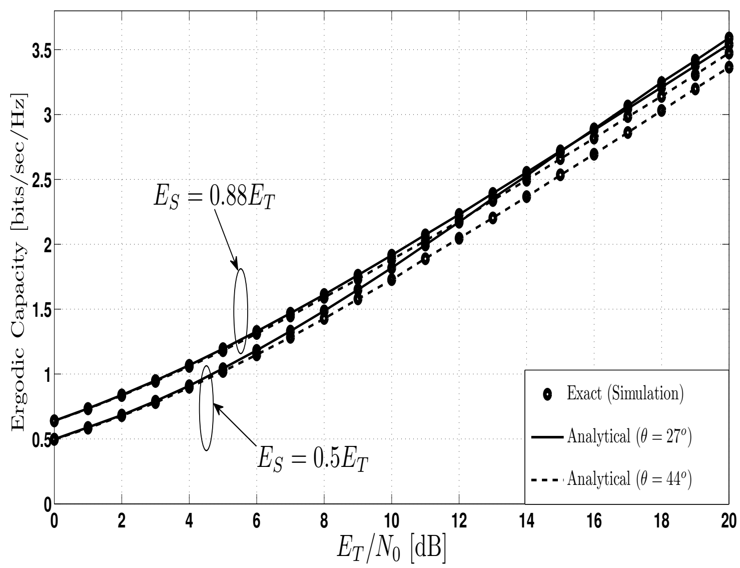

Figure 5.7: Ergodic capacity for different source energy values in two cases for the constellation rotation angle.

Chapter 6

Analysis of Reactive Multi-Branch Relaying under Interference and Nakagami-m fading [1]

6.1 Introduction

In this Chapter, performance of decode-and-forward multi-branch relaying networks operating in the presence of CCI is investigated. Relays assisting the transmission from the source to the end destination, are selected from a decoding set, which consists of the intermediate relays that decode the source message correctly, in a reactive way. In the reactive scheme, the relay whose corresponding branch results in the highest SINR at the destination is chosen. First, the exact end-to-end SINR is obtained, considering transmissions over Nakagami-m fading channels. Afterwards, using the theorem of total probability, the exact unconditional PDF of the end-to-end SINR is obtained. Based on the latter, exact closed-form expressions for the error and outage probabilities are derived. Furthermore, asymptotic expressions for the error probability are found according to the asymptotic analysis for the unconditional PDF of the end-to-end SINR, which provide better insights into

[1] Part of the material in this chapter is extracted from:
[76] A. H. Forghani, M. Xia, and S. Aïssa, "Analysis of reactive multi-branch relaying under interference and Nakagami-m fading," Submitted to *IEEE Trans. Veh. Tech.*, July 2014.

the impact of the system parameters on performance, such as determining the diversity order. Finally, the analysis is corroborated by comparing the numerical results with Monte Carlo simulations.

Using the concept of relaying, larger network coverage can be achieved by employing dual-hop transmissions, whereby the communication between a source and its far-end destination is performed over a single branch comprising an intermediate relay [77], or through multiple single-relay branches, where significant diversity gain can be achieved [55]. Such gains, however, can get significantly reduced due to the CCI originating from the frequency reuse for high spectrum efficiency. In the context of dual-hop relaying, considering that multiple relays work simultaneously together to forward their received signals to the destination, the inter-relay interference was analyzed in [14]. To avoid inter-relay interference, the technique of relay selection can be applied. In this vein, and for ease of mathematical tractability, the max-min criterion was generally applied in the related literature, see e.g. [16] and references therein. On the other hand, considering that the interference originates from external interfering sources, the effect of CCI at the destination was studied in [15], where the relaying nodes were assumed to be interference-free. In [78], the CCI was considered at both, the relaying nodes and the destination, but the AWGN was neglected at any node in the network, which makes the corresponding results inaccurate in the low and medium SNR regions. Taking CCI and AWGN into account, at both the relaying nodes and the destination node, the system performance of DF relaying over Rayleigh fading channels were investigated in [79].

Recently, the performance of optimum combining used in a DF relaying network operating in the presence of Nakagami fading and CCI at the relaying nodes and at the destination was analyzed in [80]. However, the simultaneous functioning of multiple relays will introduce inter-relay interference if relays operate in the same band, or require larger bandwidth if they work in different band slots, needless to say that the synchronization among relays is challenging in practice.

In this Chapter, a general and comprehensive analysis of dual-hop multi-branch reactive relaying in the presence of CCI and AWGN is presented. The generality stems from the fact that Nakagami-m fading (which is a general type of fading by itself) is not only considered for all the desirable channels but also for all the interference channels that impact all the relays of the network as well as the destination node. Moreover, a practical scenario for the relay transmission is considered, whereby only the set of relays that detect the source signal successfully in the first transmission phase, can have an active reaction during the second transmission phase. In this reactive scheme, the relay whose corresponding branch yields the highest SINR at the destination forwards its received signal to the destination during the second phase.

In the following, after detailing the system and the channel models in section II, the system performance is analyzed in terms of the end-to-end outage and error probabilities in section III. In particular, by using the theorem of total probability, an exact expression for the unconditional PDF of the end-to-end SINR is explicitly derived. With the resulting PDF, exact closed-form expressions for the outage and error probabilities are obtained. Moreover, to assess the effect of the fading parameters and the CCI on the system performance, an asymptotic expression for the error probability is derived and the diversity order is explicitly given. Afterwards, numerical and simulation results along with insightful discussions are presented in section IV and, finally, concluding remarks are given in the last section.

6.2 System and Channel Models

We consider a reactive multi-branch dual-hop DF relaying network, where the source, S, communicates with the destination, D, via N branches, with branch n consisting of an intermediate relay, $\mathrm{R}_n = 1, \cdots, N$. Each relay as well as the destination is interfered by L external co-channel interferers, I_l, $l = 1, \cdots, L$. In general, the number and the energy of interferers at each node may vary. However, for ease of mathematical tractability and gaining insight into the system performance, we study the simplified case where the number and the energy of interferers at each node are identical.

Consider the first phase of transmission, the signal received at the relay in the n^{th} branch, is a combination of a faded noisy signal received from the source and faded CCI signals originating from L external interferers. Mathematically, the signal received at relay

R_n can be expressed as

$$y_n = \sqrt{E_{\mathrm{S}}}\alpha_{\mathrm{S},n}x_{\mathrm{S}} + \sqrt{E_{\mathrm{I}}}\sum_{l=1}^{L}\beta_{l,n}d_{l,n} + w_n, \tag{6.1}$$

where E_{S} denotes the energy of the transmit signal at the source; $\alpha_{\mathrm{S},n}$ is the channel coefficient from the source to relay R_n, subject to Nakagami-m fading, and x_{S} refers to the normalized transmit signal from the source (i.e. $\mathbf{E}\left\{|x_{\mathrm{S}}|^2\right\} = 1$, where the operator $\mathbf{E}$ means mathematical expectation). Also, in (6.1), the signal from the l^{th} interferer impacting the n^{th} relay is represented by $d_{l,n}$ with $\mathbf{E}\left\{|d_{l,n}|^2\right\} = 1$; the energy of each interferer is denoted by E_{I}; the channel coefficient from the l^{th} CCI to relay R_n is given by $\beta_{l,n}$ subject to Nakagami-m fading, and the last term, w_n, denotes the AWGN at R_n, with zero mean and variance N_0.

When a relay fails to decode the source message successfully, it remains silent and does not participate in the second transmission phase. Accordingly, we define a decoding set, C, which consists of the relays successfully decoding the source message. In the second phase, only the relays belonging to C are allowed to be active and may forward the processed signal to the destination in a reactive way. In other words, there are $K = |C|$ intermediate relays which may forward their received signals to the destination. For each of these relays, $c \in C$, the received signal at the destination can be written as

$$y_{c,\mathrm{D}} = \sqrt{E_{\mathrm{R}}}\alpha_{c,\mathrm{D}}x_c + \sqrt{E_{\mathrm{I}}}\sum_{l=1}^{L}\beta_{l,\mathrm{D}}d_{l,\mathrm{D}} + w_{\mathrm{D}}, \qquad c = 1, 2, \cdots, K, \tag{6.2}$$

where E_{R} denotes the energy of the signal transmitted from the c^{th} relay; $\alpha_{c,\mathrm{D}}$ is the Nakagami fading coefficient of the channel from the c^{th} relay to the destination, and x_c represents the transmit signal from the c^{th} relay, with $\mathbf{E}\left\{|x_c|^2\right\} = 1$. Also, in (6.2), the signal from the l^{th} interferer, $l = 1, 2, \cdots, L$, impacting the destination is represented by $d_{l,\mathrm{D}}$ with $\mathbf{E}\left\{|d_{l,\mathrm{D}}|^2\right\} = 1$; the energy of the interfering signal is identical to that as defined in (6.2) (i.e. E_{I}); the channel coefficient from the l^{th} interferer to the destination is represented by $\beta_{l,\mathrm{D}}$, subject to Nakagami fading with parameter m_{I}, and the last term, w_{D}, denotes the AWGN at the destination, with zero mean and variance N_0.

6.3 Exact PDF of the End-To-End SINR

In this section, we derive the exact PDF of the end-to-end SINR, starting with its conditional PDF given the set of successfully decoding relays.

6.3.1 Conditional PDF of the End-to-End SINR Given the Decoding Set

Based on the highest SINR criterion for relay selection, the end-to-end SINR at the destination node of the multi-branch DF relaying system, given C as the decoding set with $K = |C|$, can be expressed as

$$\gamma_{e2e|K} = \frac{\max\limits_{c \in C} \gamma_{c,\mathrm{D}}}{1 + \sum\limits_{\mathrm{l}=1}^{L} \gamma_{\mathrm{I}_{l,\mathrm{D}}}}, \tag{6.3}$$

where $\max\limits_{c \in C} \gamma_{c,\mathrm{D}}$ represents the maximum value among the terms $\gamma_{c,\mathrm{D}}$, $c \in C$, with $\gamma_{c,\mathrm{D}} = |\alpha_{c,\mathrm{D}}| \, E_{\mathrm{R}}/N_0$ being the SNR at the destination with respect to the transmission from the c^{th} relay, and where $\gamma_{\mathrm{I}_{l,\mathrm{D}}} = |\beta_{l,\mathrm{D}}|^2 \, E_{\mathrm{I}}/N_0$ denotes the INR at the destination with respect to the l^{th} interferer. Assuming that the channel from the c^{th} relay to the destination is subject to Nakagami fading with parameter m_g, the PDF of $\gamma_{c,\mathrm{D}}$ has Gamma distribution, given by

$$f_{\gamma_{c,\mathrm{D}}}(\gamma) = \left(\frac{m_g}{\bar{\gamma}_g}\right)^{m_g} \frac{\gamma^{m_g - 1}}{\Gamma(m_g)} \exp\left(-\gamma \frac{m_g}{\bar{\gamma}_g}\right), \tag{6.4}$$

where $\bar{\gamma}_g \triangleq \mathbf{E}\left\{|\alpha_{c,\mathrm{D}}|^2\right\} E_{\mathrm{R}}/N_0$ is the average SNR at the destination and $\Gamma(x) = \int_0^\infty t^{x-1} e^{-t} \mathrm{d}t$ is the Gamma function. In light of (6.4), the CDF of $\gamma_{c,\mathrm{D}}$ can be readily shown as

$$F_{\gamma_{c,\mathrm{D}}}(\gamma) = 1 - \sum_{i=0}^{m_g - 1} \frac{1}{i!} \left(\frac{m_g \gamma}{\bar{\gamma}_g}\right)^i \exp\left(-\frac{m_g \gamma}{\bar{\gamma}_g}\right). \tag{6.5}$$

In order to get the distribution function of the end-to-end SINR, we start with the numerator in the right-hand-side (RHS) of (6.3). Specifically, let $Z \triangleq \max_{c \in C} \gamma_{c,\mathrm{D}}$, in light of (6.5), the CDF of Z can be written as

$$F_Z(\gamma|K) = \left(1 - \sum_{i=1}^{m_g} \frac{1}{(i-1)!} \left(\frac{m_g\gamma}{\bar{\gamma}_g}\right)^{(i-1)} \exp\left(-\frac{m_g\gamma}{\bar{\gamma}_g}\right)\right)^K. \tag{6.6}$$

Moreover, in view of (6.4) and (6.5) and by recalling the theory of order statistics, the PDF of Z can be readily shown as

$$f_Z\left(\gamma|\, K\right) = K f_{\gamma_{c,\mathrm{D}}} F_{\gamma_{c,\mathrm{D}}}^{K-1} =$$

$$K\left(\frac{m_g}{\bar{\gamma}_g}\right)^{m_g} \frac{\gamma^{m_g-1}}{\Gamma(m_g)} \exp\left(-\gamma\frac{m_g}{\bar{\gamma}_g}\right)\left[1 - \sum_{i=1}^{m_g} \frac{1}{(i-1)!} \left(\frac{m_g\gamma}{\bar{\gamma}_g}\right)^{(i-1)} \exp\left(-\frac{m_g\gamma}{\bar{\gamma}_g}\right)\right]^{K-1}. \tag{6.7}$$

For further proceeding, the multi-nominal theorem is exploited to expand the last power term in the RHS of (6.7). More specifically, by recalling the multi-nominal theorem, it is clear that

$$\left(\sum_{i=1}^{p} \gamma_i\right)^q = \sum_{k_1,k_2,\cdots,k_p} \binom{q}{k_1, k_2, \cdots, k_p} \prod_{i=1}^{p} \gamma_i^{k_i}, \tag{6.8}$$

here the summation operator means to take over all possible sequences of non-negative integer indices k_i, $i = 1, \cdots, p$, such that $\sum_{i=1}^{p} k_i = q$. The term $\binom{q}{k_1,k_2,\cdots,k_p} = \frac{q!}{k_1!k_2!\cdots k_p!}$ is known as a multi-nomial coefficient. In the case of $p = 2$, (6.8) reduces to the binomial theorem. Then, by comparing (6.8) with the last power term on the RHS of (6.7), we have

$$\begin{aligned}
&\gamma_1^{k_1} = 1\\
&\gamma_2^{k_2} = \frac{-1}{[(1-1)!]^{k_2}} \left(\frac{m_g\gamma}{\bar{\gamma}_g}\right)^{k_2(1-1)} \exp\left(-\frac{k_2 m_g\gamma}{\bar{\gamma}_g}\right)\\
&\cdots\\
&\gamma_t^{k_t} = \frac{-1}{[(t-2)!]^{k_t}} \left(\frac{m_g\gamma}{\bar{\gamma}_g}\right)^{k_t(t-2)} \exp\left(-\frac{k_t m_g\gamma}{\bar{\gamma}_g}\right)\\
&\cdots
\end{aligned}$$

$$\gamma_{m_g+1}^{k_{m_g+1}} = \frac{-1}{[(m_g-1)!]^{k_{m_g+1}}} \left(\frac{m_g\gamma}{\bar{\gamma}_g}\right)^{k_{m_g+1}(m_g-1)} \exp\left(-\frac{k_{m_g+1}m_g\gamma}{\bar{\gamma}_g}\right). \tag{6.9}$$

Subsequently, the product of the above terms can be written as

$$\gamma_1^{k_1}\prod_{t=2}^{m_g+1}\gamma_t^{k_t} = \left(\frac{m_g\gamma}{\bar{\gamma}_g}\right)^{\sum_{t=2}^{m_g+1}k_t(t-2)} \exp\left(-\frac{m_g\gamma}{\bar{\gamma}_g}\sum_{t=2}^{m_g+1}k_t\right)\prod_{t=2}^{m_g+1}\frac{-1}{[(t-2)!]^{k_t}}. \tag{6.10}$$

Finally, by applying (6.8) and (6.10) to (6.7) and performing some algebraic manipulations, $f_Z(\gamma|\, K)$ can be rewritten as

$$\begin{aligned} f_Z(\gamma|K) =& \frac{K}{\Gamma(m_g)}\sum_{k_1,k_2,\cdots,k_{m_g+1}}\binom{K-1}{k_1,k_2,\cdots,k_{m_g+1}}\left(\frac{m_g}{\bar{\gamma}_g}\right)^{m_g+\sum_{t=2}^{m_g+1}k_t(t-2)} \\ &\times\gamma^{m_g-1+\sum_{t=2}^{m_g+1}k_t(t-2)}\exp\left(-\frac{\gamma m_g\left(1+\sum_{t=2}^{m_g+1}k_t\right)}{\bar{\gamma}_g}\right)\prod_{t=2}^{m_g+1}\frac{-1}{[(t-2)!]^{k_t}}. \end{aligned} \tag{6.11}$$

Now, let $Y \triangleq \sum_{l=1}^{L}\gamma_{\mathrm{I}_{l,\mathrm{D}}}$. Since the variables $\gamma_{\mathrm{I}_{l,\mathrm{D}}}$, $l = 1, 2, \cdots, L$, are i.i.d., the PDF of Y is known to be given by [81]

$$f_Y(y) = \left(\frac{m_I}{\bar{\gamma}_I}\right)^{m_I L}\frac{y^{m_I L-1}}{\Gamma(m_I L)}\exp\left(-\frac{m_I}{\bar{\gamma}_I}y\right), \tag{6.12}$$

where $\bar{\gamma}_{\mathrm{I}} = \mathbf{E}\left\{|\beta_{l,\mathrm{D}}|^2\right\}E_{\mathrm{I}}/N_0$ denotes the average INR at the destination. In light of (6.3) and the definitions of Z and Y described earlier, we have $\gamma_{e2e|K} = \frac{Z}{1+Y}$ for short. Thus, it is straightforward that the PDF of $\gamma_{e2e|K}$ can be computed by

$$f_{\gamma_{e2e|K}}(\gamma|\, K) = \int_0^\infty (1+y)f_Z\left((1+y)\,\gamma|K\right)f_Y(y)\,dy. \tag{6.13}$$

Then, substituting (6.11) and (6.12) into (6.13) and performing some integration operations yield

$$f_{\gamma_{e2e|K}}\left(\gamma|\, K\right) = \sum_{k_1,k_2\cdots,k_{m_g+1}} A\gamma^B \left(\frac{m_I}{\bar{\gamma}_I}\right)^{m_I L} \exp\left(-\gamma D\right) U\left(m_I L; B + m_I L + 2; \gamma D + \frac{m_I}{\bar{\gamma}_I}\right), \tag{6.14}$$

where

$$A = \binom{K-1}{k_1, k_2, \cdots, k_{m_g+1}} \left(\frac{m_g}{\bar{\gamma}_g}\right)^{m_g + \sum_{t=2}^{m_g+1} k_t (t-2)} \times \prod_{t=2}^{m_g+1} \frac{-1}{\left[(t-2)!\right]^{k_t}}, \tag{6.15}$$

$$B = m_g - 1 + \sum\nolimits_{t=2}^{m_g+1} k_t \left(t-2\right), \tag{6.16}$$

$$D = \frac{m_g \left(1 + \sum_{t=2}^{m_g+1} k_t\right)}{\bar{\gamma}_g}, \tag{6.17}$$

and $U\left(a, b, x\right) = \frac{1}{\Gamma(a)} \int_0^\infty t^{a-1} \left(1+t\right)^{b-a-1} \exp\left(-xt\right) dt$ denotes the confluent hypergeometric function of the second kind [82, Eq. (13.4.4)]. In particular, if B takes integer values, (6.14) reduces to [82, Eq. (13.2.8)]

$$\begin{aligned} f_{\gamma_{e2e|K}}\left(\gamma|\, K\right) = &\sum_{k_1,k_2\cdots,k_{m_g+1}} A\gamma^B \left(\frac{m_I}{\bar{\gamma}_I}\right)^{m_I L} \exp\left(-\gamma D\right) \\ &\times \sum_{k=0}^{B+1} \binom{B}{k} \frac{\left(m_I L\right)_k}{\left(\gamma D + \frac{m_I}{\bar{\gamma}_I}\right)^{m_I L + k}}, \end{aligned} \tag{6.18}$$

where the binomial coefficient $\binom{N}{k} = \frac{N!}{(N-k)!k!}$, and the Pochhammer's symbol $\left(x\right)_k = \Gamma\left(x+k\right)/\Gamma\left(x\right)$ if $k = 1, 2, \cdots$, and $\left(x\right)_0 = 1$.

6.3.2 Exact PDF of the End-To-End SINR

By recalling the theorem of total probability, the unconditional PDF of the end-to-end SINR can be expressed as

$$f_{\gamma_{\mathrm{e2e}}}(\gamma) = (P_{\mathrm{off}})^N \delta(\gamma) + \sum_{t=1}^{N} \binom{N}{t} (P_{\mathrm{off}})^{N-t} (1 - P_{\mathrm{off}})^t f_{\gamma_{\mathrm{e2e}}}(\gamma|t), \tag{6.19}$$

where P_{off} denotes the probability that a relay is off (i.e. inactive) during the second transmission phase while $(1 - P_{\mathrm{off}})$ represents the probability that a relay is on (i.e. active), and $\delta(\cdot)$ denotes the Dirac delta function. Notice that the first term on the RHS of (6.19) corresponds to the case where none of the N relays can decode their respective received signal successfully and, thus, the signal from the source cannot be delivered to the destination. In other words, in such a case the received SINR at the destination is zero, which is reflected by the Dirac delta function $\delta(\gamma)$. In order to obtain P_{off} involved in (6.19), we resort to the received SINR at a particular relay, given by

$$\gamma_n = \frac{\gamma_{\mathrm{S},n}}{1 + \sum\limits_{l=1}^{L} \gamma_{\mathrm{I}_{l,n}}}, \quad n = 1, \cdots, N, \tag{6.20}$$

where $\gamma_{\mathrm{S},n} = |\alpha_{\mathrm{S},n}| E_{\mathrm{S}}/N_0$ denotes the received SNR at the n^{th} relay, and $\gamma_{\mathrm{I}_{l,n}} = |\beta_{l,n}|^2 E_{\mathrm{I}}/N_0$ represents the INR at this relay with reference to the $l\mathrm{th}$ interferer. By using a similar method to the development of (6.14), the PDF of γ_n can be shown as

$$\begin{aligned} f_{\gamma_n}(\gamma) = \frac{1}{\Gamma(m_h)} \left(\frac{m_h}{\bar{\gamma}_h}\right)^{m_h} \left(\frac{m_I}{\bar{\gamma}_I}\right)^{m_I L} \gamma^{m_h - 1} \exp\left(-\frac{m_h}{\bar{\gamma}_h}\gamma\right) \\ \times U\left(m_I L; m_h + m_I L + 1; \frac{m_h}{\bar{\gamma}_h}\gamma + \frac{m_I}{\bar{\gamma}_I}\right), \end{aligned} \tag{6.21}$$

where m_h is the Nakagami fading parameter of the channel from the source and relays, and $\bar{\gamma}_h = \mathbf{E}\left\{|\alpha_{\mathrm{S},n}|^2\right\} E_{\mathrm{S}}/N_0$ means the average SNR at the $n\mathrm{th}$ relay. Hence, P_{off} can be computed as [39]:[2]

$$P_{\text{off}} = a\int_0^{\infty} \text{erfc}\left(\sqrt{b\gamma}\right) f_{\gamma_{S,n}}(\gamma)d\gamma$$
$$= a\left\{1 - \frac{(1-\mu)^{1/2}}{\mu^{m_{\text{I}}L}}\sum_{k=0}^{m_h-1}\left(\begin{array}{c}2k\\k\end{array}\right)\left(\frac{\mu}{4}\right)^k\sum_{i=0}^{k}\left(\begin{array}{c}k\\i\end{array}\right)\frac{(m_{\text{I}}L)}{\mu^i}\right.$$
$$\left.\times \text{U}\left(m_{\text{I}}L+i, m_{\text{I}}L+i-k+\frac{1}{2}, \frac{m_{\text{I}}}{\mu\bar{\gamma}_{\text{I}}}\right)\right\}, \tag{6.22}$$

where $\mu = m_h/(b\bar{\gamma}_h + m_h)$; parameter pair (a, b) are constants depending upon the type of modulation used, e.g. $(a, b) = (0.5, 1)$ for BPSK and $(a, b) = (0.5, 0.5)$ for QPSK, and $erfc\,(x)$ denotes the complementary error function. In particular, in order to derive (6.22) from (6.21), we first replace the hypergeometric function in (6.21) with its integral expression described earlier and, then, take the Laplace transform of $\gamma^{m_h-1}erfc\left(\sqrt{b\gamma}\right)$ with respect to γ, which results in an expression involving Gaussian hypergeometric function, denoted by ${}_2F_1\,(a, b; c; x)$ in general.

Then, rewriting Gaussian hypergeometric function by its series expansion shown in [83] and evaluating the resulting integral expression yields the intended (6.22).

Finally, by substituting (6.14) (or (6.18)) and (6.22) into (6.19), a closed-form expression for the PDF of the end-to-end SINR, i.e. $f_{\gamma_{e2e}}\,(\gamma)$, can be readily obtained. In the next section, the resulting $f_{\gamma_{e2e}}\,(\gamma)$ will be used to determine the error and outage probabilities of the considered system.

6.4 The System Performance Analysis

In this section, exact outage probability of the considered system is first derived. Then, the average error probability is obtained, upon which an asymptotic analysis is performed such that the diversity order is disclosed.

[2]In the presence of a large number of interferers, which is common in wireless environment, calculation of the error probability is carried out considering Gaussian distribution for the interference by using the central limit theorem (cf. [84] and references therein).

6.4.1 Exact Outage Probability

Now, we determine the end-to-end outage probability of the considered system. By definition, outage probability can be computed as per the CDF of the end-to-end SINR, namely,

$$\bar{P}_{\text{out}} = \int_0^{\gamma_{\text{th}}} f_{\gamma_{\text{e2e}}^{\text{Reac}}}(\gamma) d\gamma =$$

$$(P_{\text{off}})^N + \sum_{t=1}^{N} \binom{N}{t} (P_{\text{off}})^{N-t} (1 - P_{\text{off}})^t \underbrace{\int_0^{\gamma_{\text{th}}} f_{\gamma_{\text{e2e}}}(\gamma | t) d\gamma}_{P_{\text{out}|t}^{\text{Reac}}}, \tag{6.23}$$

where $P_{\text{out}|t}$ represents the outage probability given that the decoding set C consists of t relays.

If B takes non-integer values, by virtue of (6.14), $P_{\text{out}|t}$ can be readily shown to be given by

$$P_{\text{out}|t} = \sum_{k_1, k_2, \cdots, k_{m_g+1}} A \frac{\left(\frac{m_I}{\bar{\gamma}_I}\right)^{m_I L} D^{-B+1}}{\Gamma(m_I L)} \frac{(\gamma_{\text{th}} D)^{B+1} \Gamma(m_I L + B + 1)}{(B+1) \left(\gamma_{\text{th}} D + \frac{m_I}{\bar{\gamma}_I}\right)^{m_I L + B + 1}}$$

$$\times {}_2F_1\left(1, m_I L + B + 1; B + 1; \frac{\bar{\gamma}_I \gamma_{\text{th}} D}{\bar{\gamma}_I \gamma_{\text{th}} D + m_I}\right). \tag{6.24}$$

On the other hand, if B takes integer values, in light of (6.18), $P_{\text{out}|t}$ can be shown to expressed as

$$P_{\text{out}|t} = \sum_{k_1, k_2, \cdots, k_{m_g+1}} \frac{A D^{-B+1} B!}{\left(D \gamma_{\text{th}} + \frac{m_{\text{I}}}{\bar{\gamma}_{\text{I}}}\right)^{m_{\text{I}} L}}$$

$$\times\left[1-\sum_{i=0}^{B}\frac{(D_{\gamma_{\rm th}})^i}{i!}\left(\frac{m_{\rm I}}{\bar{\gamma}_{\rm I}}\right)^{m_{\rm I}L}\exp\left(-D_{\gamma_{\rm th}}\right)\sum_{K=0}^{i}\left(\begin{array}{c} i \\ k \end{array}\right)\frac{(m_I L)_k}{\left(D_{\gamma_{\rm th}}+\frac{m_{\rm I}}{\bar{\gamma}_{\rm I}}\right)^k}\right]. \tag{6.25}$$

Replacing $P_{{\rm out}|t}$ in (6.23) with its corresponding value in (6.24) or (6.25), the end-to-end outage probability can be readily obtained.

6.4.2 Exact Error Probability and the Diversity Order

With the resulting $f_{\gamma_{\rm e2e}}(\gamma)$ given by (6.19), the average error probability of the considered system can be shown to be expressed as [39]

$$\bar{P}_e = a\int_0^\infty {\rm erfc}\left(\sqrt{b\gamma}\right)f_{\gamma_{\rm e2e}}(\gamma)d\gamma \tag{6.26}$$

$$= (P_{\rm off})^N + a\sum_{t=1}^{N}\binom{N}{t}(P_{\rm off})^{N-t}(1-P_{\rm off})^t\underbrace{\int_0^\infty {\rm erfc}\left(\sqrt{b\gamma}\right)f_{\gamma_{\rm e2e}}(\gamma|t)d\gamma}_{\lambda_t}, \tag{6.27}$$

where λ_t can be evaluated as

$$\lambda_t^{=}\sum_{k_1,k_2\cdots,k_{m_g+1}} a - a\frac{(1-\sigma)^{1/2}}{\sigma^{m_I L}}\sum_{k=0}^{B}\binom{2k}{k}\left(\frac{\sigma}{4}\right)^k$$

$$\times\sum_{i=0}^{k}\binom{k}{i}\frac{(m_I L)_i}{\sigma^i}U\left(m_I L+i; m_I L+i-k+\frac{1}{1}; \frac{m_I}{\sigma\bar{\gamma}_I}\right), \tag{6.28}$$

where $\sigma \triangleq \frac{D}{b+D}$. Finally, replacing $P_{\rm off}$ and λ_t in (6.27) with their corresponding values given by (6.22) and (6.28), the average error probability is obtained.

Since the exact expressions pertaining to the outage probability and the error probability are very complex, to gain insight into the system performance, we perform an asymptotic analysis for the error probability so as to get the diversity order of the considered system. This parameter reveals the impact of the channel fading parameter and the CCI on the system performance. To this end, we consider an ideal case where all relaying nodes can decode the source signal successfully. In other words, the cardinality of the successfully decoding set is the total number of relays, i.e. $K = |C| = N$. Subsequently, the Taylor's series expansion of $f_{\gamma_{\mathrm{e2e}}}(\gamma)$ obtained based on (6.18) can be expressed as

$$f_{\gamma_{\mathrm{e2e}}}(\gamma) \approx \sum_{k_1, k_2, \cdots, k_{m_g+1}} A\gamma^B \sum_{k=0}^{B+1} \binom{B+1}{k} (m_I L)_k \left(\frac{\bar{\gamma}_I}{m_I}\right)^k, \tag{6.29}$$

where $k_1 + k_2 + \cdots + k_{m_g+1} = N - 1$. Then, substituting (6.29) into (6.26) and performing some algebraic manipulations, the average error probability can be shown to be approximately given by

$$\bar{P}_e \approx \sum_{k_1, k_2, \cdots, k_{m_g+1}} aA \frac{\Gamma\left(B + \frac{2}{1}\right)}{b^{B+1}\sqrt{\pi}} \frac{1}{B+1} \sum_{k=0}^{B+1} \binom{B+1}{k} (m_I L)_k \left(\frac{\bar{\gamma}_I}{m_I}\right)^k, \tag{6.30}$$

Finally, inserting the expression of A and B given respectively by (6.15) and (6.16) into (6.30) yields

$$\bar{P}_e \approx \sum_{k_1, k_2, \cdots, k_{m_g+1}} a \binom{|N| - 1}{k_1, k_2, \cdots, k_{m_g+1}} \prod_{t=2}^{m_g+1} \frac{-1}{[(t-2)!]^{k_t}} \frac{\Gamma\left(B + \frac{2}{1}\right)}{b^{B+1}\sqrt{\pi}}$$
$$\times \frac{1}{B+1} (m_I L)_k \left(\frac{\bar{\gamma}_I}{\bar{\gamma}_g}\right)^{m_g + \sum_{t=2}^{m_g+1} k_t (t-2)}. \tag{6.31}$$

Case I (Fixed CCI): In these conditions, the value of $\bar{\gamma}_{\mathrm{I}}$ is a constant regardless of $\bar{\gamma}_g$. Then, it is observed from (6.31) that the diversity order equals to the minimum among all the possible values of $m_g + \sum_{t=2}^{m_g+1} k_t (t-2)$ corresponding to all the possible cases with $k_1 + k_2 + \cdots + k_{m_g+1} = N - 1$. It is remarkable that the diversity order of each case with its specific k_t for $t = 1, 2, \cdots, m_g + 1$, is equal to $m_g + \sum_{t=2}^{m_g+1} k_t (t-2)$, due to the last term on the RHS of (6.31).

Case II (Fixed ratio of $\bar{\gamma}_{\mathrm{I}}/\bar{\gamma}_g$): In this case, the value of $\bar{\gamma}_{\mathrm{I}}$ increases linearly with $\bar{\gamma}_g$. It is seen from (6.31) that $\bar{P}_e$ depends only on the ratio of $\bar{\gamma}_{\mathrm{I}}/\bar{\gamma}_g$, regardless of the particular value of $\bar{\gamma}_{\mathrm{I}}$ or $\bar{\gamma}_g$. Therefore, increasing $\bar{\gamma}_g$ will not improve the error performance. Accordingly, the diversity order is zero and error floors will appear.

6.5 Numerical Results and Discussions

Numerical results are now presented to corroborate the analytical results obtained in relation with the outage probability and the error probability. In the Monte-Carlo simulation experiments, the modulation scheme is set to BPSK and the number of interferers impacting each relay and the destination is set to $L = 6$. The main target of the simulation experiments is to investigate the impact of varying channel parameters m_g (corresponding to the channel from relays to the destination) and m_{I} (corresponding to the channel from interferers to relays or the destination), as well as the ratio of $\bar{\gamma}_{\mathrm{I}}/\bar{\gamma}_g$, on the system performance. The simulation results are compared with the corresponding numerical results, and they are illustrated in Fig. 6.1 and Fig. 6.2 below as a function of E_{T}/N_0, where E_{T} denotes the total energy, defined by $E_{\mathrm{T}} = E_{\mathrm{S}} + NE_{\mathrm{R}}$ with E_{S} and E_{R} being the energies of the transit signals from the source and a relay, respectively. Also, the effect of large-scale path-loss is neglected by assuming a cluster of relaying nodes, which means that the distances between all the relays and the destination are identical.

Fig. 6.1 depicts the outage probability of dual-branch network $(N = 2)$ in the presence of fixed CCI ($\bar{\gamma}_{\mathrm{I}} = 0.02E_{\mathrm{T}}/N_0$), versus E_{T}/N_0 normalized to the outage threshold γ_{th}. Also, three different fading scenarios with $m_g = m_{\mathrm{I}} = 2, 3, 4$ are considered. For comparison purposes, under each fading scenario the simulation results in the absence of CCI are presented as well, as shown by the straight lines in Fig. 6.1.

It is seen from Fig. 6.1 that the numerical results computed as per (6.23) coincide perfectly with the simulation results, which demonstrates the effectiveness of the previous analysis. On the other hand, when the values of m_g and m_{I} increase from 2 to 3 till 4, the outage probability decreases accordingly, as expected. Finally, it is observed that the outage probability decreases slightly with E_{T}/N_0 at the low and medium range whereas an error floor appears at the high E_{T}/N_0 region. This is because the system performance is dominated by noise at the low and medium E_{T}/N_0 whereas by CCI in the high E_{T}/N_0 region. To the contrary, if there is no CCI at all, the outage probability decreases linearly with E_{T}/N_0, as shown by the straight lines in Fig. 6.1.

On the other hand, Fig. 6.2 depicts the bit error probability versus E_{T}/N_0, under three different interfering cases with fixed $\bar{\gamma}_{\mathrm{I}}/\bar{\gamma}_g$, i.e., the value of $\bar{\gamma}_{\mathrm{I}}$ increases linearly with $\bar{\gamma}_g$.

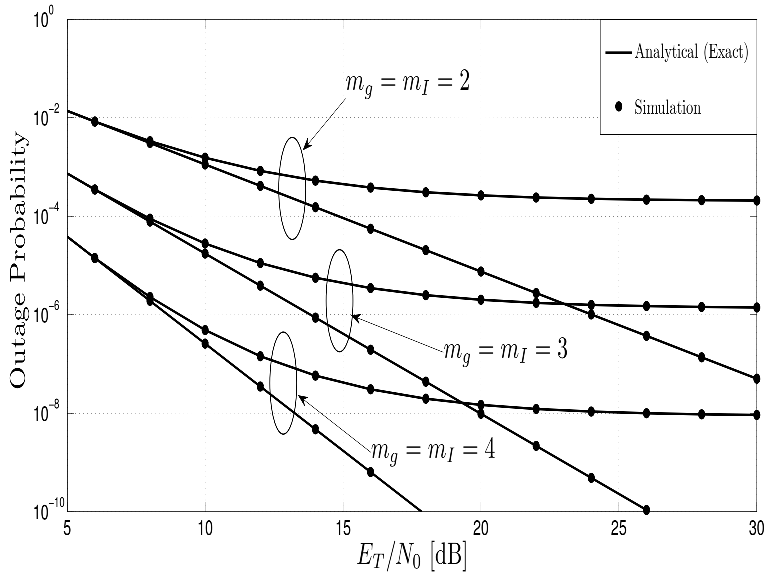

Figure 6.1: Outage probability of a dual-branch network ($N = 2$) in the presence of CCI (the number of interferers $L = 6$ and the average INR ($\bar{\gamma}_I = 0.02\frac{E_T}{N_0}$), for three different fading scenarios ($m_g = m_\mathrm{I} = 2, 3, 4$). For each scenario, the upper curve corresponds to the case in the presence of CCI whereas the lower straight line corresponds to the case in the absence of CCI.

Also, the fading parameters are set to $m_g = m_\mathrm{I} = 2$ in the ensuing simulation experiments. It is seen that the numerical results of the exact error probability computed by (6.27) agree very well with the simulation results and the asymptotic results computed by (6.31) are very tight with the simulation results. Also, an error floor appears in the high E_T/N_0 region, as predicated by the preceding analysis of the diversity order.

6.6 Summary

In this Chapter, the impact of CCI on the performance of reactive multi-branch dual-hop DF relaying systems was analytically investigated, assuming that the desired signals and all the interfering signals are subject to independent but not necessarily identical Nakagami-m fading. Based on the decoding set consisting of the relays which successfully decode the received signal, the best relay with the highest end-to-end SINR was chosen to assist the communication between the source and the destination. In such a scenario, the distribution

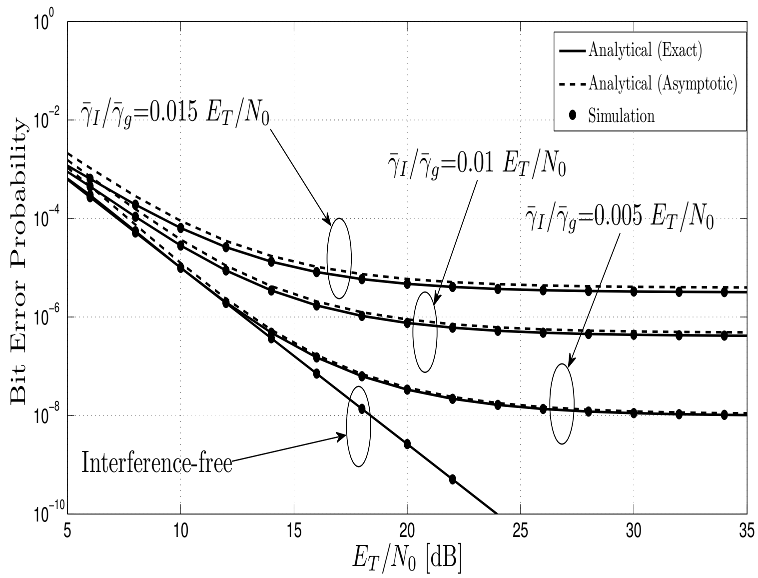

Figure 6.2: Bit error probability of a triple-branch network $(N = 3)$ in the presence of CC, where three different interfering cases $(\bar{\gamma}_I/\bar{\gamma}_g = 0.005, 0.01, 0.015)$ and the ideal interference-free scenario are considered.

functions of the end-to-end SINR were analytically obtained, which were further applied to derive the average error probability of the system. Our results can be used to efficiently evaluate the system performance without resort to time-consuming simulation experiments. In particular, our result pertaining to the diversity order predicts that an error floor will appear when the ratio of the total transmit power to noise power is high, since the system performance is strictly interference-limited.

Chapter 7

Conclusion

7.1 Conclusions of the Dissertation

In this thesis, tools for the design and management of different kinds of relaying networks in the field of wireless communications were provided. Several gaps in the performance analysis of practical relaying networks and the improvement in their performance were filled. In particular, performance evaluation and enhancement of MHMB relaying networks taking into account the practical issue of CCI were considered. Specifically, the focus was on the performance of MHMB relaying networks with multiple co-channel interferers affecting all nodes that take part in the end-to-end transmission from the source node to its final destination. Two scenarios were studied: with equal power or non-equal power interferers were assumed to affect each relay node in the network. The optimal gain, i.e., variable-gain coefficient, was applied at each relay. The performance of the network was assessed in terms of important performance criteria, namely, the bit error probability and the outage probability. Moreover, optimal power allocation was considered in order to improve the overall performance of the network.

Furthermore, signal space diversity as a technique to improve the performance was studied. The performance of relaying networks benefiting from SSD was investigated in terms of error probability, outage probability, Ergodic capacity (for slow fading channels) and outage capacity (for fast fading channels). Moreover, in order to enhance the system performance, the error probability of these networks were minimized subject to constraint on the total energy budget. The optimization of the performance whereby the total energy was minimized under constraint on the error probability was also investigated.

In addition to the above, by using a decoding set C in a cooperative network, the system performance was enhanced. The idea of using a decoding set implied that the relays which fail to decode their received signal in the first phase of signal transmission, do not take part in the second phase of signal transmission.

In Chapter 2, a closed-form approximate expression was derived to calculate the average bit error probability of MHMB cooperative networks considering transmission in the environment with independent and non-identical Rayleigh fading channels.

In Chapter 3, the performance of opportunistic AF MHMB relaying networks operating in the presence of CCI was investigated. Exact and upper-bound expressions for the end-to-end SINR were obtained, considering transmissions over independent non-identical Rayleigh fading channels. The CDF and the PDF of the upper-bound end-to-end SINR were obtained. Accordingly, a lower-bound closed-form expression for the outage probability was derived. Moreover, an approximation function for the PDF of the end-to-end SINR was obtained. Subsequently, simple expressions for the approximate error and outage probabilities were provided. the optimization of the power allocation among the transmit nodes was addressed to enhance the overall system performance.

Chapter 4 examined the performance of MHMB relaying networks using AF protocol and operating in practical environments with unequal-power interferers. Exact and upper-bound expressions were derived for the end-to-end SINR. Then, the MGF of the upper-bound end-to-end SINR was obtained. Based on this, the error and outage probabilities were assessed in closed form. Following that, simple expressions for the outage and error probabilities were provided.

The performance of relaying systems benefiting from SSD was studied in Chapter 5. Performance metrics such as error probability, asymptotic error probability, outage probability, Ergodic capacity and outage capacity were derived. In addition, a two-phase optimization procedure was presented. By applying the two-phase optimization, the performance of the system increased significantly. Furthermore, to significantly preserve the total energy, another optimization procedure was presented. In this optimization process, aiming at minimizing the total energy expenditure, the optimum source and relay energies were obtained subject to the error probability constraint.

In Chapter 6, the impact of CCI on the performance of reactive multi-branch dual-hop DF relaying systems was analytically investigated, assuming that the desired signals and all the interfering signals are subject to independent but not necessarily identical Nakagami-m fading. Based on the decoding set consisting of the relays which successfully decode the received signal, the best relay with the highest end-to-end SINR was chosen to assist the communication between the source and the destination. In such a scenario, the distribution functions of the end-to-end SINR were analytically obtained, which were further applied to derive the average error probability of the system. Our results can be used to efficiently evaluate the system performance without resort to time-consuming simulation experiments. In particular, our result pertaining to the diversity order predicts that an error floor will appear when the ratio of the total transmit power to noise power is high, since the system performance is strictly interference-limited.

7.2 Topics for Future Research

To the best of my knowledge, investigation of the performance and the optimization of MHMB relaying networks benefiting from the SSD technique in the presence of CCI has not been done so far, and therefore future research can be done in this direction. Although, studying the performance and the optimization of such systems might be extremely difficult, if it is properly done, it can provide tools for the design and management of relaying systems benefiting from the technique of SSD in the presence of CCI, in practice.

Furthermore, another interesting topic of research which has recently received a lot of attention is hybrid AF/DF relaying. Hybrid AF/DF relaying implies that each relay in a cooperative system can operate in AF or DF mode, depending on the decoding result of its received signal. Indeed, if a relay decodes its received signal correctly, it works in DF mode, otherwise, the relay switches to AF mode. In other words, the relay always transmits regardless of the decoding result of its received signal. This is a topic I am currently working on in the context of my postdoctoral research position.

Appendix A

Résumé de la Thèse

A.1 Motivation

A.1.1 Diversité Coopérative

Dans les communications sans fil, la mise en œuvre de plusieurs antennes afin d'offrir la diversité spatiale n'est pas tout le temps réalisable en pratique. C'est pourquoi la diversité coopérative qui emploie des relais pour aider les communications entre la source et la destination est apparu, et offre la diversité spatiale, sans l'exigence d'avoir plusieurs antennes [3,4] pour les émetteurs et/ou les récepteurs. En effet, la source, ensemble avec le(s) relais, offre un réseau virtuel d'antennes pour créer, d'une façon alternative, une diversité spatiale lorsque plusieurs antennes physiques ne sont pas disponibles. Dans cette thèse, des réseaux coopératifs, constitués de relais, sont étudiées. Avec la communication coopérative, il est possible de lutter contre l'évanouissement du signal dû à la propagation par trajets multiples et par conséquent, améliorer la performance du système ainsi que d'étendre la zone de couverture [5]. Deux stratégies de transmission bien connus, sont utilisés pour les relais en termes de traitement du signal qu'il reçoivent. La première stratégie consiste à amplifier et envoyer (*amplify-and-forward* (AF)), tandis que la deuxième consite à décoder et envoyer (*decode-and-forward* (DF)) le signal reçu. Sur la base sur la stratégie de relayage adoptée, je mets en œuvre différents protocoles de coopération, pour atteindre les critères de performance cibles, généralement définis en termes de la probabilité d'erreur, probabilité de coupure, et capacité [5].

A.2 Réseaux à Relais Multiples et Multi-sauts

En général, deux types de coopération sont possibles, dépendamment du nombre de sauts et de branches considérés, entre la source et la destination finale. Un saut consiste au passage d'un nœud à un autre, et une branche est le chemin entre le nœud source et le nœud de destination. Deux types de systèmes sont envisageables. Dans le premier type, les systèmes coopératifs à multi-saut avec branche unique sont considérés, tandis que dans l'autre type on considère les transmissions à saut double avec des relais sur branches multiples [11–13]. Avec la transmission multi-saut, il est possible d'atteindre une couverture plus élevée, tout en diminuant les effets liés aux défauts du canal de transmission. Par ailleurs, il est également très clair qu'en utilisant diverses branches qui sont différentes et indépendants, au lieu d'une seule branche, le gain de diversité peut être encore augmenté. Dans ce cas, plusieurs techniques de combinaison telles que la combinaison à rapport maximal (*maximal ratio combining (MRC)* ou la combinaison par sélection (*selection combining (SC)*), peuvent être appliquées au niveau du récepteur final.

A.2.1 Interférence Co-canal

La performance des réseaux coopératifs, dans leur forme générale de réseaux de relais avec multi-sauts et multi-branches (MSMB), dépend fortement de l'environnement dand lequel ils fonctionnent. Dans un contexte de transmission sans fil, en plus des dégradations liées à la propagation radio, l'interférence co-canal (CCI) peut affecter les performances du réseau de manière significative. La CCI est une forme de diaphonie qui provient de la réutilisation de fréquence, c'est à dire lorsque deux ou plusieurs émetteurs radio sont actifs dans la même bande de fréquence. Dans les réseaux de relais MSMB, plusieurs brouilleurs en dehors du réseau source-destination cible peuvent être actifs et donc agir en tant que sources d'interférences. Ces signaux indésirables peuvent dégrader la qualité du signal à la destination cible. Il est donc très important de les considérer lors de l'évaluation de la performance des réseaux de relais MSMB, et lors de la conception de stratégies de communication, afin d'assurer une grande efficacité dans la pratique. En fait, comme on le verra plus loin dans ce rapport, l'impact de la CCI peut affecter considérablement la performance, et nécessite des contre-mesures pour améliorer la performance de ces réseaux. Ces contre-mesures peuvent aller de l'optimisation de la façon dont les ressources sont partagées entre différents nœuds participants dans le réseau, à la mise en œuvre de techniques sophistiquées comme la diversité spatiale de signal (SSD).

Dans des études récentes sur les réseaux MSMB, l'accent est mis principalement sur la transmission elle-même, et on suppose que le réseau fonctionne dans un environnement sans interférences. Toutefois, l'étude de l'impact de la CCI sur les réseaux coopératifs MSMB n'est pas seulement importante, mais aussi nécessaire pour l'exploitation de systèmes sans fil coopératifs, dans la pratique. L'impact de la CCI sur l'efficacité des systèmes coopératifs est analytiquement étudié dans [14–17]. Dans ces articles, les auteurs supposent que l'interférence influe sur la destination et les nœuds relais, pour le type bien connu de réseau à double sauts. Par exemple, il est indiqué dans [16] que des interférences limitent le gain de diversité de systèmes à relais dit *channel state information (CSI)-assisted amplify-and-forward (AF)*, et peut réduire considérablement les performances des dits systèmes. L'interférence existe généralement en raison de la réutilisation du canal relais-destination, où le canal qui réutilise la fréquence peut créer des interférences, ce qui à son tour affecte la performance des autres nœuds de destination [14]. Dans [15], l'effet d'interférence sur la probabilité de coupure d'un réseau de relais AF dans un environnement à évanouissements Rayleigh est analysé.

A.2.2 Amélioration de la Performance

Différentes techniques peuvent être mises en œuvre pour accroître la performance de transmission dans les réseaux de relais. Ces techniques sont variées, et peuvent aussi être combinées ensemble, afin d'améliorer la performance. L'optimisation des ressources (par allocation optimale de la puissance), la diversité spatiale de signal (SSD), le choix d'un ensemble de décodage et l'utilisation de gain variable dans le relais, sont quelques unes de ces techniques. Nous les présentons brièvement dans ce qui suit.

A.2.3 Optimisation des ressources

Deux procédés d'optimisation pour les réseaux à relais peuvent être présentés, en considérant deux critères d'optimisation. Dans ces deux procédés d'optimisation, la répartition optimale de la puissance est réalisée entre le nœud source et le(s) nœud(s) relais participant à la transmission du signal. Tout d'abord, afin d'améliorer les performances du système, nous pouvons minimiser la probabilité d'erreur (et/ou la probabilité de coupure) du système, avec une contrainte sur la quantité totale d'énergie. Cela augmente considérablement la performance du système. Dans le second scénario, afin de préserver la quantité d'énergie totale, nous pouvons minimiser la dépense énergétique totale du système, avec une contrainte sur la probabilité d'erreur/coupure. Ainsi, l'énergie totale est conservée de manière significative.

A.2.4 Diversité Spatiale de Signal

La diversité spatiale de signal (SSD), également connue sous le nom de diversité de modulation, est considérée comme une technique pour améliorer la performance. En fait, l'application de la technique SSD dans un réseau de transmission peut améliorer la performance de ce réseau. Selon qu'on a l'évanouissement rapide ou l'évanouissement sélective en fréquence, ou si les canaux sont à antennes multiples (MIMO), la technique SSD apporte des gains en termes de diversité dans le temps, diversité de fréquence, et de diversité spatiale, respectivement. En utilisant la diversité de modulation, les vecteurs de symboles sont mis en rotation par une matrice d'étalement carré de telle sorte que deux vecteurs de symboles peuvent être distingués par le nombre maximal d'éléments distincts. Dans un réseau coopératif avec un relais, étant donné que ces composantes du vecteur de signal sont transmises à travers les chemins indépendants de la source vers la destination (un composant est envoyé à travers le trajet source-destination, tandis que l'autre composant est envoyé à travers le chemin relais-destination), le signal reçu à la destination est plus fiable et donc, le rendement du réseau est amélioré. En effet, en supposant qu'un évanouissement profond affecte un seul des composantes du vecteur de signal, la constellation tournée fournit une protection contre les effets défavorables du bruit comparé à la constellation non-tournée.

A.2.5 Sélection de Relais

Il peut y avoir une possibilité que le relais ne parvienne pas à décoder le signal reçu correctement, en supposant que le relais utilise la technique *decode-and-forward* pour générer et transmettre le signal traité aux relais suivants ou à la destination. Par conséquent, dans un réseau MSMB avec plusieurs relais, seuls les relais qui sont en mesure de décoder le signal reçu correctement, doivent participer à la transmission du signal. Soit C l'ensemble de décodage. Cet ensemble est constitué des relais qui sont en mesure de décoder le signal reçu correctement. Dans la deuxième phase, à savoir la phase de transmission, seuls les relais qui appartiennent à la série C sont autorisés à être actifs, et donc de retransmettre leurs signaux traités aux relais ultérieurs ou à la destination. L'utilisation de l'ensemble de décodage C mentionné ci-dessus peut améliorer les performances, car les relais qui ne parviennent pas à décoder leur signal reçu ne participent pas à la transmission du signal. Une telle approche est utilisée par le standard IEEE802.16j et la LTE version 10, et sa mise en œuvre en pratique nécessite l'utilisation de méthodes de détection d'erreurs telles que la redondance cyclique.

A.2.6 Relayage par Gain Variable

Il existe plusieurs choix pour le gain du relais, par exemple, le gain variable ou gain fixe. Le coefficient de gain variable est le gain optimal sur le relais. Une performance maximale peut être atteinte en utilisant ce gain. D'autres types de gains peuvent également être utilisés au niveau des relais, mais ils ne donneront pas une performance optimale, tant qu'ils ne sont pas des gains optimaux. En fait, le gain variable au relais est utilisé pour garantir la contrainte de puissance. L'utilisation du coefficient de gain variable au relais implique que toutes l'information d'état du canal est disponible dans le relais.

A.3 Objectifs de Recherche

Dans cette dissertation, nous nous concentrons sur l'évaluation de la performance et l'amélioration des réseaux de relais MSMB en tenant compte de l'aspect pratique de la CCI. Plus précisément, nous étudions la performance des réseaux de relais MSMB avec plusieurs brouilleurs co-canal affectant tous les nœuds qui participent à la transmission de bout-à-bout, depuis le nœud source vers sa destination finale. En particulier, les brouilleurs de puissance égales, ou de puissance non-égales, sont supposés avoir un impact sur chaque nœud relais dans le réseau. Le gain optimal, c'est à dire le coefficient de gain variable, est utilisé à chaque relais. La performance du réseau est évaluée en termes de critères de performance importants, à savoir la probabilité d'erreur binaire, la probabilité de coupure et la capacité. En outre, la répartition optimale de la puissance est prise en compte dans le but d'améliorer la performance globale du réseau.

La technique SSD est aussi considérée pour améliorer les performances. Nous étudions la performance des réseaux de relais bénéficiant de la technique SSD, en termes de probabilité d'erreur, de probabilité de coupure, de capacité ergodique (pour des canaux à évanouissements lents) et en termes de capacité de coupure (pour des canaux à évanouissements rapides). En outre, afin d'améliorer les performances du système, nous minimisons la probabilité d'erreur de ces réseaux, avec une contrainte sur la quantité totale de l'énergie. Nous considérons également l'optimisation de la performance pour minimiser l'énergie totale, sous contrainte sur la probabilité d'erreur.

Enfin, en utilisant un ensemble de décodage C dans un réseau coopératif, nous pouvons améliorer les performances du système. L'idée d'utiliser un ensemble de décodage implique que les relais qui ne parviennent pas à décoder leur signal reçu dans la première phase de transmission du signal, ne participent pas à la deuxième phase de la transmission du signal. ¡

A.4 Contributions

Les contributions de la thèse figurent sous forme d'articles dejà publiés ou en cours d'evaluation.

A.4.1 Articles

[1] A. H. Forghani, S. S. Ikki, and S. Aissa, "Novel approach for approximating the performance of multi-hop multi-branch relaying over Rayleigh fading channels," in *Proc. Wire-*

less Days Conf. (WD'11), Niagara Falls, Ontario, Canada, Oct. 2011.

[2] A. H. Forghani, S. S. Ikki, and S. Aissa, "Performance evaluation of multi-hop multi-branch relaying networks with multiple co-channel interferers," in *Proc. IEEE International Conf. Commun. (ICC'12)*, Ottawa, Ontario, Canada, 2012.

[3] A. H. Forghani, S. S. Ikki, and S. Aissa, "On the performance and power optimization of multi-hop multi-branch relaying networks with co-channel interferers," *IEEE Trans. Veh. Tech.*, vol. 62, no. 7, pp. 3437–3443, Sep. 2013.

[4] A. H. Forghani, S. S. Ikki, and S. Aissa, "Performance of non-symmetric relaying networks in the presence of interferers with unequal powers," *IEEE Wireless Commun. Lett.*, vol. 2, no. 1, pp. 106–109, Feb. 2013.

[5] A. H. Forghani and S. Aissa, "Signal space diversity based relaying: performance analysis and optimization," Submitted to *IEEE Trans. Veh. Tech.*, Sep. 2014.

[6] A. H. Forghani, M. Xia, and S. Aissa, "Analysis of reactive multi-branch relaying under interference and Nakagami-m fading," Submitted to *IEEE Trans. Veh. Tech.*, July 2014.

A.4.2 Résumé des Contributions des Publications

- **Article [1]:** Dans cet article, une expression approximative et sous forme fermée de la probabilité d'erreur binaire moyen (ABEP) de réseaux coopératifs MSMB, est trouvée. Le schéma de relais AF coopératifs regroupe M branches séparées entre le nœud source et le nœud de destination, et chaque branche comprend un certain nombre de relais. En outre, nous considérons des liens de transmission à évanouissements Rayleigh, indépendants et non-identiques, entre des nœuds successifs dans chaque branche. Les résultats numériques sont également proposés et comparés aux resultats de simulations Monte Carlo.

- **Articles [2] et [3]:** Dans ces articles, nous étudions les performances des réseaux à relais opportunistes à MSMB AF opérant en présence d'interférences co-canal. Nous obtenons des expressions exactes de bornes supérieures sur le rapport signal-à-bruit-plus-interférences (SINR) de bout-à-bout, en supposant des transmissions sur des canaux Rayleigh indépendants et non identiques. Ensuite, la fonction cumulative

(CDF) et la densité de probabilité (PDF) de la limite supérieure du SINR de bout-à-bout, sont étudiées. Sur la base de ces données statistiques, nous obtenons une expression sous forme fermée, minorant la probabilité de coupure. En outre, une expression approximative de la PDF du SINR bout-à-bout est calculée. Par la suite, des expressions simples pour l'erreur approximative et les probabilités de coupure sont fournies. Ces expressions permettent une plus grande compréhension de l'effet des différents paramètres du système, sur les performances. Par ailleurs, dans l'article [3], nous nous focalisons sur l'optimisation de la répartition de puissance entre les nœuds de transmission, pour améliorer la performance globale du système. En ayant en main une solution pour le problème d'allocation de ressources, l'attribution de puissance adaptative minimise la probabilité d'erreur, sous la contrainte de puissance combinée sur la branche avec le SINR maximum. Il est démontré qu'en appliquant les énergies obtenues à travers le processus d'optimisation, la performance du réseau augmente de manière significative. En dernier lieu, la précision de l'analyse est validée en comparant les résultats numériques avec les simulations Monte Carlo, et d'importantes discussions sont fournies.

- **Article [4]:** Dans ce travail, la performance des réseaux à relais non symétriques, à MSMB, et utilisant le protocole AF en fonctionnant dans des environnements pratiques avec des brouilleurs à puissance inégale, est examinée. Il est supposé que les canaux, aussi bien pour les signaux désirés que pour les interférence, sont sujets à des évanouissements Rayleigh. Tout d'abord, des expressions exactes de bornes supérieures sur le rapport SINR bout-à-bout, sont calculées. Ensuite, on calcule la fonction génératrice des moments (MGF) pour la borne supérieure sur le rapport SINR. Sur la base de cette dernière (c'est à dire la MGF), les probabilités d'erreurs et de coupure sont évaluées sous forme fermée. En outre, des expressions asymptotiques simples et générales pour les probabilités d'erreurs et de coupure, qui montrent explicitement les gain de codage et de diversité, sont dérivées et discutées. Enfin, l'analyse est validée en comparant les résultats numériques à des simulations Monte Carlo, le tout soutenues par d'importantes discussions.

- **Article [5]:** Cet article étudie la performance et l'optimisation d'un système de relais qui bénéficie de la diversité spatiale de signal. La technique SSD consiste en une rotation de la constellation, et l'entrelacement sur les composantes des points de signal. La détection à la destination dépend du décodage correct ou incorrect au niveau du relais. Les mesures de performance telles que la probabilité d'erreur, la probabilité d'erreur asymptotique, la probabilité de coupure et la capacité ergodique sont obtenues pour les canaux indépendants non identiques, et les canaux indépendants et identiques. En outre, une procédure d'optimisation à deux phases est présentée. Nous obtenons, dans la première phase, l'angle de rotation optimal. Dans la deuxième phase, les énergies optimales de la source et des relais sont obtenues sous la contrainte de la quantité totale de l'énergie, afin de minimiser la probabilité d'erreur. En utilisant l'optimisation à deux phases, la performance du système augmente considérablement. En outre, pour conserver sensiblement l'énergie totale, une autre procédure d'optimisation est présentée. Dans cette dernière, qui vise à minimiser la dépense énergétique totale, les énergies optimales de la source et du relais sont obtenues sous la contrainte de la probabilité d'erreur. Finalement, la validité de notre structure proposée est authentifiée par les résultats numériques et les simulations Monte Carlo. Nos résultats obtenus dans cet article facilitent la gestion et la conception des systèmes pratiques de relais basés sur la diversité spatiale de signal.

- **Article [6]:** Dans cet article, la performance des réseaux de relais, multi-branches, utilisant la technique du *decode-and-forward*, et opérant en présence d'interférences co-canal, est étudiée. Les relais assistant la transmission depuis la source jusqu'à la destination finale sont choisis parmi un ensemble de décodage, qui est constitué des relais intermédiaires qui décodent le message source correctement, de façon réactive. Dans le schéma réactif, le relais dont la branche correspond au plus grand SINR à la destination, est choisi. Nous obtenons tout d'abord le SINR exact bout-en-bout, en supposant des transmissions via des canaux où l'évanouissement du signal est régie par la loi Nakagami-m. Ensuite, la PDF inconditionnelle du SINR bout-en-bout, est obtenue. Sur la base de ces résultats, les expressions exactes sous forme fermée des probabilités d'erreur et de coupure, sont dérivées. En outre, afin d'avoir un meilleur aperçu sur l'impact des paramètres du système sur la performance, une analyse asymptotique sur la probabilité d'erreur, est faite. Enfin, l'analyse est corroborée par la comparaison des résultats numériques avec des simulations Monte Carlo.

A.5 Organisation de la Dissertation

La thèse est organisé comme suit.

Dans le chapitre 2, nous présentons une expression approximative et sous forme fermée, pour calculer la probabilité moyenne d'erreur binaire dans les réseaux coopératifs MSMB, en supposant une transmission dans un environnement à canaux Rayleigh, indépendants et non identiques.

Le chapitre 3 examine la performance des réseaux de relais AF MSMB opportunistes, opérant en présence d'interférences de co-canal. Les expressions exactes de bornes supérieures sur le SINR bout-à-bout sont obtenues, en tenant compte des transmissions via des canaux de transmision Rayleigh, indépendants et non identiques. Nous étudions la CDF et la PDF de la borne supérieure du SINR bout-à-bout. Nous obtenons également une expression sous forme fermée de la borne supérieure sur la probabilité de coupure. En outre, une expression approchée de la PDF du SINR bout-à-bout est dérivée. Par la suite, nous fournissons des expressions simples pour les probabilités d'erreur et de coupure. Nous nous penchons ensuite sur l'optimisation de la répartition de puissance entre les nœuds de transmission pour améliorer la performance globale du système.

Dans le chapitre 4, nous examinons la performance des réseaux de relais MSMB utilisant le protocole AF, et fonctionnant dans des environnements pratiques avec des brouilleurs de puissances inégales. Nous obtenons des expressions exactes pour la borne supérieure sur le SINR bout-à-bout. Ensuite, nous calculons la MGF de la borne supérieure sur le SINR. Sur la base de ce dernier, les probabilités d'erreur et de coupure sont évaluées sous forme fermée. Par la suite, des expressions simples pour les probabilités d'erreur et de coupure sont fournis.

Le chapitre 5 étudie la performance des systèmes de relais bénéficiant de la diversité spatiale de signal. Nous obtenons des mesures de performance telles que la probabilité d'erreur, la probabilité d'erreur asymptotique, la probabilité de coupure, la capacité ergodique et la capacité de coupure. Pour le réseau considéré, lors de la phase de diffusion du processus de communication, le relais reste silencieux en cas de problème dans le décodage du message provenant de la source. Dans le cas contraire, lorsque le relais décode correctement le signal de radiodiffusion, il génère le signal traité et le transmet à la destination. Une procédure d'optimisation à deux phases est présentée. En appliquant l'optimisation à deux phases, la performance du système augmente considérablement. Par ailleurs, pour préserver considérablement l'énergie totale, une autre procédure d'optimisation est présentée. Dans ce processus d'optimisation, visant à minimiser la dépense énergétique totale, la source optimale et les énergies de relais sont obtenus sous la contrainte de probabilité d'erreur.

Le chapitre 6 étudie la performance des réseaux de relais multi-branches, opérant en présence d'interférences co-canal. Les relais assistant la transmission depuis la source jusqu'à la destination finale sont choisis parmi un ensemble de décodage, qui est constitué des relais intermédiaires qui décodent le message source correctement, de façon opportuniste ou réactive. Dans le schéma opportuniste, tous les relais dans l'ensemble de décodage sont exploitées pour la transmission pendant la phase de relais, et la technique de la combinaison de rapport maximal est utilisée au noeud de destination. Dans le schéma réactif, le relais dont la branche correspond au plus grand SINR à la destination, est choisie. Pour chacun des deux régimes (opportuniste ou réactif), nous obtenons tout d'abord le SINR exact, en supposant des transmissions via des canaux où l'évanouissement du signal est régie par la loi Nakagami-m. Ensuite, la PDF inconditionnelle des SINR bout-en-bout, sont obtenus. Sur la base de ces résultats, les expressions exactes sous forme fermée des probabilités d'erreur et de coupure, sont dérivées. En outre, afin d'avoir un meilleur aperçu sur l'impact des paramètres du système sur la performance, une analyse asymptotique de la probabilité d'erreur, est faite. Enfin, l'analyse est corroborée par la comparaison des résultats numériques avec des simulations Monte Carlo.

Enfin, dans le chapitre 7, nous présentons les conclusions de ce travail et proposons des orientations pour des travaux de recherche futurs.

References

[1] M. R. Bhatnagar, "On the capacity of decode-and-forward relaying over Rician fading channels," *IEEE Commun. Lett.*, vol. 17, no. 6, pp. 1100–1103, June 2013.

[2] M. K. Arti, R. K. Mallik, and R. Schober, "Beamforming and combining in two-way AF MIMO relay networks," *IEEE Commun. Lett.*, vol. 17, no. 7, pp. 1400–1403, July 2013.

[3] S. S. Ikki and M. H. Ahmed, "Performance analysis of cooperative diversity wireless networks over Nakagami-m fading channel," *IEEE Commun. Lett.*, vol. 11, no. 4, pp. 334–336, Apr. 2007.

[4] L. L. Yang and H. H. Chen, "Error probability of digital communications using relay diversity over Nakagami-m fading channels," *IEEE Trans. Wireless Commun.*, vol. 7, no. 5, pp. 1806–1811, May 2008.

[5] M. O. Hasna and M. S. Alouini, "End-to-end performance of transmission systems with relays over Rayleigh-fading channels," *IEEE Trans. Wireless Commun*., vol. 2, no. 6, pp. 1126–1131, Nov. 2003.

[6] A. Bansal, M. R. Bhatnagar, A. Hjørungnes, and Z. Han, "Low-complexity decoding in DF MIMO relaying system," *IEEE Trans. Veh. Technol.*, vol. 62, no. 3, pp. 1123–1137, 2013.

[7] M. R. Bhatnagar and M. K. Arti, "Selection beamforming and combining in decode-and-forward MIMO relay networks," *IEEE Commun. Lett.*, vol. 17, no. 8, pp. 1556–1559, 2013.

[8] M. R. Bhatnagar, "Average BER analysis of relay selection based decode-and-forward cooperative communication over Gamma-Gamma fading FSO links," in *Proc. IEEE International Conf. Commun. (ICC'13)*, Budapest, Hungary, 2013.

[9] B. Maham and A. Hjorungnes, "Opportunistic relaying for MIMO amplify-and-forward cooperative networks," *Springer: Wireless Personal Commun.*, 2012.

[10] M. K. Arti, R. K. Mallik, and R. Schober, "Channel estimation and decoding of os-tbc in two-way AF MIMO relay networks," *IEEE Vehicular Technology Conference* (VTC'13), Nevada, Las Vegas, USA, Sept. 2013.

[11] M. O. Hasna and M-S. Alouini, "Outage probability of multihop transmission over Nakagami fading channels," *IEEE Commun. Lett.*, vol. 7, no. 5, pp. 216–218, May 2003.

[12] D. B. Costa and S. Aïssa, "End-to-end performance of dual-hop semi-blind relaying systems with partial relay selection," *IEEE Trans. Wireless Commun.*, vol. 8, no.8, pp. 4306–4315, Aug.2009.

[13] V. Asghari, A. Maaref, and S. Aïssa, "Symbol error probability analysis for multi-hop relaying over Nakagami fading channels," in *Proc. IEEE Wireless Commun. and Networking Conf. (WCNC'10)*, pp. 1–6, Sydney, Australia, Apr. 2010.

[14] A. Agustin and J. Vidal, "Amplify-and-forward cooperation under interference-limited spatial reuse of the relay slot," *IEEE Trans. Wireless Commun.*, vol. 7, no. 5, pp. 1952–1962, May 2008.

[15] C. Zhong, S. Jin, and K.-K. Wong, "Dual-hop systems with noisy relay and interference-limited destination," *IEEE Trans. Commun.*, vol. 58, no. 3, pp. 764–768, Mar. 2010.

[16] I. Krikidis, J. S. Thompson, S. McLaughlin, and N. Goertz, "Max-min relay selection for legacy amplify-and-forward systems with interference," *IEEE Trans. Wireless Commun.*, vol. 8, no. 6, pp. 3016–3027, June 2009.

[17] S. S. Ikki and S. Aïssa, "Effects of co-channel interference on the error probability performance of multi-hop relaying networks," *IEEE Trans. Veh. Technol.*, vol. 61, no. 2, pp. 566–573, Feb. 2012.

[18] J. N. Laneman, D. N. C. Tse, and G. W. Wornell, "Cooperative diversity in wireless networks: efficient protocols and outage behavior," *IEEE Trans. Inf. Theory.*, vol. 50, no. 12, pp. 3062–3080, Dec. 2004.

[19] A. Muller and J. Speidel, "Exact symbol error probability of M-PSK for multihop transmission with regenerative relays," *IEEE Commun. Lett.*, vol. 11, no. 12, pp. 952–954, Dec. 2007.

[20] Z. Bin and M. C. Valenti, "Practical relay networks: a generalization of hybrid-ARQ," *IEEE J. Sel. Areas Commun.*, vol. 23, no. 1, pp. 7–18, Jan. 2005.

[21] J. Boyer, D. D. Falconer, and H. Yanikomeroglu, "Multihop diversity in wireless relaying channels," *IEEE Trans. Commun.*, vol. 52, no. 10, pp. 1820–1830, Oct. 2004.

[22] G. Farhadi and N. Beaulieu, "Fixed relaying versus selective relaying in multi-hop diversity transmission systems," *IEEE Trans. Commun.*, vol. 58, no. 3, pp. 956–965, Mar. 2010.

[23] M. Safari and M. Uysal, "Cooperative diversity over log-normal fading channels: performance analysis and optimization," *IEEE Trans. Wireless Commun.*, vol. 7, no. 5, pp. 1963–1972, May 2008.

[24] M. Di Renzo, F. Graziosi, and F. Santucci, "A comprehensive framework for performance analysis of cooperative multi-hop wireless systems over log-normal fading channels," *IEEE Trans. Commun.*, vol. 58, no. 2, pp. 531–544, Feb. 2010.

[25] G. Farhadi and N. C. Beaulieu, "On the performance of amplify-and-forward cooperative systems with fixed gain relays," *IEEE Trans. Wireless Commun.*, vol. 7, no. 5, pp. 1851–1856, May 2008.

[26] R. Nikjah and N. C. Beaulieu, "Exact capacity analysis of rate adaptive power nonadaptive multi-branch multi-hop decode-and-forward relaying networks," in *Proc. IEEE Global Telecommun. Conf.(GLOBCOM'09)*, Honolulu, Hawaii, USA, 2009.

[27] H. A. Suraweera, H. K. Garg, and A. Nallanathan, "Performance analysis of two hop amplify-and-forward systems with interference at the relay," *IEEE Commun. Lett.*, vol. 14, no. 8, pp. 692–694, Aug. 2010.

[28] H. A. Suraweera, D. S. Michalopoulos, R. Schober, G. K. Karagiannidis, and A. Nallanathan, "Fixed gain amplify-and-forward relaying with co-channel interference," in *Proc. IEEE International Conf. Commun. (ICC'11)*, Kyoto, Japan, 2011.

[29] A. M. Cvetkovic, G. T. Dordevic, and M. C. Stefanovic, "Performance of interference-limited dual-hop non-regenerative relays over Rayleigh fading channels," *IET Commun.*, vol. 5, no. 2, pp. 135–140, Jan. 2010.

[30] S. Chen, X. Zhang, F. Liu, and D. Yang, "Outage performance of dual-hop relay network with co-channel interference," in *Proc. IEEE Veh. Technol. Conf. (VTC'10)*, Ottowa, Ontario, Canada, 2010.

[31] S. S. Ikki and S. Assa, "Performance analysis of dual-hop relaying systems in the presence of co-channel interference," in *Proc. IEEE Global Telecommun. Conf.*, Miami, Florida, USA, 2010.

[32] A. Nasri, R. Schober, and I. Blake, "Performance and optimization of amplify-and-forward cooperative diversity systems in generic noise and interference," *IEEE Trans. Wireless Commun.*, vol. 10, no. 4, pp. 1132–1143, Apr. 2011.

[33] D. Benevides da Costa, H. Ding, and J. Ge, "Interference-limited relaying transmissions in dual-hop cooperative networks over Nakagami-m fading," *IEEE Commun. Lett.*, vol. 15, no. 5, pp. 503–505, May 2011.

[34] D. Lee and J. H. Lee, "Outage probability for dual-hop relaying systems with multiple interferers over Rayleigh fading channels," *IEEE Trans. Veh. Technol.*, vol. 60, no. 1, pp. 333–338, Jan. 2011.

[35] H. Yu, I. -H. Lee, and G. L. Stuber, "Outage probability of decode-and-forward cooperative relaying systems with co-channel interference," *IEEE Trans. Wireless Commun.*, vol. 11, no. 1, pp. 266–274, Jan. 2012.

[36] J. Boutros and E. Viterbo, "Signal space diversity: a power and bandwidth-efficient diversity technique for the Rayleigh fading channel," *IEEE Trans. Inf. Theory*, vol. 44, no. 7, pp. 1453–1467, July 1998.

[37] A. H. Forghani, S. S. Ikki, and S. Aïssa, "Novel approach for approximating the performance of multi-hop multi-branch relaying over Rayleigh fading channels," in *Proc. Wireless Days Conf. (WD'11)*, Niagara Falls, Ontario, Canada, Oct. 2011.

[38] M. Di Renzo, F. Graziosi, and F. Santucci, "On the performance of CSI-assisted cooperative communications over generalized fading channels," *IEEE Commun. Lett.*, vol. 2, no. 6, pp. 1001-1007, May 2008.

[39] M. K. Simon and M.-S. Alouini, *Digital Communication over Fading channels: A Unified Approach to Performance Analysis, John Wiley & Sons Inc.*, 2nd ed., Nov. 2004.

[40] J. G. Proakis, *Digital Communications, McGraw-Hill*, 4th ed., Aug. 2000.

[41] M. D. Renzo, F. Graziosi, and F. Santucci, "A unified framework for performance analysis of CSI-assisted cooperative communications over fading channels," *IEEE Trans. Commun.*, vol. 57, no. 9, pp. 2551-2557, Sep. 2009.

[42] I. S. Gradshteyn and I. M. Ryzhik, *Table of Integrals, Series, and Products, Elsevier Academic Press publications*, 7th ed. San Diego, California: Academic Press, 2007.

[43] M. Chiani, D. Dardari, and M. K. Simon, "New exponential bounds and approximations for the computation of error probability in fading channels," *IEEE Trans. Wireless Commun.*, vol. 2, no. 4, pp. 840-845, July 2003.

[44] A. H. Forghani, S. S. Ikki, and S. Aïssa, "Performance evaluation of multi-hop multi-branch relaying networks with multiple co-channel interferers," in *Proc. IEEE International Conf. Commun. (ICC'12)*, Ottawa, Ontario, Canada, 2012.

[45] A. H. Forghani, S. S. Ikki, and S. Aïssa, "On the performance and power optimization of multi-hop multi-branch relaying networks with co-channel interferers," *IEEE Trans. Veh. Tech.*, vol. 62, no. 7, pp. 3437–3443, Sep. 2013.

[46] Y. Hyungseok and G. L. Stuber, "Outage analysis for general decode-and-forward cooperative relaying systems with co-channel interference," in *Proc. IEEE Wireless Commun. and Networking Conf. (WCNC'12)*, pp. 65–69, Paris, France, Apr. 2012.

[47] S. S. Ikki and S. Aïssa, "Multihop wireless relaying systems in the presence of cochannel interferences: Performance analysis and design optimization," *IEEE Trans. Veh. Technol.*, vol. 61, no. 2, pp. 566–573, Feb. 2012.

[48] Y. Chen and C. Tellambura, "Distribution function of selection combiner output in equally correlated Rayleigh, Rician, and Nakagami-m fading channels," *IEEE Trans. Commun.*, vol. 52, no. 11, pp. 1948–1956, Nov. 2004.

[49] D. S. Michalopoulos, H. A. Suraera, G. K. Karagiannidis and R. Schober, "Amplify-and-forward relay selection with outdated channel estimates," *IEEE Trans. Commun.*, vol. 60, no. 5, pp. 1278–1290, May 2012.

[50] C. Shao-I, "Performance of amplify-and-forward cooperative diversity networks with generalized selection combining over Nakagami-m fading channels," *IEEE Commun. Lett.*, vol. 16, no. 5, pp. 634–637, May 2012.

[51] M. Seyfi, S. Muhaidat and L. Jie, "Amplify-and-forward selection cooperation over Rayleigh fading channels with imperfect CSI," *IEEE Trans. Wireless Commun.*, vol. 11, no. 1, pp. 199–209, Jan. 2012.

[52] A. Papoulis and S. U. Pillai, *Random Variables and Stochastic Processes, McGraw-Hill*, 4th edition, 2004.

[53] Z. Wang and G. B. Giannakis, "A simple and general parameterization quantifying performance in fading channels," *IEEE Trans. Commun.*, vol. 51, no. 8, pp. 1389–1398, Aug. 2003.

[54] A. Ribeiro, X. Cai, and G. B. Giannakis, "Symbol error probabilities for general cooperative links," *IEEE Trans. Wireless Commun.*, vol. 4, no. 3, pp. 1264–1273, May 2005.

[55] A. H. Forghani, S. S. Ikki, and S. Aïssa, "Performance of non-symmetric relaying networks in the presence of interferers with unequal powers," *IEEE Wireless Commmun. Lett.*, vol. 2, no. 1, pp. 106–109, Feb. 2013.

[56] S. S. Ikki and S. Aïssa, "Effects of co-channel interference on the error probability performance of multi-hop relaying networks," in *Proc. IEEE Global Commun. Conf. (GLOBCOM'11)*, Houston, Texas, USA, 2011.

[57] M. K. Simon and M.-S. Alouini, *Digital Communication over Fading Channels, John Wiley & Sons Inc.*, 2nd ed., Feb. 2005.

[58] M. R. McKay, A. Zanella, I. B. Collings and M. Chiani, "Error probability and SINR analysis of optimum combining in Rician fading," *IEEE Trans. Commun.*, vol. 57, no. 3, pp. 676–687, Mar. 2009.

[59] A. H. Forghani and S. Aïssa, "Relaying with signal space diversity: performance analysis and optimization," Submitted to *IEEE Trans. Veh. Tech.*, Sep. 2014.

[60] K. Boulle and J. C. Belfiore, "Modulation schemes designed for the Rayleigh fading channel," in *Proc. Conf. Inform. Sci. Syst. (CISS'92)*, Princeton, New Jersey, USA, 1992.

[61] X. Giraud, E. Boutillon, and J. C. Belfiore, "Algebraic tools to build modulation schemes for fading channels," *IEEE Trans. Inf. Theory*, vol. 43, no. 3, pp. 938–952, May 1997.

[62] Y. Shang, D. Wang, and X. G. Xia, "Flexible signal space diversity techniques from MDS codes with fast decoding," in *Proc. IEEE Global Commun. Conf. (GLOBCOM'10)*, Miami, Florida, USA, 2010.

[63] S. A. Ahmadzadeh, S. A. Motahari, and A. K. Khandani, "Signal space cooperative communication," *IEEE Trans. Wireless Commun.*, vol. 9, no. 4, pp. 1266–1271, Apr. 2010.

[64] C. C. Kuo, S. H. Tsai, L. Tadjpour, and Y. H. Chang, *Precoding Techniques for Digital communication systems, Springer*, New York, 2008.

[65] M. L. McCloud, "Analysis and design of short block OFDM spreading matrices for use on multipath fading channels," *IEEE Trans. Commun.*, vol. 53, no. 4, pp. 656–665, Apr. 2005.

[66] A. Bury, J. Egle, and J. Lindner, "Diversity comparison of spreading transforms for multicarrier spread spectrum transformation," *IEEE Trans. Commun.*, vol. 51, no. 5, pp. 774–781, May 2003.

[67] D. Goeckel and G. Ananthaswamy, "On the design of multidimensional signal sets for OFDM systems," *IEEE Trans. Commun.*, vol. 50, no. 3, pp. 442–452, Mar. 2002.

[68] J. Hagenauer, "Rate-compatible punctured convolutional codes (RCPC codes) and their applications," *IEEE Trans. Commun.*, vol. 36, no. 4, pp. 389–400, Apr. 1988.

[69] M. Janani, A. Hedayat, T. E. Hunter, and A. Nosratinia, "Coded cooperation in wireless communications: space-time transmission and iterative decoding," *IEEE Trans. Signal Procesing*, vol. 52, no. 2, pp. 362–371, Feb. 2004.

[70] B. Zhao and MC Valenti, "Distributed turbo coded diversity for relay channel," *Electron. Lett.*, vol. 39, no. 10, pp. 786–787, May 2003.

[71] W. Tairan, A. Cano, G. B. Giannakis, and J. N. Laneman, "High-Performance cooperative demodulation with decode-and-forward relays," *IEEE Trans. Commun.*, vol. 55, no. 7, pp. 1427–1438, July 2007.

[72] E. Viterbo and F. Oggier, "Tables of algebraic rotations," http://www.tlc.polito.it /∼viterbo/rotations/rotations.html.

[73] J. Kim, W. Lee, J. K. Kim, and I. Lee, "On the symbol error rates for signal space diversity schemes over a Rician fading channel," *IEEE Trans. Commun.*, vol. 57, no. 8, pp. 2204–2209, Aug. 2009.

[74] S. A. Ahmadzadeh, S. A. Motahari, and A. K. Khandani, "Signal space cooperative communication for single relay model," Tech. Rep. 2009-01, Department of ECE, University of Waterloo, 2009.

[75] S. S. Ikki and S. Aïssa, "A study of optimization problem for amplify-and-forward relaying over ibull fading channels with multiple antennas," *IEEE Commun. Lett.*, vol. 15, no. 11, pp. 1148–1151, Nov. 2011.

[76] A. H. Forghani, M. Xia, and S. Aïssa, "Analysis of reactive multi-branch relaying under interference and Nakagami-m fading," Submitted to *IEEE Trans. Veh. Tech.*, July 2014.

[77] H. A. Suraweera, G. K. Karagiannidis, and P. J. Smith, "Performance analysis of the dual-hop asymmetric fading channel," *IEEE Trans. Wireless Commun.*, vol. 8, no. 6, pp. 2783–2788, June 2009.

[78] Q. Yang, K. S. Kwak, and F. Fu, "Closed-form expression for outage probability of DF relaying with unequal Nakagami interferers in Nakagami fading," in *Proc. IEEE Int. Symp. Personal, Indoor Mobile Radio Commun.*, pp. 335–339, Sept. 2009.

[79] J. B. Kim and D. Kim, "Exact and closed-form outage probability of opportunistic decode-and-forward relaying with unequal-power interferers," *IEEE Trans. Commun.*, vol. 9, no. 12, pp. 3601–3606, Feb. 2010.

[80] N. Suraweera and N. C. Beaulieu, "Outage probability of decode-and-forward relaying with optimum combining in the presence of co-channel interference and Nakagami fading," *IEEE Wireless Commmun. Lett.*, vol. 2, pp. 495–498, Oct. 2013.

[81] A. A. Abu-Dayya and N. C. Beaulieu, "Outage probabilities of cellular mobile radio systems with multiple Nakagami interferers," *IEEE Trans. Veh. Technol.*, vol. 40, no. 4, pp. 757–768, Nov. 1991.

[82] F. W. J. Olver, *Handbook of Mathematical Functions*, Cambridge University Press, 2010.

[83] T. Eng and L. B. Milstein, "Coherent DS-CDMA performance in Nakagami multipath fading," *IEEE Trans. Commun.*, vol. 43, no. 234, pp. 1134–1143, Feb./Mar./Apr. 1995.

[84] K. S. Ahn and R. W. Heath, "Performance analysis of maximum ratio combining with imperfect channel estimation in the presence of cochannel interferences," *IEEE Trans. Wireless Commun.*, vol. 8, no. 3, pp. 1080–1085, Mar. 2009.